Physik-Department

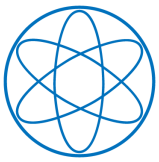

Minimal Flavour Violation in the Quark and Lepton Sector and the Impact of Extra Dimensions on Flavour Changing Neutral Currents and Electroweak Symmetry Breaking

Dissertation
von

Andreas Weiler

Technische Universität
München

Physik-Department
Technische Universität München
Institut für Theoretische Physik
Lehrstuhl Univ.-Prof. Dr. Andrzej J. Buras

Minimal Flavour Violation in the Quark and Lepton Sector and the Impact of Extra Dimensions on Flavour Changing Neutral Currents and Electroweak Symmetry Breaking

Andreas Weiler

Vollständiger Abdruck der von der Fakultät für Physik der Technischen Universität München zur Erlangung des akademischen Grades eines

Doktors der Naturwissenschaften (Dr. rer. nat.)

genehmigten Dissertation.

Vorsitzender:		Univ.-Prof. Dr. Lothar Oberauer
Prüfer der Dissertation:	1.	Univ.-Prof. Dr. Andrzej J. Buras
	2.	Univ.-Prof. Dr. Wolfgang Hollik

Die Dissertation wurde am 10 .1.2007 bei der Technischen Universität München eingereicht und durch die Fakultät für Physik am 16 .1.2007 angenommen.

Minimal Flavour Violation in the Quark and Lepton Sector and the Impact of Extra Dimensions on Flavour Changing Neutral Currents and Electroweak Symmetry Breaking

DISSERTATION

zur Erlangung des Grades
Doktor der Naturwissenschaften (Dr. rer. nat.)
am Fachbereich Physik
der Technischen Universität München

vorgelegt von
Andreas Weiler

Physik-Department T31
Technische Universität München
Januar 2007

Abstract

We study flavor-changing decays of hadrons and leptons and an extra-dimensional approach to electroweak symmetry breaking. Specifically,

- We study the framework of Minimal Flavour Violation (MFV) as an explanation of the flavour problem.
- We discuss the impact of a specific extra-dimensional model of the MFV class on flavour changing neutral currents.
- We derive model-independent upper bounds on rare decays.
- We discuss the extension of the MFV framework from the quark to the lepton sector and show how baryogenesis through leptogenesis can be achieved and examine if possible correlations with charged lepton flavour violation exist.
- We discuss the dynamical breaking of the electroweak symmetry in extra dimensions by unifying gauge and higgs fields and we show that realistic models are possible once the extra dimension is strongly curved.

Contents

Chapter 1

Introduction

The physical laws provided by the Standard Model (SM) of particle physics are currently in spectacular agreement with everything that is known about the interactions of elementary particles. Our understanding of these laws, however, is far from complete. One manifestation of this incompleteness is that the theory has nineteen free parameters which we are not able to predict or explain but must be provided by experiment[1]. For example, the energy scale v at which the electroweak symmetry $SU(2) \times U(1)$ is broken to the electro-magnetic $U(1)$ is not predicted in the SM: it is set to $v \sim 174$ GeV by the measured mass of the Z gauge boson, which is about $M_Z = 91$ GeV. Another example are the masses of the quarks and leptons, or more precisely the ratio of the masses to the weak scale v, the so called Yukawa couplings. Those are also free parameters. The lack of understanding regarding the origin of these parameters is obvious: the measured Yukawa couplings for the quarks and leptons show a striking hierarchy in sizes, from 3×10^{-6} for the electron to ~ 1 for the top quark. There must be a deeper explanation for this pattern, but this explanation lies beyond the SM.

The SM is incomplete in another important respect. It fails to provide a consistent framework for a quantum theory of gravity. Phenomenologically this is not a problem, since quantum gravitational effects are not expected to play an important role until the Planck energy scale $M_{Pl} = (hc/2\pi G_N)^{1/2} = 2 \times 10^{19}$ GeV, which is more than sixteen orders of magnitude larger than the highest energies tested at current and foreseeable particle accelerators. This fact, however, raises the questions: why are there such large hierarchies in Nature? Why is one fundamental mass scale, the Planck scale, so large compared to the other scale known, the weak scale?

These two puzzling hierarchies, the hierarchy in fermion masses and the hierarchy between the Planck and the electroweak scale, can be reformulated as questions about awkwardly small dimensionless parameters. Why is the electron coupling $\lambda_e \sim 3 \times 10^{-6}$ and what is the origin of $M_Z/M_{Pl} \sim 10^{-17}$?

[1]Including the neutrino masses, mixing angles and CP violation phases adds nine more parameters.

Small quark and lepton Yukawa couplings in the SM are at least technically natural in the sense defined by `t Hooft. As λ_i is taken to zero, the fermion becomes massless and left and right helicity states decouple. The theory then has an enlarged chiral symmetry $U(1)_{iL} \times U(1)_{iR}$, which ensures that at least perturbative quantum corrections to the Yukawa coupling vanish to all orders. As a consequence, if λ_i is small at the classical level, all quantum corrections are proportional to its tree-level value and therefore even smaller in magnitude. Small Yukawa couplings are in this sense at least technically natural that quantum corrections do not significantly change the size of λ_i. This is, however, little help in understanding the origin of the small coupling and the pattern of the Yukawa couplings in the SM in general.

The situation is dramatically different in the case of the hierarchy between Planck and weak-scale. In the SM, the breaking of the electroweak symmetry is accomplished by a vacuum expectation value of the scalar Higgs doublet. The negative mass squared of the Higgs m_H^2 is a dimensionful parameter put in by hand which sets (together with the self-coupling) the value of the weak scale. It is well-known that unlike the Yukawa couplings, this parameter is not protected from quantum corrections. The theory becomes classically scale invariant if m_H^2 is taken to zero and so on first glance one could think that a small Higgs mass would also be technically natural. Quantum corrections, however, do not respect the conformal symmetry as it is reflected in the logarithmic running of the gauge coupling constants. Contrary to the common lore, however, within the SM, m_H^2 is not quadratically sensitive to the cut-off, because this would mean a hard breaking of scale invariance by the regulator beyond the one given by m_H^2 and the anomalous running of couplings [1]. The Higgs mass squared becomes unnatural, as soon as one introduces a new explicit high-energy scale Λ in the theory, say the scale of a grand unified theory. Quantum corrections then generally pull the Higgs mass to the value of the new scale and any new physics at a higher energy scale renders the value of m_H^2 unnatural. The correct weak scale can then only result if the tree-level value of m_H^2 is very finely tuned to precisely cancel all the huge quantum corrections, up to an accuracy of $(v/\Lambda)^2$, which has to be as good as one in 10^{34} if Λ is of the order of the Planck scale.

Those two hierarchies set the stage for the problems discussed in this thesis. We expect new degrees of freedom to naturally stabilize the weak scale against quantum corrections. In order to alleviate the fine-tuning we expect the scale of new physics Λ at or not far beyond the TeV range. Since the new degrees of freedom generically couple to the SM quark flavours, they induce new sources of flavour violation. Together with the specific hierarchy of Yukawa couplings in the SM, which the new sources of flavour violation need not to respect, this leads to a tension between the scale of new flavour violation and the scale at which the quadratic Higgs mass is expected to be regularized.

The SM exhibits the accidental property at tree level that flavour change happens only in interactions with fermions which differ in their electromagnetic

charge by one unit. Flavour changing neutral current (FCNC) interactions appear first at the one-loop level. They are additionally suppressed by the particular pattern of the Yukawa couplings: mixings within the first two generations are GIM suppressed and the third generation mixes only weakly with the first two. Due to the double suppression in the SM, quantum fluctuations of new degrees of freedom can in principle contribute in an equally important way. Another particularly interesting property of the SM quark flavour sector is that all CP violation is determined by one universal phase. This correlates many CP violating observables in the SM and provides stringent constraints on scenarious beyond the SM.

Our main interest will be the phenomenological investigation of potential deviations of quark and lepton flavour observables from their SM expectations. Currently, the Tevatron and soon the LHC will hunt for direct signatures for new physics in that they strive to actually produce new particles not contained in the SM. At the same time, CLEO, Belle and BaBar are probing and spectacularly confirming the SM quark flavour sector. Even more excitingly, one hopes to find indirect evidence for new physics in the deviation from SM expectations due to quantum fluctuations of new degrees of freedom. In the future, LHCb, SuperBelle, and rare Kaon experiments at J-PARC and CERN will take over and will herald the era of precision flavour physics.

In the lepton sector, one of the most exciting measurements in the following years will be the MEG experiment which is trying to achieve a sensitivity of 5×10^{-14} for the branching ratio of the leptonic FCNC $\mu^+ \to e^+\gamma$, improving the current bound by two orders of magnitude. Charged lepton flavour violation in the SM is strongly GIM suppressed by the small neutrino masses. In many extension of the SM, however, it can be significantly enhanced, even close to current bounds. We expect that both direct and indirect searches will further complement and assist each other. We will most probably not be able to exactly pin down what waits for us beyond the SM on the results of a proton collider alone.

In the first part of the thesis we will discuss a possible solution to the aforementioned tension between the scale of the new physics solving the hierarchy problem and the scale that suppresses new sources of flavour violation. We will assume the most pessimistic scenario in which the only sources of flavour violation are the SM Yukawa couplings. This is the framework of Minimal Flavour Violation (MFV). In Section 2, we first introduce the general formalism and then in Section 2.3 review the analysis of a specific extra-dimensional model. Finally, in Section 2.4, we discuss a model-independent analysis of minimal flavour violation. Employing the mild assumption that the dominant contribution originates from penguin diagrams we find model independent upper bounds on yet to be measured rare decays.

In Section 3, we show how the MFV framework can be extended to the lepton sector. After motivating this generalization we show how baryogenesis through

leptogenesis can be achieved and including flavour effects in the calculation we show how this compares to the results of a previous analysis. Finally we discuss correlations with the lepton flavour violating process $\mu \to e\gamma$.

The third part of the thesis is mainly concerned with a possible solution of the gauge-hierarchy problem by unifying gauge and Higgs fields in five dimensions. In Section 4, we first motivate the calculation of the effective potential of the Wilson line phase in warped extra dimensions by showing the problems of gauge-Higgs-unification in flat extra-dimensions. We then discuss our calculation of the effective potential of the Wilson line phase and the Hosotani effect in warped extra dimensions. Finally we show how warped gauge-Higgs unification can lead to realistic models of electroweak symmetry breaking. We conclude and give an outlook in chapter 5.

Chapter 2

Minimal Flavour Violation in the quark sector

2.1 Motivation

In recent years great progress has been made in the study of flavour changing neutral (FCNC) decays, leading to an impressively precise extraction of the CKM parameters and more importantly to tight constraints on new sources of flavour violation beyond the SM. The biggest unknown of the SM, the nature of electroweak symmetry breaking (EWSB), will most likely be explored in the coming years at the LHC. The theoretical mystery of EWSB, namely the large hierarchy between the Planck scale and the EWSB scale, however, seems to imply new degrees of freedom beyond the ones in the SM. The proposed solutions include among others supersymmetry [2], technicolor [3, 4], composite Higgs [5], topcolor [6], little Higgs models [7] in 4d and also Arkani-Hamed-Dimopoulos-Dvali (ADD) [8] and Randall-Sundrum I (RS1) [9] models with extra dimensions.
All of these models have new physics (NP) degrees of freedom around the TeV scale. The tight experimental bounds and the non-observation of any deviation from the SM in the flavour sector however generically need this scale to be much higher. An important constraint for example is ϵ_K. NP generically induces a four-fermion operator $(\bar{s}d)^2/\Lambda_{NP}^2$, where the *effective scale* Λ_{NP} has to roughly satisfy $\Lambda_{NP} > 4\pi S_0 M_W/(g^2\lambda^5) \approx 10^3$ TeV in oder to be compatible with experiment. The actual scale of the NP scenario can be lower, if e.g. the contributions are loop suppressed or protected by some GIM like mechanism. In any case such heavy particles can hardly be involved in regularization the quadratic divergency of the Higgs mass. This tension between scales is the so called flavour puzzle.
If in a model the scale responsible for the mediation of flavour violation is much higher than the EWSB scale, then the new sources of flavour violation become irrelevant at energies around the EW scale and the only relevant sources of flavour and CP violation come from the Yukawa matrices of the SM. Most of the present

constraints can then be elegantly avoided and the flavour problem is evaded. This is the framework of minimal flavour violation.

2.2 Basic Framework

2.2.1 Definition

A first definition has been given in [10], where the non-standard contributions have been reabsorbed into a redefinition of the SM electroweak parameters. In the MFV models there are no new complex phases and flavour changing transitions are governed by the CKM matrix. Moreover, the only relevant operators are those already present in the SM[1]. Consequently, new physics enters only through the Wilson coefficients of the SM operators that can receive additional contributions due to the exchange of new virtual particles beyond the SM ones.
Any weak decay amplitude can be then cast in the simple form

$$\mathrm{A(Decay)} = \sum_i B_i \eta^i_{\mathrm{QCD}} V^i_{\mathrm{CKM}} F_i(v), \qquad F_i(v) = F^i_{\mathrm{SM}} + F^i_{\mathrm{New}} \ \ \text{(real)}, \tag{2.1}$$

where $F_i(v)$ are the *master functions* of MFV models [11]

$$S(v),\ X(v),\ Y(v),\ Z(v),\ E(v),\ D'(v),\ E'(v) \tag{2.2}$$

with v denoting collectively the parameters of a given MFV model. Examples of models in this class are the Two Higgs Doublet Model II and the Minimal Supersymmetric Standard Model (MSSM) without new sources of flavour violation and for small or moderate $\tan\beta$. Also models with one universal extra dimension [12, 13] and the simplest little Higgs models are of MFV type [14].
We have the following correspondence between the most interesting FCNC processes and the master functions in the MFV models [11, 15]:

$K^0 - \bar{K}^0$-mixing (ε_K)	$S(v)$
$B^0_{d,s} - \bar{B}^0_{d,s}$-mixing ($\Delta M_{s,d}$)	$S(v)$
$K \to \pi\nu\bar{\nu}$, $B \to X_{d,s}\nu\bar{\nu}$	$X(v)$
$K_{\mathrm{L}} \to \mu\bar{\mu}$, $B_{d,s} \to l\bar{l}$	$Y(v)$
$K_{\mathrm{L}} \to \pi^0 l^+ l^-$	$Y(v)$, $Z(v)$, $E(v)$
ε', $\Delta S = 1$	$X(v)$, $Y(v)$, $Z(v)$, $E(v)$
Nonleptonic $\Delta B = 1$	$X(v)$, $Y(v)$, $Z(v)$, $E(v)$, $E'(v)$
$B \to X_s\gamma$	$D'(v)$, $E'(v)$
$B \to X_s$ gluon	$E'(v)$
$B \to X_s l^+ l^-$	$Y(v)$, $Z(v)$, $E(v)$, $D'(v)$, $E'(v)$

[1]This holds for low and moderate $\tan\beta$ in Two Higgs Doublet Model II models. For large $\tan\beta$ the normalization of the Yukawa couplings changes and operators previously suppressed by light quark masses may become relevant.

This table means that the observables like branching ratios, mass differences $\Delta M_{d,s}$ in $B^0_{d,s} - \bar{B}^0_{d,s}$-mixing and the CP violation parameters ε and ε', can all be to a very good approximation expressed in terms of the corresponding master functions and the relevant CKM factors.

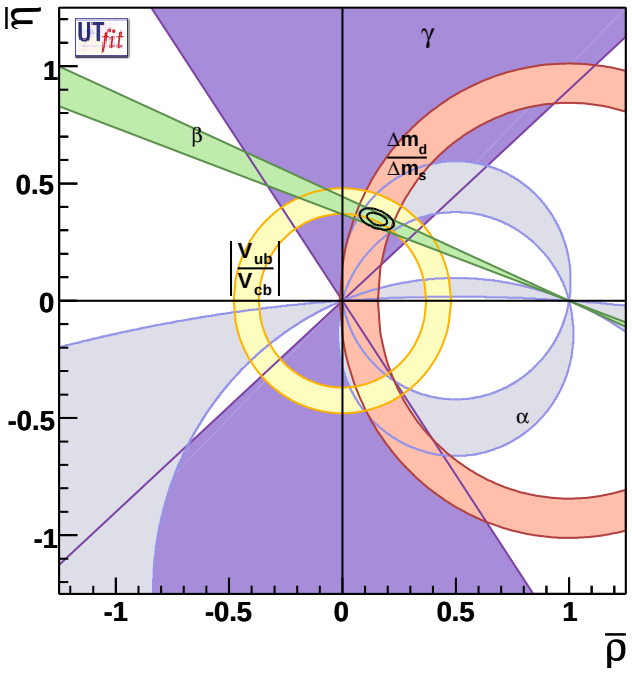

Figure 2.1: *The universal unitarity triangle (UUT) as of 2006 determined by the UTfit group [16]. The quality of the fit is almost as good as within the SM. The analysis shown in the plot results in* $\bar{\rho} = 0.154 \pm 0.032$ *and* $\bar{\eta} = 0.347 \pm 0.018$

The remaining entries in the formulae for these observables are low-energy quantities such as the parameters B_i, that can be calculated within the SM and the QCD factors $\eta^i_{\rm QCD}$ describing the renormalization group evolution of operators for scales $\mu \leq M_W$. These factors being universal can be calculated, similarly to B_i, in the SM. The remaining, model-specific QCD corrections can be absorbed in the functions F_i.
As pointed out in [10], there exists a universal unitarity triangle (UUT) valid in all these models, that can be constructed independently of the parameters specific to a given model. A recent determination of the UUT is shown in Fig. 2.1

2.2.2 Phenomenologically relevant Master Functions

This class of models can be formulated to a very good approximation in terms of eleven parameters: four parameters of the CKM matrix and seven values of the universal master functions $F_i(v)$ that parametrize the short distance contributions to rare decays with v denoting symbolically the parameters of a given MFV model. However, as argued in [11], the new physics contributions to the functions

$$S(v), \qquad C(v), \qquad D'(v), \tag{2.3}$$

representing respectively $\Delta F = 2$ box diagrams, Z^0-penguin diagrams and the magnetic photon penguin diagrams, are the most relevant ones for phenomenology, with the remaining functions producing only minor deviations from the SM in low-energy processes. Several explicit calculations within models with MFV confirm this conjecture. We have checked the impact of these additional functions on our analysis, and we will comment on it in Section 3.4.

Now, the existence of a UUT implies that the four CKM parameters can be determined independently of the values of the functions in (2.3). Moreover, only $C(v)$ and $D'(v)$ enter the branching ratios for radiative and rare decays so that constraining their values by (at least) two specific branching ratios allows to obtain straightforwardly the ranges for all branching ratios within the class of MFV models. Analyses of that type can be found in [11, 17, 18].[2]

2.2.3 Effective Field Theory Framework

For all practical purposes an equivalent result can be derived using an effective field theory framework [17]. One starts from the observation that without the Yukawa couplings the SM exhibits a large chiral flavour symmetry $G = U(3)^5$. Formally, we can recover invariance under G if we promote the Yukawa couplings to fields transforming under the appropriate subgroups of G. The SM Yukawa couplings are the vacuum expectation values of these fields [3] which break the flavour symmetry $\mathrm{SU}(3)_q^3 \otimes \mathrm{SU}(3)_\ell^2 \otimes \mathrm{U}(1)_{\mathrm{PQ}} \otimes \mathrm{U}(1)_{E_R}$ leading to the standard Lagrangian

$$\mathcal{L} = \bar{Q}_L Y_D D_R H + \bar{Q}_L Y_U U_R H_c + \bar{L}_L Y_E E_R H \ + \ \text{h.c.} \ . \tag{2.4}$$

Since the SM Yukawa couplings except the top are small, we find that the only relevant non-diagonal structure is obtained by contracting two Y_U. We define

[2] An alternative approach is to extract from rare decays the relevant Wilson coefficients [19, 20, 21]. However, since in MFV models these coefficients have nontrivial correlations among themselves, we find it more transparent to express the physical quantities in terms of the functions in eq. (2.3).

[3] Since G is spontaneously broken, one generally expects so called familon degrees of freedom [22]. In the case of G being a global symmetry the spontaneous breaking would lead to axion-like particles with a generic coupling of the form $1/F \partial_\mu f^a \bar{\psi} \gamma^\mu T^a \psi$, with F as the family breaking scale, f^a as the familon and T^a as the broken generators of G.

$(\lambda_{\rm FC})_{ij} \approx \lambda_t^2 V_{3i}^* V_{3j}$ for $i \neq j$. Higher orders of $\lambda_{\rm FC}$ are still proportional to $\lambda_t^2 V_{3i}^* V_{3j}$ due to the unitarity of the CKM matrix. We can therefore parameterize all FCNC processes with the effective flavour changing coupling $\lambda_{\rm FC}$.
The construction of the most general, renormalization group invariant, operator basis up to dimension 6 compatible with G is performed in [17]. We list the operators in Appendix A. After integrating out off-shell gauge fields and after breaking the electroweak symmetry the operators with down type quarks relevant for our phenomenological applications[4] are given as
1) Quark-lepton currents:

$$\begin{aligned} \mathcal{Q}_{\nu\bar{\nu}} &= \bar{d}_i\gamma_\mu(1-\gamma_5)d_j\ \bar{\nu}\gamma_\mu(1-\gamma_5)\nu \\ \mathcal{Q}_{10A} &= \bar{d}_i\gamma_\mu(1-\gamma_5)d_j\ \bar{\ell}\gamma_\mu\gamma_5\ell \\ \mathcal{Q}_{9V} &= \bar{d}_i\gamma_\mu(1-\gamma_5)d_j\ \bar{\ell}\gamma_\mu\ell \end{aligned} \tag{2.5}$$

2) Dipole operators:

$$\begin{aligned} \mathcal{Q}_{7\gamma} &= \frac{1}{g^2} m_{d_i}\bar{d}_i(1-\gamma_5)\sigma_{\mu\nu}d_j(eF_{\mu\nu}) \\ \mathcal{Q}_{8G} &= \frac{1}{g^2} m_{d_i}\bar{d}_i(1-\gamma_5)\sigma_{\mu\nu}T^a d_j(g_s G^a_{\mu\nu}) \end{aligned} \tag{2.6}$$

We can recover the master formula (2.1) with the identifications given in coefficients ϵ_i of the general operator basis as follows (the ϵ_i are defined in A.1)

$$\begin{aligned} \delta C_{\nu\bar{\nu}} &= \epsilon_Z + \epsilon_{\ell 1} - \epsilon_{\ell 2} = X_{new} \\ \delta C_{10A} &= \epsilon_Z - \epsilon_{\ell 1} - \epsilon_{\ell 2} + \epsilon_{\ell 3} = Y_{new} \\ \delta C_{9V} &= \epsilon_{\ell 1} + \epsilon_{\ell 2} + \epsilon_{\ell 3} - \left[(1-4\sin^2\theta_{\rm W})\epsilon_Z + 2e\epsilon_{F2}\right] = 4\sin^2\theta_{\rm W} Z_{new} - Y_{new} \\ \delta C_{7\gamma} &= \frac{2g^2}{e}\epsilon_{F1} = -\frac{1}{2}D'_{new} \\ \delta C_{8G} &= \frac{2g^2}{g_s}\epsilon_{G1} = -\frac{1}{2}E'_{new} \end{aligned} \tag{2.7}$$

where $\delta C_i = C_i(M_W^2) - C_i^{\rm SM}(M_W^2)$ and $\epsilon_Z = (\epsilon_{H1}+\epsilon_{H2})/2$. Ignoring the admixture of the gluon penguin encoded in the E function in the master formula above[5], we see that the number of independent, relevant parameters is the same in the effective field theory framework as in the original approach given in (2.1). In MFV we therefore find five independent contributions which govern all $d_i \to d_j\gamma, l^+l^-, \bar{\nu}\nu$ processes. We will see in Section 2.4, how one can further reduce the amount of freedom in order to correlate rare K and B decays with the radiative

[4] We ignore the electroweak and QCD penguin operators.

[5] The admixture of the gluon penguin contribution E at NLO into $\tilde{C}_9^{\rm NDR}(\mu)$ relevant for $B \to X_s l^+l^-$ and $K_L \to \pi_0 l^+l^-$ is of the order of $\mathcal{O}(10^{-2})$.

decays $B \to X_s\gamma$ and $B \to X_s l^+ l^-$.
Together with the universal contribution to the $\Delta F = 2$ amplitude

$$\mathcal{H}_{\rm eff}^{\Delta F=2} = \frac{G_F^2 M_W^2}{16\pi^2}(V_{3i}^* V_{3j})^2 S(v) \left[\bar{d}_i \gamma_\mu (1-\gamma_5) d_j\right]^2 \ , \tag{2.8}$$

we can perform a complete analysis of the MFV flavour interactions.

2.3 A specific model: Universal Extra Dimensions

2.3.1 Introduction

As an example for a specific MFV model we discuss an extension of the SM to extra spatial dimensions. Models in more than three spatial dimensions ($D > 4$) have been with us for more than 80 years beginning with the work of Kaluza and Klein, who used this idea in an attempt to unify gravity and electromagnetism in a five dimensional model with the extra compact dimension characterized by a radius R [23].

While Kaluza, Klein and many authors afterwards considered very small extra dimensions with the compactification scale $1/R = \mathcal{O}(M_{\rm Planck})$, in recent years there has been an increasing interest in models with large extra dimensions, in which $1/R = \mathcal{O}(1\ \text{TeV})$. A special role is played by models with universal extra dimensions (UED) in which all the SM field are democratically allowed to propagate in flat, compact extra dimensions of size 10^{-18} m or smaller. We will concentrate on these models assuming one extra dimension in what follows.

Above the compactification scale $1/R$ a given UED model becomes a higher dimensional field theory whose equivalent description in four dimensions consists of the SM fields, the towers of their Kaluza-Klein (KK) partners and additional towers of KK modes that do not correspond to any field in the SM. Every SM particle has heavy KK partners similar to the case of the MSSM, providing a wealth of possible implications for particle physics and cosmology.

The simplest model of this universal type is the Appelquist, Cheng and Dobrescu (ACD) model [24] with one universal extra dimension. In what follows we will briefly describe this model and subsequently report on the results of two papers [12, 13] in which we investigated the impact of the KK modes on FCNC processes in this model.

2.3.2 The ACD Model

The full Lagrangian of this model includes both the bulk and the boundary Lagrangian. The bulk Lagrangian is determined by the SM parameters after an appropriate rescaling. The coefficients of the boundary terms, however, although

volume suppressed, are free parameters and will get renormalized by bulk interactions. Flavor non-universal boundary terms would lead to large FCNCs. In analogy to a common practice in the MSSM where the soft supersymmetry breaking couplings are chosen to be flavour universal we assume negligible boundary terms at the cut-off scale, which defines what is now called minimal UED or mUED. With this choice contributions from boundary terms are of higher order and we only have to consider the bulk Lagrangian for the calculation of the impact of the ACD model.

Since all our calculations are cut-off independent (see below) the only additional free parameter relative to the SM is the compactification scale $1/R$.

Thus all the tree-level masses of the KK particles and their interactions among themselves and with the SM particles are described in terms of $1/R$ and the parameters of the SM. This economy in new parameters should be contrasted with supersymmetric theories and models with an extended Higgs sector. All Feynman rules necessary for the evaluation of FCNC processes can be found in [12, 13].

A very important property of the ACD model is the conservation of KK parity that implies the absence of tree level KK contributions to low energy processes taking place at scales $\mu \ll 1/R$. In this context the flavour changing neutral current (FCNC) processes like particle-antiparticle mixing, rare K and B decays and radiative decays are of particular interest. Since these processes first appear at one-loop in the SM and are strongly suppressed, the one-loop contributions from the KK modes to them could in principle be important.

The effects of the KK modes on various processes of interest have been investigated in a number of papers. In [24, 25] their impact on the precision electroweak observables assuming a light Higgs ($m_H \leq 250$ GeV) and a heavy Higgs led to the lower bound $1/R \geq 300\,\text{GeV}$ and $1/R \geq 250\,\text{GeV}$, respectively. Subsequent analyses of the anomalous magnetic moment [26] and the $Z \to b\bar{b}$ vertex [27] have shown the consistency of the ACD model with the data for $1/R \geq 300\,\text{GeV}$. The latter calculation has been confirmed in [12]. The scale of $1/R$ as low as 300 GeV would also lead to an exciting phenomenology in the next generation of colliders and could be of interest in connection with dark matter searches [28]. Particle physics alone does not lead to an upper bound on $1/R$, but the thermal relic density of the lightest Kaluza-Klein particle (LKP) increases with $1/R$, and LKPs would overclose the universe for $1/R > 1.5$ TeV [28], providing motivation for considering weak-scale KK particles.

The question then arises whether such low compactification scales are still consistent with the data on FCNC processes. This question has been addressed in detail in [12, 13]. Before presenting the results of these papers let us recall the particle content of the ACD model that has been described in detail in [12] .

In the effective four dimensional theory, in addition to the ordinary particles of the SM, denoted as zero ($n = 0$) modes, there are infinite towers of the KK modes ($n \geq 1$). There is one such tower for each SM boson and two for each SM

fermion, while there also exist physical neutral ($a^0_{(n)}$) and charged ($a^\pm_{(n)}$) scalars with ($n \geq 1$) that do not have any zero mode partners. The masses of the KK particles are universally given by

$$(m^2_{(n)})_{\rm KK} = m_0^2 + \frac{n^2}{R^2}\ . \tag{2.9}$$

Here m_0 is the mass of the zero mode, M_W, M_Z, m_t respectively. For $a^0_{(n)}$ and $a^\pm_{(n)}$ this is M_Z and M_W, respectively. In phenomenological applications it is more useful to work with the variables x_t and x_n defined through

$$x_t = \frac{m_{\rm t}^2}{M_{\rm W}^2}, \qquad x_n = \frac{m_n^2}{M_{\rm W}^2}, \qquad m_n = \frac{n}{R} \tag{2.10}$$

than with the masses in (2.9).

2.3.3 The ACD Model and FCNC Processes

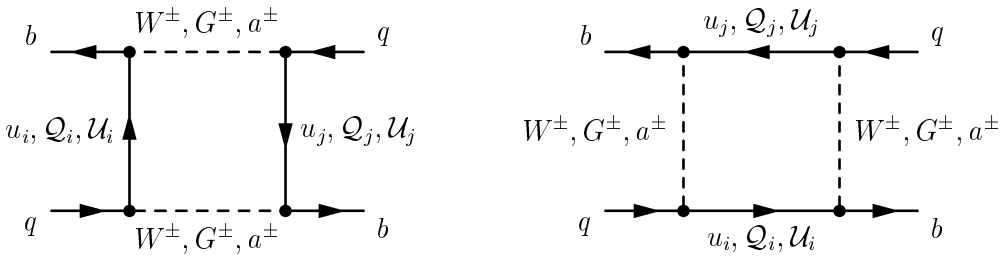

Figure 2.2: Box diagrams contributing to $S_n(x_t, x_n)$. We suppress the KK mode number.

As our analysis of [12, 13] shows, the ACD model with one extra dimension has a number of interesting properties from the point of view of FCNC processes discussed here. These are:

- GIM mechanism [29] that improves significantly the convergence of the sum over the KK modes corresponding to the top quark, removing simultaneously to an excellent accuracy the contributions of the KK modes corresponding to lighter quarks and leptons. This feature removes the sensitivity of the calculated branching ratios to the scale $M_s \gg 1/R$ at which the higher dimensional theory becomes non-perturbative and at which the towers of the KK particles must be cut off in an appropriate way. This should be contrasted with models with fermions localized on the brane, in which the KK parity is not conserved and the sum over the KK modes diverges. In these models the results are sensitive to M_s and for instance in $\Delta M_{s,d}$, the KK effects are significantly larger [30] than found by us. We expect similar behaviour in other processes considered below.

- The low energy effective Hamiltonians are governed by local operators already present in the SM. As flavour violation and CP violation in this model is entirely governed by the CKM matrix, the ACD model belongs to the class ofmodels with minimal flavour violation (MFV) as defined in the previous section. This has automatically the following important consequence for the FCNC processes considered in [12, 13]: the impact of the KK modes on the processes in question amounts only to the modification of the Inami-Lim one-loop functions [31].

- Thus in the case of $\Delta M_{d,s}$ and of the parameter ε_K, that are relevant for the standard analysis of the Unitarity Triangle, these modifications have to be made in the function S [32]. In the case of the rare K and B decays that are dominated by Z^0 penguins the functions X and Y [33] receive KK contributions. Finally, in the case of the decays $B \to X_s\gamma$, $B \to X_s$ gluon, $B \to X_s\mu\bar{\mu}$ and $K_L \to \pi^0 e^+ e^-$ and the CP-violating ratio ε'/ε the KK contributions to new short distance functions have to be computed. These are the functions D (the γ penguins), E (gluon penguins), D' (γ-magnetic penguins) and E' (chromomagnetic penguins).

Thus each function mentioned above, that in the SM depends only on m_t, becomes now also a function of $1/R$:

$$F(x_t, 1/R) = F_0(x_t) + \sum_{n=1}^{\infty} F_n(x_t, x_n), \quad F = B, C, D, E, D', E', \tag{2.11}$$

with x_n defined in (2.10). The functions $F_0(x_t)$ result from the penguin and box diagrams in the SM and the sum represents the KK contributions to these diagrams.

In the phenomenological applications it is convenient to work with the gauge invariant functions [33]

$$X = C + B^{\nu\bar{\nu}}, \qquad Y = C + B^{\mu\bar{\mu}}, \qquad Z = C + \frac{1}{4}D. \tag{2.12}$$

The functions $F(x_t, 1/R)$ have been calculated in our papers [12, 13] with the results given in table 2.1. Our results for the function S have been confirmed in [34]. For $1/R = 300$ GeV, the functions S, X, Y, Z are enhanced by 8%, 10%, 15% and 23% relative to the SM values, respectively. The impact of the KK modes on the function D is negligible. The function E is moderately enhanced but this enhancement plays only a marginal role in the phenomenological applications. The most interesting are very strong suppressions of D' and E', that for $1/R = 300\,\text{GeV}$ amount to 36% and 66% relative to the SM values, respectively. However, the effect of the latter suppressions is softened in the relevant branching ratios through sizable additive QCD corrections.

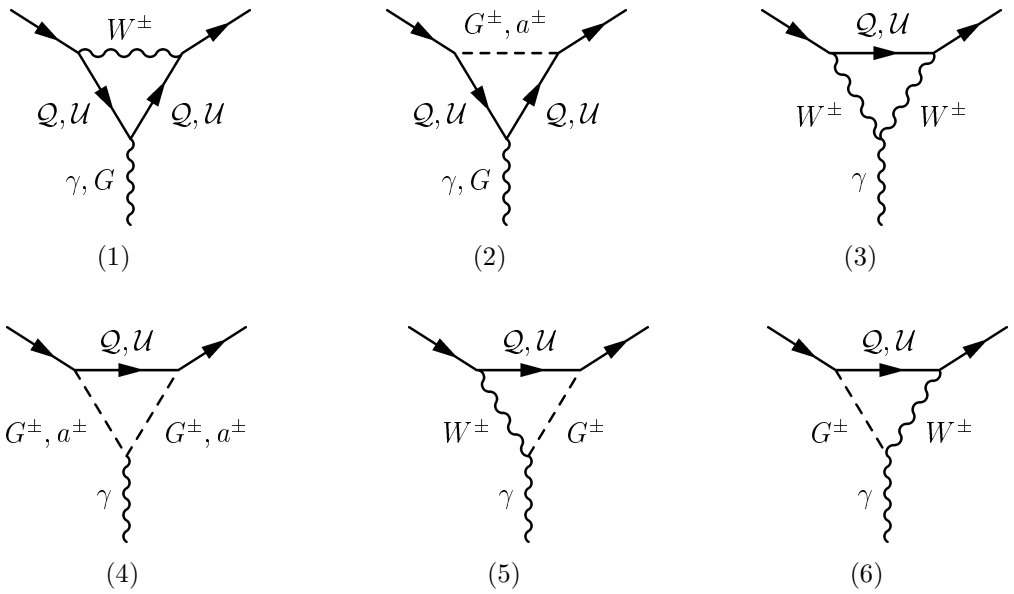

Figure 2.3: Penguin diagrams contributing to $F_n(x_t, x_n)$.

$1/R$	S	X	Y	Z	E	D'	E'	C	D
200	2.813	1.826	1.281	0.990	0.342	0.113	−0.053	1.099	−0.479
250	2.664	1.731	1.185	0.893	0.327	0.191	0.019	1.003	−0.470
300	2.582	1.674	1.128	0.835	0.315	0.242	0.065	0.946	−0.468
400	2.500	1.613	1.067	0.771	0.298	0.297	0.115	0.885	−0.469
SM	2.398	1.526	0.980	0.679	0.268	0.380	0.191	0.798	−0.476

Table 2.1: Values of S, X, Y, Z, E, D', E', C and D as functions of $1/R$ in GeV.

2.3.4 The Impact of the KK Modes on Specific Decays

2.3.4.1 The Impact on the Unitarity Triangle

Here the function S plays the crucial role. Consequently the impact of the KK modes on the UT is rather small. For $1/R = 300\,\text{GeV}$, $|V_{td}|$, $\bar{\eta}$ and γ are suppressed by 4%, 5% and 5°, respectively. It will be difficult to see these effects in the $(\bar{\varrho}, \bar{\eta})$ plane. On the other hand a 4% suppression of $|V_{td}|$ means a 8% suppression of the relevant branching ratio for a rare decay sensitive to $|V_{td}|$ and this effect has to be taken into account. Similar comments apply to $\bar{\eta}$ and γ. Let us also mention that for $1/R = 300\,\text{GeV}$, ΔM_s is enhanced by 8% that in view of the sizable uncertainty in $\hat{B}_{B_s}\sqrt{F_{B_s}}$ will also be difficult to see.

2.3.4.2 The Impact on Rare K and B decays

Here the dominant KK effects enter through the function C or equivalently X and Y, depending on the decay considered. In table 2.2 we show seven branching ratios as functions of $1/R$ for central values of all remaining input parameters. The hierarchy of the enhancements of branching ratios can easily be explained by inspecting the enhancements of the functions X and Y that is partially compensated by the suppression of $|V_{td}|$ in decays sensitive to this CKM matrix element but fully effective in decays governed by $|V_{ts}|$.

$1/R$	200 GeV	250 GeV	300 GeV	400 GeV	SM
$Br(K^+ \to \pi^+\nu\bar{\nu}) \times 10^{11}$	8.70	8.36	8.13	7.88	7.49
$Br(K_{\rm L} \to \pi^0\nu\bar{\nu}) \times 10^{11}$	3.26	3.17	3.09	2.98	2.80
$Br(K_{\rm L} \to \mu^+\mu^-)_{\rm SD} \times 10^{9}$	1.10	1.00	0.95	0.88	0.79
$Br(B \to X_s\nu\bar{\nu}) \times 10^{5}$	5.09	4.56	4.26	3.95	3.53
$Br(B \to X_d\nu\bar{\nu}) \times 10^{6}$	1.80	1.70	1.64	1.58	1.47
$Br(B_s \to \mu^+\mu^-) \times 10^{9}$	6.18	5.28	4.78	4.27	3.59
$Br(B_d \to \mu^+\mu^-) \times 10^{10}$	1.56	1.41	1.32	1.22	1.07

Table 2.2: Branching ratios for rare decays in the ACD model and the SM as discussed in the text.

For $1/R = 300\,\text{GeV}$ the following enhancements relative to the SM predictions are seen: $K^+ \to \pi^+\nu\bar{\nu}$ (9%), $K_{\rm L} \to \pi^0\nu\bar{\nu}$ (10%), $B \to X_d\nu\bar{\nu}$ (12%), $B \to X_s\nu\bar{\nu}$ (21%), $K_L \to \mu\bar{\mu}$ (20%), $B_d \to \mu\bar{\mu}$ (23%) and $B_s \to \mu\bar{\mu}$ (33%). These results correspond to central values of the input parameters. The uncertainties in these parameters partly cover the differences between the ACD model and the SM model and it is essential to reduce these uncertainties considerably if one wants to see the effects of the KK modes in the branching ratios in question.

2.3.4.3 The Impact on $B \to X_s\gamma$ and $B \to X_s$ gluon

The inclusive $B \to X_s\gamma$ decay has been the subject of very intensive theoretical and experimental studies during the last 15 years. On the experimental side the world average resulting from the data by CLEO, ALEPH, BaBar and Belle reads [35]

$$\text{Br}(\bar{B} \to X_s\gamma) = (3.55 \pm 0.24^{+0.09}_{-0.10} \pm 0.03) \cdot 10^{-4} \tag{2.13}$$

where the first error is statistical, the second one systematical, the third one is due to the extrapolation from high E_0 to the reference value, and the last error accounts for the subtraction of $\bar{B} \to X_d\gamma$ background. It is about 1.4 standard deviations above the recently reported NNLO SM result [36]

$$\text{Br}(\bar{B} \to X_s\gamma) = (2.98 \pm 0.26) \cdot 10^{-4} \tag{2.14}$$

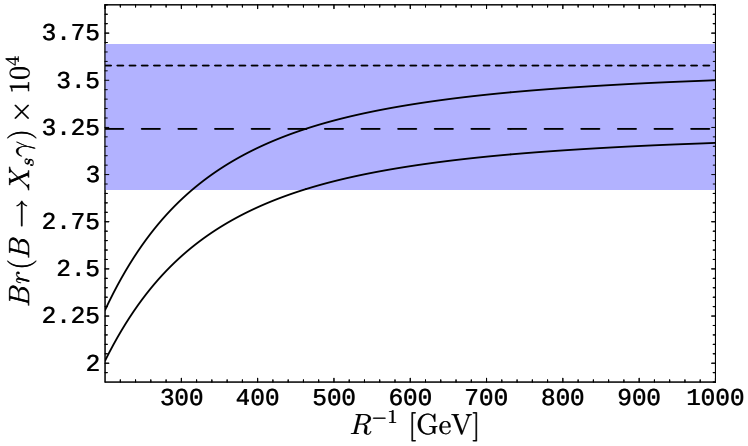

Figure 2.4: The branching ratio for $B \to X_s\gamma$ and $E_\gamma > 1.6$ GeV as a function of $1/R$. See text for the meaning of various curves.

The theoretical status can be found in [37].

Due to strong suppressions of the functions D' and E' by the KK modes, the $B \to X_s\gamma$ and $B \to X_s$ gluon decays are considerably suppressed compared to SM estimates. For $1/R = 300\,\text{GeV}$, $Br(B \to X_s\gamma)$ is suppressed by 20%, while $Br(B \to X_s$ gluon) even by 40%. The phenomenological relevance of the latter suppression is unclear at present as $Br(B \to X_s$ gluon) suffers from large theoretical uncertainties and its extraction from experiment is very difficult if not impossible.

In fig. 2.4 we compare $Br(B \to X_s\gamma)$ in the ACD model with the experimental data. The shaded region represents the data in (2.13) and the two black lines are the theoretical ranges in the ACD model using the NNLO result for the SM contribution.

We observe that in view of the sizable deviation of experimental average and the recently improved theoretical prediction in the SM, the strong suppression of $Br(B \to X_s\gamma)$ by the KK modes does provide a powerful lower bound on $1/R$ and values $1/R \geq 500\,\text{GeV}$ have to be chosen to not deviate more than two standard deviations from the experimental result.

$Br(B \to X_s\gamma)$ provides a very powerful bound on $1/R$ that is substantially stronger than the bounds obtained from the electroweak precision data.

The suppression of $Br(B \to X_s\gamma)$ in the ACD model has already been found in [38]. Our result presented above is consistent with the one obtained by these authors but differs in details as only the dominant diagrams have been taken into account in the latter paper and the analysis was performed in the LO approximation. Their bound is considerably weaker since our strong constraint relies on the fact that we used the NNLO SM prediction.

2.3.4.4 The Impact on $B \to X_s\mu^+\mu^-$ and $A_{FB}(\hat{s})$

The inclusive $B \to X_s\mu^+\mu^-$ decay has been the subject of very intensive theoretical and experimental studies during the last 15 years. On the experimental side only the BELLE collaboration reported the observation of this decay[6] with [39]

$$Br(B \to X_s\mu^+\mu^-) = (7.9 \pm 2.1^{+2.0}_{-1.5}) \cdot 10^{-6} \ . \tag{2.15}$$

For the decay to be dominated by perturbative contributions one has to remove $\bar{c}c$ resonances by appropriate kinematic cuts in the dilepton mass spectrum. The SM expectation [19] for the low dilepton mass window is given by

$$\tilde{B}r(B \to X_s\mu^+\mu^-)_{\rm SM} = (2.75 \pm 0.45) \cdot 10^{-6} \tag{2.16}$$

where the dilepton mass spectrum has been integrated between the limits:

$$\left(\frac{2m_\mu}{m_b}\right)^2 \leq \hat{s} \leq \left(\frac{M_{J/\psi} - 0.35\,\text{GeV}}{m_b}\right)^2 \tag{2.17}$$

where $\hat{s} = (p_+ + p_-)^2/m_b^2$.

This cannot be directly compared to the experimental result in (2.15) that is supposed to include the contributions from the full dilepton mass spectrum. Fortunately future experimental analyses should give the results corresponding to the low dilepton mass window so that a direct comparison between the experiment and the theory will be possible. The most recent reviews summarizing the theoretical status can be found in [40, 19].

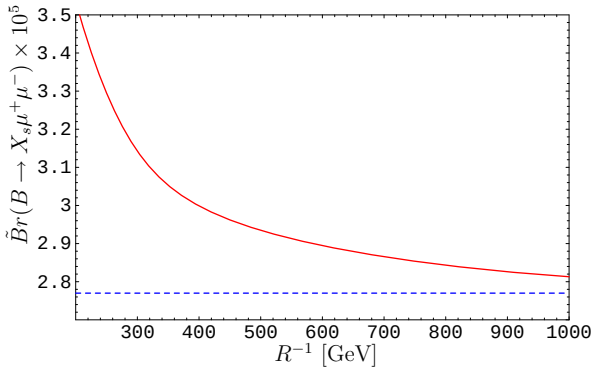

Figure 2.5: $\tilde{B}r(B \to X_s\mu^+\mu^-)$ in the SM (dashed line) and in the ACD model. The integration limits are discussed in the text.

[6] The situation on the experimental side has changed since this analysis had been performed. Belle and BaBar have since measured these decays in various perturbative windows of the dilepton mass spectrum. The result of these measurements does, however, not impact our analysis. The recent NNLO SM prediction of the decay $Br(B \to X_s\gamma)$ on the other hand, has been included and its analysis has been updated for this dissertation.

In fig. 2.5 we show the branching ratio $\tilde{B}r(B \to X_s\mu^+\mu^-)$ as a function of $1/R$ that corresponds to the SM result of (2.16). The observed enhancement is mainly due to the function Y that enters the Wilson coefficient of the operator $(\bar{s}b)_{V-A}(\bar{\mu}\mu)_A$. The Wilson coefficient of $(\bar{s}b)_{V-A}(\bar{\mu}\mu)_V$, traditionally denoted by C_9, is essentially unaffected by the KK contributions.

Of particular interest is the Forward-Backward asymmetry $A_{\rm FB}(\hat{s})$ in $B \to X_s\mu^+\mu^-$ that similarly to the case of exclusive decays [41] vanishes at a particular value $\hat{s} = \hat{s}_0$. The fact that $A_{\rm FB}(\hat{s})$ and the value of $\hat{s}_0$ being sensitive to short distance physics are in addition subject to only very small non-perturbative uncertainties makes them particularly useful quantities to test physics beyond the SM.

The calculations for $A_{\rm FB}(\hat{s})$ and of $\hat{s}_0$ have been done including NNLO corrections [42, 43] that turn out to be significant. In particular they shift the NLO value of $\hat{s}_0$ from 0.142 to 0.162 at NNLO. In fig. 2.6 (a) we show the normalized Forward-Backward asymmetry that we obtained by means of the formulae and the computer program of [19, 42] modified by the KK contributions calculated in [13]. The dependence of $\hat{s}_0$ on $1/R$ is shown in fig. 2.6 (b).

We observe that the value of $\hat{s}_0$ is considerably reduced relative to the SM result obtained by including NNLO corrections [19, 42, 43]. This decrease is related to the decrease of $Br(B \to X_s\gamma)$ as discussed below. For $1/R = 300\,\text{GeV}$ we find the value for $\hat{s}_0$ that is very close to the NLO prediction of the SM. This result demonstrates very clearly the importance of the calculations of the higher order QCD corrections, in particular in quantities like $\hat{s}_0$ that are theoretically clean. We expect that the results in figs. 2.6 (a) and (b) will play an important role in the tests of the ACD model in the future.

In MFV models there exist a number of correlations between different measurable quantities that do not depend on specific parameters of a given model [10, 44]. In [13] a correlation between $\hat{s}_0$ and $Br(B \to X_s\gamma)$ has been pointed out. It is present in the ACD model and in a large class of supersymmetric models discussed for instance in [19]. We show this correlation in fig. 2.7. We refer to [13] for further details.

2.3.4.5 The Impact on $K_L \to \pi^0 e^+ e^-$ and ε'/ε

The impact of the KK modes on the rare decay $K_L \to \pi^0 e^+ e^-$ is at most 10% but it is substantially larger on ε'/ε. The most recent discussion on ε'/ε can be found in [45]. As the Z^0 penguins are enhanced in the ACD model, the ratio ε'/ε is suppressed relative to the SM expectations with the size of the suppression depending sensitively on the hadronic matrix elements. In view of this no useful bound on $1/R$ can be obtained from ε'/ε at present.

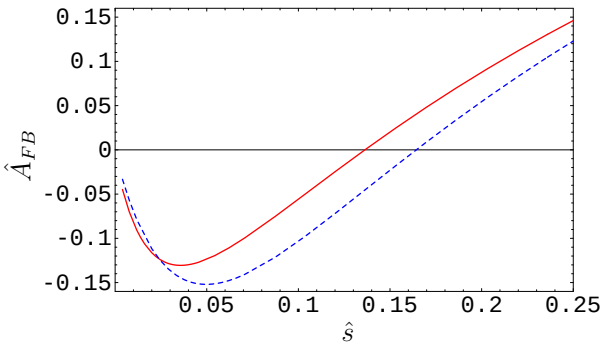

(a)

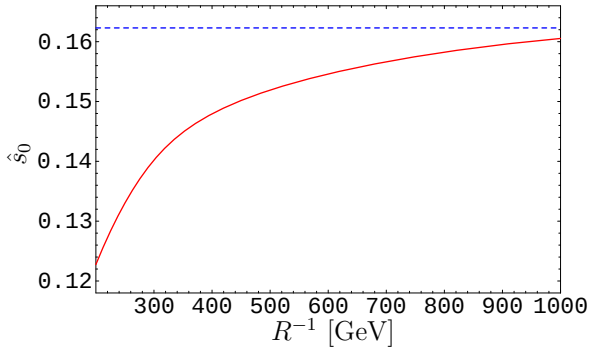

(b)

Figure 2.6: (a) Normalized Forward-Backward asymmetry in the SM (dashed line) and ACD for $R^{-1} = 250$ GeV. (b) Zero of the forward backward asymmetry A_{FB} in the SM (dashed line) and the ACD model.

2.3.5 Concluding Remarks

Our analysis of the ACD model shows that all the present data on FCNC processes are consistent with $1/R$ as low as 500 GeV. Possibly, the most interesting results of our analysis is the suppression of $Br(B \to X_s\gamma)$ which leads to the strongest lower bound currently available on the compactification scale $1/R$. Also interesting is the enhancement of $Br(K^+ \to \pi^+\nu\bar{\nu})$, the sizable downward shift of the zero ($\hat{s}_0$) in the $A_{\rm FB}$ asymmetry and .

The nice feature of this extension of the SM is the presence of only one additional parameter, the compactification scale. This feature allows a unique determination of various enhancements and suppressions relative to the SM expectations. We find

- Enhancements: $K_L \to \pi^0 e^+ e^-$, ΔM_s, $K^+ \to \pi^+\nu\bar{\nu}$, $K_{\rm L} \to \pi^0\nu\bar{\nu}$, $B \to X_d\nu\bar{\nu}$, $B \to X_s\nu\bar{\nu}$, $K_L \to \mu^+\mu^-$, $B_d \to \mu^+\mu^-$, $B \to X_s\mu^+\mu^-$ and $B_s \to \mu^+\mu^-$.

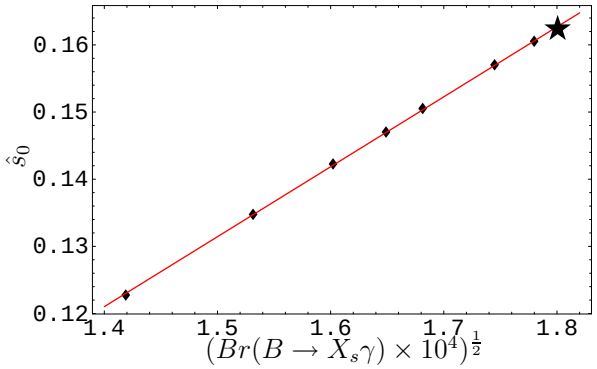

Figure 2.7: Correlation between $\sqrt{Br(B \to X_s\gamma)}$ and $\hat{s}_0$. The straight line is a least square fit to a linear function. The dots are the results in the ACD model for $1/R = 200, 250, 300, 350, 400, 600$ and 1000 GeV and the star denotes the SM value.

- Suppressions: $B \to X_s\gamma$, $B \to X_s$ gluon, the value of $\hat{s}_0$ in the forward-backward asymmetry and ε'/ε.

We would like to emphasize that violation of this pattern by the future data will exclude the ACD model. For instance the measurement of $\hat{s}_0$ that is higher than the SM estimate would automatically exclude this model as there is no compactification scale for which this could be satisfied. Whether these enhancements and suppressions are required by the data or whether they exclude the ACD model with a low compactification scale, will depend on the precision of the forthcoming experiments and the efforts to decrease the theoretical uncertainties.

2.4 Model Independent Upper bounds on rare B and K decays

Now we discuss model-independent upper bounds and correlations resulting from the assumption of MFV[7]. As all information on NP is encoded solely in the functions listed in (2.2), we will now devise a strategy to identify and to determine the dominant contributions.

2.4.1 Strategy

In order to find the functions $F_i(v)$ in (2.2), one first looks at various functions resulting from penguin diagrams: C (Z^0 penguin), D (γ penguin), E (gluon penguin), D' (γ-magnetic penguin) and E' (chromomagnetic penguin). Subsequently box diagrams have to be considered. Here we have the box function S ($\Delta F = 2$ transitions), as well as the $\Delta F = 1$ box functions $B^{\nu\bar{\nu}}$ and $B^{l\bar{l}}$ relevant for decays with $\nu\bar{\nu}$ and $l\bar{l}$ in the final state, respectively.

While the $\Delta F = 2$ box function S and the penguin functions E, D' and E' are gauge independent, this is not the case for C, D and the $\Delta F = 1$ box diagram functions $B^{\nu\bar{\nu}}$ and $B^{l\bar{l}}$. In phenomenological applications it is more convenient to work with gauge independent functions [33]

$$X(v) = C(v) + B^{\nu\bar{\nu}}(v), \qquad Y(v) = C(v) + B^{l\bar{l}}(v), \qquad Z(v) = C(v) + \frac{1}{4}D(v). \tag{2.18}$$

The formulae for the processes in the SM, given in terms of the master functions and CKM factors can be found in many papers. The full list using the same notation is given in [47]. An update of these formulae with additional references is given in two papers on universal extra dimensions [12, 13], where one has to replace $F_i(v, 1/R)$ by $F_i(v)$ to obtain the formulae in a general MFV model. In what follows we will use the formulae of [12, 13] except that:

- We will set the functions

$$B^{\nu\bar{\nu}}(v), \qquad B^{l\bar{l}}(v), \qquad E(v) \tag{2.19}$$

  to their SM values and we will trade the functions $D'(v)$ and $E'(v)$ for the low-energy coefficient $C_7^{\text{eff}}(\mu_b)$ which enters both $b \to s\gamma$ and $b \to sl^+l^-$. In this manner the only free variables are the functions listed in (2.3) plus the $D(v)$ function. As remarked below, this latter function has only a minor impact on our analysis. We have also explored the possible impact of NP contributions to $B^{\nu\bar{\nu}}(v)$ and $B^{l\bar{l}}(v)$, as will be discussed at the end of Section 2.4.2.

[7] This section based on our paper [46].

- In obtaining $Br(K^+ \to \pi^+ \nu\bar{\nu})$ we have included the recently calculated long distance contributions [48] that enhance the branching ratio by roughly 6%. This amounts effectively to a charm parameter of $P_c = 0.43 \pm 0.07$. [8]
- We will use the formula for $(K_{\rm L} \to \pi^0 l^+ l^-)_{\rm CPV}$ from [50, 51].
- We used the complete NLO formulae for $B \to X_s\gamma$ from [52]. This has been the best available calculation at the time. Now a almost complete NNLO treatment is available [37, 36].
- We used the complete NNLO formulae for $B \to X_s l^+ l^-$ from [53, 20].

Branching Ratios	Formula	Reference	Parameters
$Br(K^+ \to \pi^+ \nu\bar{\nu})$	(4.24)	[12]	$Br(K^+ \to \pi^0 e^+ \nu)$, m_c
$Br(K_{\rm L} \to \pi^0 \nu\bar{\nu})$	(4.27)	[12]	$Br(K^+ \to \pi^0 e^+ \nu)$
$Br(K_{\rm L} \to \mu^+\mu^-)_{\rm SD}$	(4.32)	[12]	m_c
$Br(K_{\rm L} \to \pi^0 l^+ l^-)_{\rm CPV}$	(43)	[51]	see [51]
$Br(B \to X_s \nu\bar{\nu})$	(4.29)	[12]	$Br(B \to X_c l\bar{\nu})$
$Br(B \to X_d \nu\bar{\nu})$	(4.29)	[12]	$Br(B \to X_c l\bar{\nu})$
$Br(B_s \to \mu^+\mu^-)$	(4.30)	[12]	F_{B_s}
$Br(B_d \to \mu^+\mu^-)$	(4.30)	[12]	F_{B_d}

Table 2.3: *Guide to the formulae. See text for explanations. The dependence of all branching ratios on CKM parameters and the top quark mass is not explicitly reported.*

In Table 2.3 we indicate where the formulae in question can be found and which additional input parameters are involved in them. In Table 2.4 we give the numerical values of all the parameters involved in the analysis.

Finally, for the reader's convenience, and in order to show the relative importance of NP contributions to the processes we consider, we report below numerical formulae for the branching ratios in terms of $F^i_{\rm New}$ in eq. (2.1). These numerical expressions have been obtained for central values of the parameters in Table 2.4, as functions of $\Delta C \equiv C(v) - C_{\rm SM}$, $\Delta C_7^{\rm eff} \equiv C_7^{\rm eff} - C_{7\,\rm SM}^{\rm eff}$, $\Delta D \equiv D(v) - D_{\rm SM}$, $\Delta B^{l\bar{l}} \equiv B^{l\bar{l}}(v) - B^{l\bar{l}}_{\rm SM}$ and $\Delta B^{\nu\bar{\nu}} \equiv B^{\nu\bar{\nu}}(v) - B^{\nu\bar{\nu}}_{\rm SM}$. With the aid of eq. (2.20), it is possible to quickly check the impact of NP contributions in any given MFV model. As a first insight, we see that the dependence of $Br(B \to X_s l^+ l^-)$ on ΔD is relatively weak, as can be read off from the small prefactors in the formulae below. From eq. (2.20) one can also check whether the NP contribution to box

[8] After the completion of this analysis a NNLO calculation of the charm contribution became available [49].

Parameter	Value	Gaussian (σ)
λ	0.2255	0.0014
$\|V_{cb}\|$	0.0415	0.0007
$\bar{\rho}$	0.191	0.046
$\bar{\eta}$	0.353	0.028
F_{B_s}	230 MeV	30 MeV
F_{B_d}	189 MeV	27 MeV
$Br(B \to X_c l \bar{\nu})$	0.1045	0.0021
$Br(K^+ \to \pi^0 e^+ \nu)$	0.0487	0.0006
$m_t^{\rm pole}$	178.0 GeV	4.3 GeV
$\overline{m}_b$	4.21 GeV	0.08 GeV
$\overline{m}_c$	1.3 GeV	0.1 GeV
$\alpha_s(M_Z)$	0.119	0.003

Table 2.4: *Values of the relevant parameters used in the analysis.*

diagrams in any given model is large enough as to modify significantly our results obtained for $\Delta B^{l\bar{l}} = \Delta B^{\nu\bar{\nu}} = 0$ in the next Section. Finally, these formulae allow

to understand the structure of our numerical results. We have[9]:

$$\begin{aligned}
Br(B \to X_s l^+ l^-, 0.04 < q^2(\mathrm{GeV}) < 1) &= 1.16 \cdot 10^{-6}(1 + 0.38\,(\Delta B^{l\bar{l}})^2 \\
&+0.46\,\Delta C_7^{\mathrm{eff}}\Delta B^{l\bar{l}} + 0.41\,\Delta C\Delta B^{l\bar{l}} - 3.47\,\Delta C_7^{\mathrm{eff}} + 0.56\,\Delta B^{l\bar{l}} \\
&+4.31(\Delta C_7^{\mathrm{eff}})^2 + 0.19\,(\Delta C)^2 + 0.38\Delta C - 0.11\,\Delta C_7^{\mathrm{eff}}\Delta D)\,, \\
Br(B \to X_s l^+ l^-, 1 < q^2(\mathrm{GeV}) < 6) &= 1.61 \cdot 10^{-6}(1 + 1.33\,(\Delta B^{l\bar{l}})^2 \\
&+1.26\,\Delta C_7^{\mathrm{eff}}\Delta B^{l\bar{l}} + 1.43\,\Delta C\Delta B^{l\bar{l}} - 0.31\,\Delta D\Delta B^{l\bar{l}} + 2.08\,\Delta B^{l\bar{l}} \\
&+1.42(\Delta C_7^{\mathrm{eff}})^2 + 0.67\,(\Delta C)^2 + 1.36\Delta C - 0.29\,\Delta C_7^{\mathrm{eff}}\Delta D - 0.18\Delta D)\,, \\
Br(B \to X_s l^+ l^-, 14.4 < q^2(\mathrm{GeV}) < 25) &= 3.70 \cdot 10^{-7}(1 + 1.18\,(\Delta B^{l\bar{l}})^2 \\
+0.70\,\Delta C_7^{\mathrm{eff}}\Delta B^{l\bar{l}} + 0.60\,\Delta C_7^{\mathrm{eff}} &+ 1.27\,\Delta C\Delta B^{l\bar{l}} - 0.27\,\Delta D\Delta B^{l\bar{l}} + 2.18\,\Delta B^{l\bar{l}} \\
&+0.21(\Delta C_7^{\mathrm{eff}})^2 + 0.60\,(\Delta C)^2 + 1.24\Delta C - 0.16\,\Delta C_7^{\mathrm{eff}}\Delta D - 0.24\Delta D)\,, \\
Br(B_d \to \mu^+\mu^-) &= 1.08 \cdot 10^{-10}(1 + \Delta B^{l\bar{l}} + \Delta C)^2\,, \\
Br(B_s \to \mu^+\mu^-) &= 3.76 \cdot 10^{-9}(1 + \Delta B^{l\bar{l}} + \Delta C)^2\,, \\
Br(B \to X_d \nu\bar{\nu}) &= 1.50 \cdot 10^{-6}(1 + 0.65\,(\Delta C + \Delta B^{\nu\bar{\nu}}))^2\,, \\
Br(B \to X_s \nu\bar{\nu}) &= 3.67 \cdot 10^{-5}(1 + 0.65\,(\Delta C + \Delta B^{\nu\bar{\nu}}))^2\,, \\
Br(K^+ \to \pi^+ \nu\bar{\nu}) &= 8.30 \cdot 10^{-11}(1 + 0.20(\Delta C + \Delta B^{\nu\bar{\nu}})^2 \\
&+0.89(\Delta C + \Delta B^{\nu\bar{\nu}}))\,, \\
Br(K_L \to \pi^0 \nu\bar{\nu}) &= 3.10 \cdot 10^{-11}(1{+}0.65(\Delta C + \Delta B^{\nu\bar{\nu}}))^2\,, \\
Br(K_L \to \mu^+\mu^-) &= 8.58 \cdot 10^{-10}(1{+}0.82(\Delta C + \Delta B^{l\bar{l}}))^2\,. \qquad (2.20)
\end{aligned}$$

2.4.2 Numerical Analysis

Our numerical analysis consists of three steps:

1. Extracting CKM parameters using the UUT analysis;
2. Determining the allowed range for ΔC and $\Delta C_7^{\mathrm{eff}}$ from presently available data;
3. Computing the expectation values of rare decays based on these allowed ranges.

For the first step, we used the 2005 results of the **UT***fit* collaboration on the UUT analysis [54]:

$$\bar{\rho} \;=\; 0.191 \pm 0.046\,, \qquad \bar{\eta} = 0.353 \pm 0.028. \qquad (2.21)$$

Since the UUT analysis is independent of loop functions, the above results are in particular independent of the top quark mass.

[9]Notice that we have discarded terms with coefficients smaller than 0.1 in $Br(B \to X_s l^+ l^-)$.

Branching Ratios	MFV (95%)	SM (68%)	SM (95%)	exp
$Br(K^+ \to \pi^+ \nu\bar{\nu}) \times 10^{11}$	< 11.9	8.3 ± 1.2	$[6.1, 10.9]$	$(14.7^{+13.0}_{-8.9})$ [59]
$Br(K_{\rm L} \to \pi^0 \nu\bar{\nu}) \times 10^{11}$	< 4.59	3.08 ± 0.56	$[2.03, 4.26]$	$< 5.9 \cdot 10^4$ [60]
$Br(K_{\rm L} \to \mu^+\mu^-)_{\rm SD} \times 10^9$	< 1.36	0.87 ± 0.13	$[0.63, 1.15]$	-
$Br(B \to X_s \nu\bar{\nu}) \times 10^5$	< 5.17	3.66 ± 0.21	$[3.25, 4.09]$	< 64 [61]
$Br(B \to X_d \nu\bar{\nu}) \times 10^6$	< 2.17	1.50 ± 0.19	$[1.12, 1.91]$	-
$Br(B_s \to \mu^+\mu^-) \times 10^9$	< 7.42	3.67 ± 1.01	$[1.91, 5.91]$	$< 2.7 \cdot 10^2$ [62]
$Br(B_d \to \mu^+\mu^-) \times 10^{10}$	< 2.20	1.04 ± 0.34	$[0.47, 1.81]$	$< 1.5 \cdot 10^3$ [62]

Table 2.5: *Upper bounds for rare decays in MFV models at* 95% *probability, the corresponding values in the SM (using inputs from the UUT analysis) and the available experimental information. See the text for details.*

In the second step, to minimize the theoretical input, we have traded $D'(v)$ and $E'(v)$ for $C_7^{\rm eff}$, which is the relevant low-energy quantity entering $Br(B \to X_s\gamma)$ and $Br(B \to X_s l^+ l^-)$. Concerning $Br(B \to X_s\gamma)$, we compare the theoretical value with the experimental results of CLEO [55], Belle [56] and BaBar [57] in the corresponding kinematic ranges, adding a conservative 10% flat theoretical error to the theoretical prediction. This error contains both the uncertainties due to the cutoff in the photon spectrum [58] and the ones related to higher order effects, which are particularly large since we are omitting here model-specific NLO terms for the NP contribution. For $Br(B \to X_s l^+ l^-)$, we use the experimental data in the q^2 regions $0.04 < q^2({\rm GeV}) < 1$, $1 < q^2({\rm GeV}) < 6$ and $14.4 < q^2({\rm GeV}) < 25$ to avoid the theoretical uncertainty due to the presence of $c\bar{c}$ resonances.

The second and third steps are carried out using the approach of ref. [63]: taking $C(v)$, $C_7^{\rm eff}(\mu_b)$ and $D(v)$ to have a flat *a-priori* distribution and using the available experimental data and theoretical inputs, we determine the *a-posteriori* probability density function (p.d.f.) for $C(v)$, $C_7^{\rm eff}(\mu_b)$ and all the rare decays listed in Table 2.5. Concerning $D(v)$, it plays only a marginal role in these decays and therefore it is not well determined by the analysis. We varied ΔD in the conservative range $\pm 4 D_{\rm SM}$. Even this rather large variation has little impact on the extraction of the allowed range for $C(v)$.

In Figure 2.8 we plot the p.d.f. for $\Delta C(v)$ and $\Delta C_7^{\rm eff}$, that represent $F^i_{\rm New}$ in (2.1) and enter eq. (2.20). In Figure 2.9 we plot the p.d.f. for the branching ratios. The corresponding upper bounds at 95% probability are reported in Table 2.5, where, for comparison, we also report the results obtained within the SM, using the same CKM parameters obtained from the UUT analysis. Finally, in Figures 2.10 and 2.11 we plot the branching ratios of the rare decays vs. $C(v)$, to make the impact of future measurements on the determination of $C(v)$ more transparent.

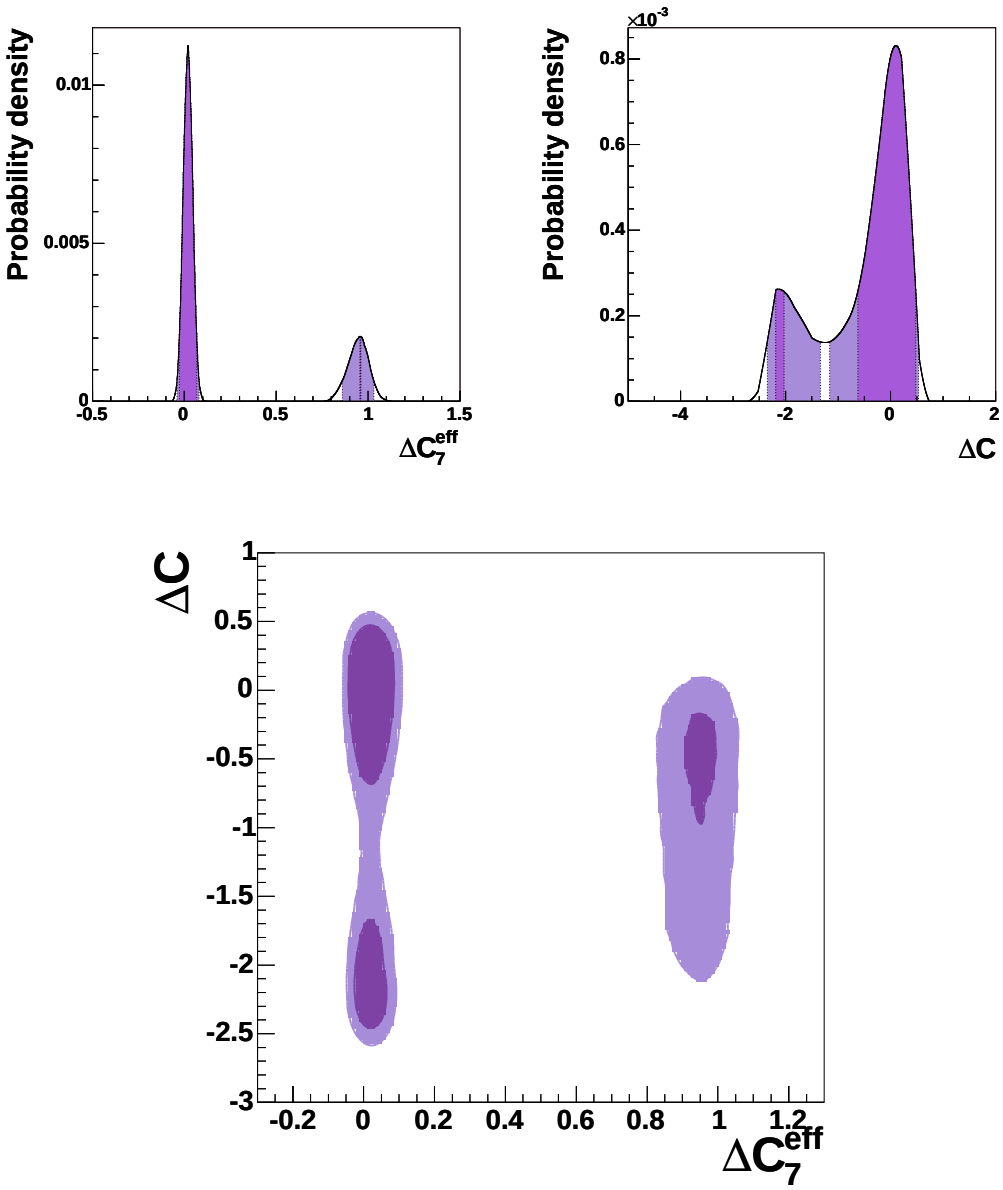

Figure 2.8: *P.d.f.'s for* $\Delta C_7^{\rm eff}$ *(top-left),* ΔC *(top-right) and* ΔC *vs.* $\Delta C_7^{\rm eff}$ *(bottom). Dark (light) areas correspond to the* 68% *(*95%*) probability region.*

Let us now comment on our results. As can be seen from Figure 2.8, we have two possible solutions for $\Delta C_7^{\rm eff}$, one very close to the SM, and the other corresponding to reversing the sign of $C_7^{\rm eff}(\mu_b)$ (recall that $C_7^{\rm eff}(\mu_b)$ is negative in the SM and equal to $C_7^{\rm eff}(\mu_b) \approx -0.33$). The second solution is disfavoured: it is barely accessible at 68% probability, in accordance with the results of [21]. This

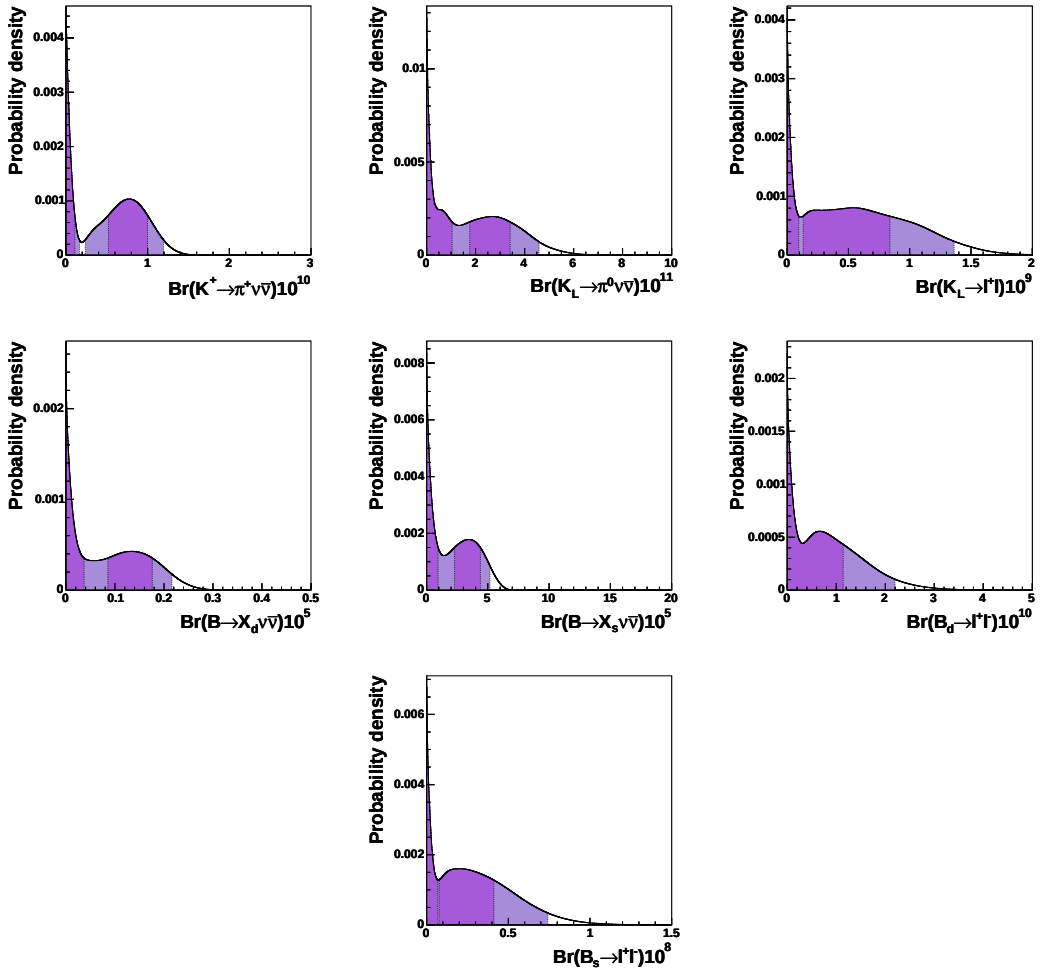

Figure 2.9: *P.d.f.'s for the branching ratios of the rare decays* $Br(K^+ \to \pi^+\nu\bar{\nu})$, $Br(K_{\rm L} \to \pi^0\nu\bar{\nu})$, $Br(K_{\rm L} \to \mu^+\mu^-)_{\rm SD}$, $Br(B \to X_{d,s}\nu\bar{\nu})$, *and* $Br(B_{d,s} \to \mu^+\mu^-)$. *Dark (light) areas correspond to the* 68% (95%) *probability region.*

result is easy to understand. In the case of the second solution for $\Delta C_7^{\rm eff}$, the branching ratio $Br(B \to X_s l^+ l^-)$ becomes larger than the experimental value. The full results are:

$$\begin{aligned} \Delta C_7^{\rm eff} &= (0.02 \pm 0.047) \cup (0.958 \pm 0.002) \text{ at } 68\% \text{ probability}, \\ \Delta C_7^{\rm eff} &= [-0.039, 0.08] \cup [0.859, 1.031] \text{ at } 95\% \text{ probability}. \end{aligned} \tag{2.22}$$

Since we have two separate ranges for $\Delta C_7^{\rm eff}$, in the following we will also present separately the results corresponding to the "LOW" or "HI" solution for $\Delta C_7^{\rm eff}$ (see Figures 2.12 and 2.13).

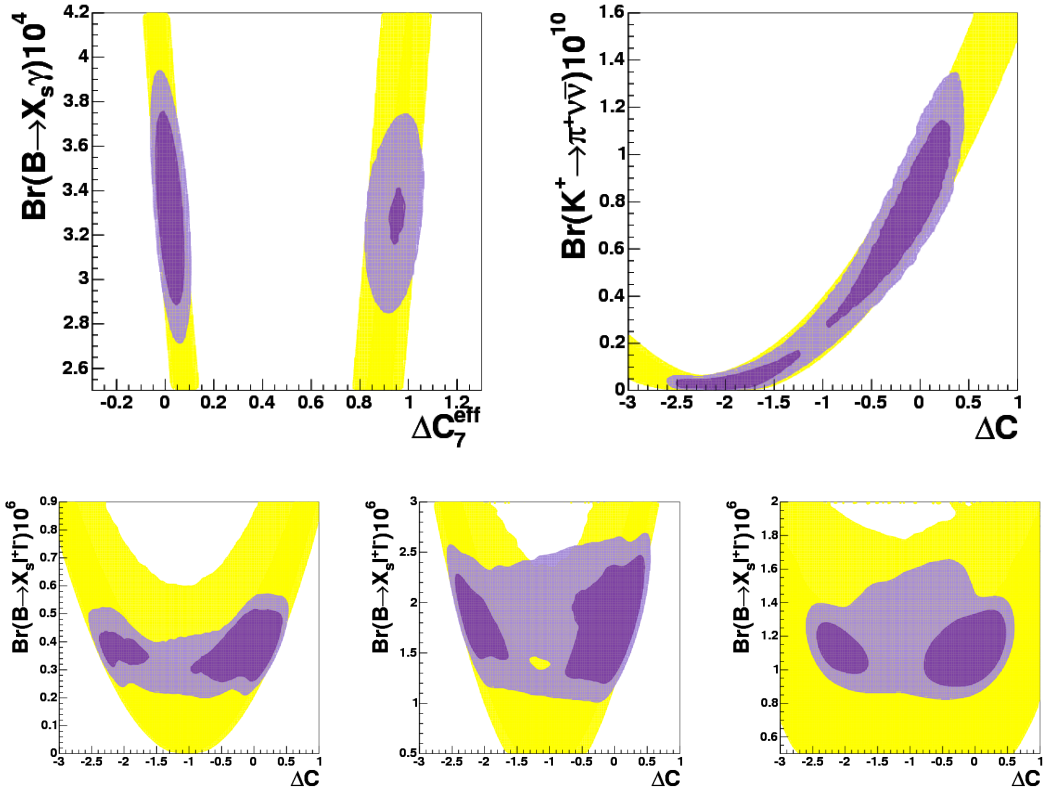

Figure 2.10: *P.d.f.'s for the branching ratios of the rare decays used to constrain* ΔC *and* $\Delta C_7^{\rm eff}$ *as a function of these parameters:* $Br(B \to X_s\gamma)_{E_\gamma > 1.8{\rm GeV}}$ *(top-left),* $Br(K^+ \to \pi^+ \nu\bar{\nu})$ *(top-right),* $Br(B \to X_s l^+ l^-)_{14.4<q^2({\rm GeV})<25}$ *(bottom-left),* $Br(B \to X_s l^+ l^-)_{1<q^2({\rm GeV})<6}$ *(bottom-center),* $Br(B \to X_s l^+ l^-)_{0.04<q^2({\rm GeV})<1}$ *(bottom-right). Dark (light) areas correspond to the* 68% *(*95%*) probability region. Very light areas correspond to the range obtained without using the experimental information.*

As can be seen in Figure 2.8 we have two solutions for ΔC, one close to the SM and the other corresponding to reversing the sign of C. We recall that $C \approx 0.81$ in the SM. The ranges obtained are

$$\begin{aligned} \Delta C &= (-0.16 \pm 0.53) \cup (-2.15 \pm 0.08) \text{ at } 68\% \text{ probability}, \\ \Delta C &= [-1.25, 0.44] \cup [-2.39, -1.45] \text{ at } 95\% \text{ probability}. \end{aligned} \tag{2.23}$$

From the plot of ΔC vs $\Delta C_7^{\rm eff}$ in Figure 2.8, it is evident that the situation is different for the HI and LOW solutions for $\Delta C_7^{\rm eff}$. Indeed, the two solutions

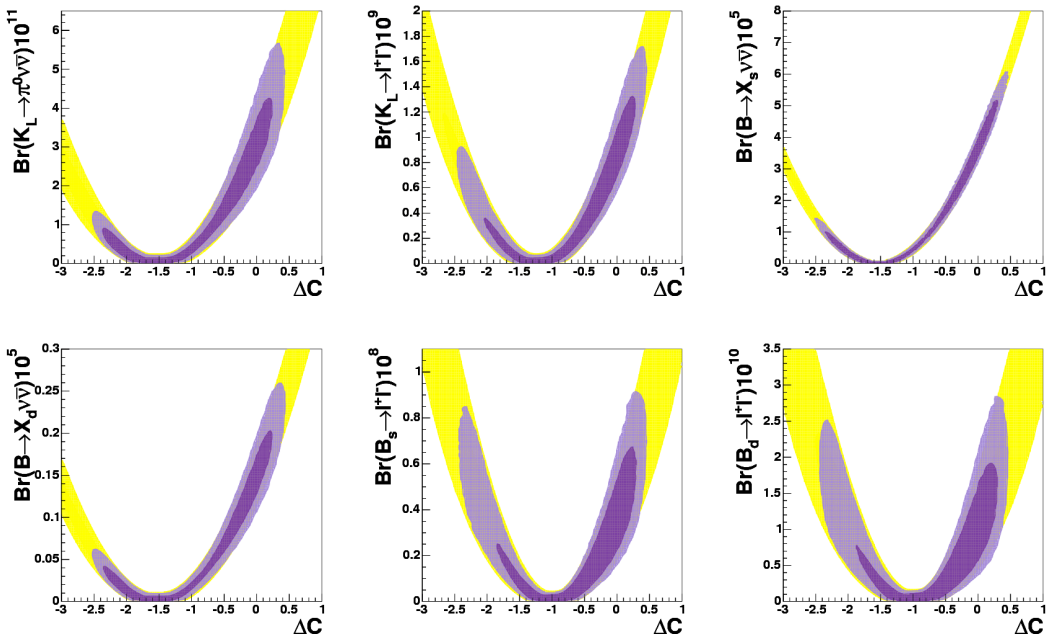

Figure 2.11: *P.d.f.'s for the branching ratios of the rare decays* $Br(K_{\rm L} \to \pi^0\nu\bar{\nu})$, $Br(K_{\rm L} \to \mu^+\mu^-)_{\rm SD}$, $Br(B \to X_{d,s}\nu\bar{\nu})$, *and* $Br(B_{d,s} \to \mu^+\mu^-)$ *as a function of* ΔC. *Dark (light) areas correspond to the* 68% (95%) *probability region. Very light areas correspond to the range obtained without using the experimental information.*

correspond to the following ranges for ΔC:

$$\begin{aligned}
\text{LOW}: \ \Delta C &= (-0.03 \pm 0.41) \cup (-2.18 \pm 0.02) \text{ at } 68\% \text{ probability}, \\
\text{LOW}: \ \Delta C &= [-0.75, 0.50] \cup [-2.49, -1.60] \text{ at } 95\% \text{ probability}, \\
\text{HI}: \ \Delta C &= (-0.68 \pm 0.58) \text{ at } 68\% \text{ probability}, \\
\text{HI}: \ \Delta C &= [-1.98, 0.04] \text{ at } 95\% \text{ probability}.
\end{aligned} \tag{2.24}$$

These results are easy to understand. For the LOW solution the solutions with ΔC being positive and negative are consistent with the data on $B \to X_s l^+ l^-$. On the other hand for the HI solution, $\Delta C < 0$ is favoured as with $\Delta C > 0$ the difficulty with a too high $Br(B \to X_s l^+ l^-)$ becomes more acute.

For the reader's convenience, we report in Table 2.6 the values of the X, Y and Z functions obtained by summing SM and NP contributions and by applying all the available experimental constraints.

The impact of $Br(K^+ \to \pi^+\nu\bar{\nu})$ on the bounds on NP contributions can be seen by comparing Figure 2.8 with Figure 2.14, where $Br(K^+ \to \pi^+\nu\bar{\nu})$

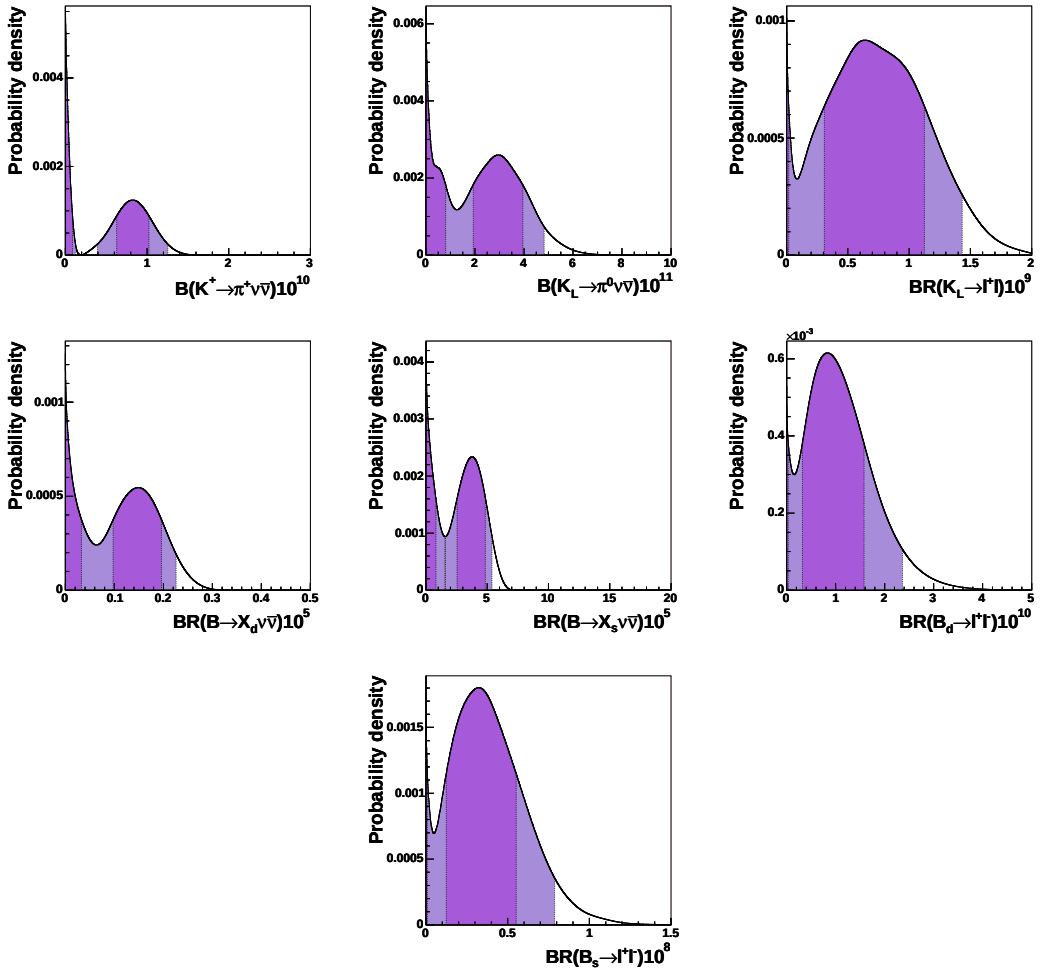

Figure 2.12: *P.d.f.'s for the branching ratios of the rare decays* $Br(K^+ \to \pi^+\nu\bar{\nu})$, $Br(K_{\rm L} \to \pi^0\nu\bar{\nu})$, $Br(K_{\rm L} \to \mu^+\mu^-)_{\rm SD}$, $Br(B \to X_{d,s}\nu\bar{\nu})$, *and* $Br(B_{d,s} \to \mu^+\mu^-)$ *considering only the LOW solution for* $\Delta C_7^{\rm eff}$. *Dark (light) areas correspond to the* 68% *(*95%*) probability region.*

was not used as a constraint.[10] As can be seen from Figure 2.14, the role of $Br(K^+ \to \pi^+\nu\bar{\nu})$ is to suppress the solution with $\Delta C \sim -2$, which corresponds to destructive interference with the SM in $Br(K^+ \to \pi^+\nu\bar{\nu})$ and in the other rare decays. In this respect, a further improvement of the experimental error on $Br(K^+ \to \pi^+\nu\bar{\nu})$ will be extremely useful in further reducing the importance

[10]In order to fully exploit the experimental information on $Br(K^+ \to \pi^+\nu\bar{\nu})$, we use directly the likelihood function obtained by deriving the experimental C The experimental CL can be found at http://www.phy.bnl.gov/e949/E949Archive/br_cls.dat, and the likelihood we use can be found at http://www.utfit.org/kpinunubar/ckm-kpinunubar.html.

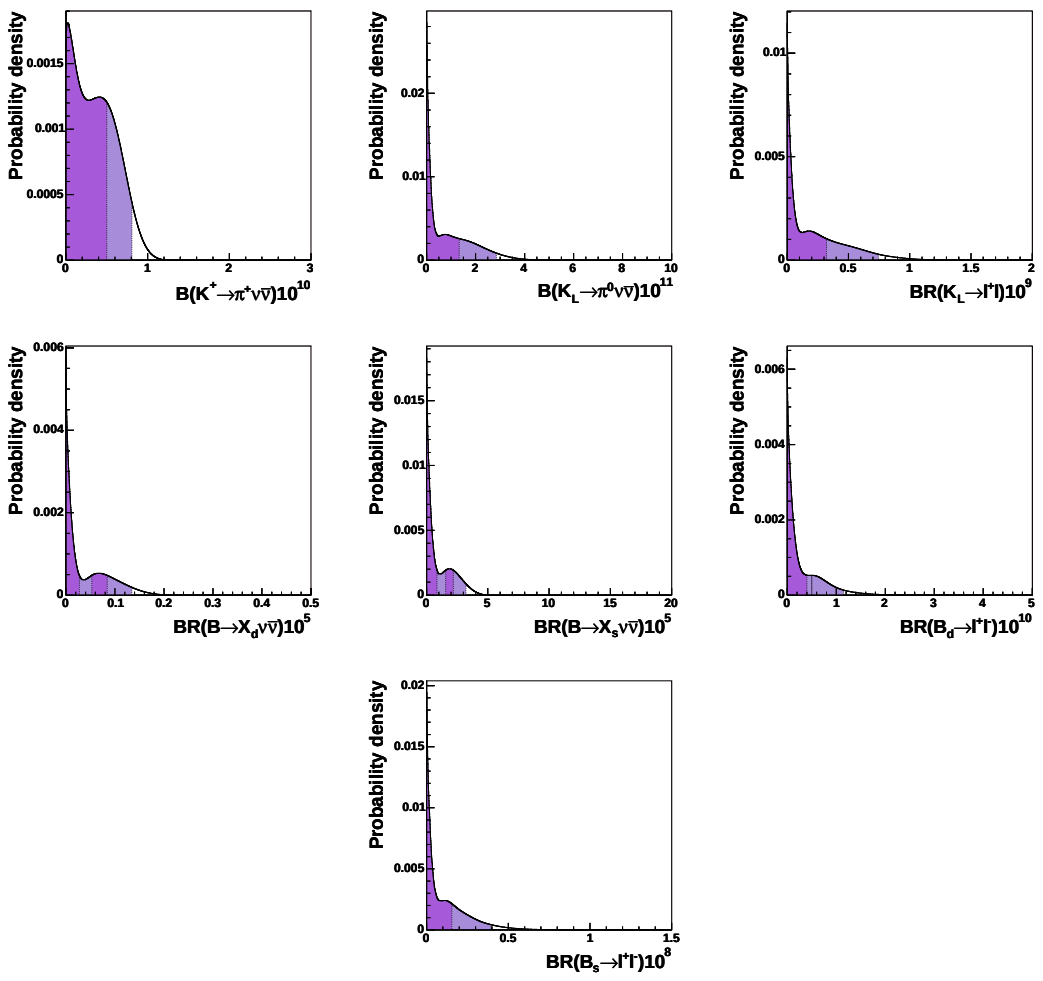

Figure 2.13: *P.d.f.'s for the branching ratios of the rare decays* $Br(K^+ \to \pi^+\nu\bar{\nu})$, $Br(K_{\rm L} \to \pi^0\nu\bar{\nu})$, $Br(K_{\rm L} \to \mu^+\mu^-)_{\rm SD}$, $Br(B \to X_{d,s}\nu\bar{\nu})$, *and* $Br(B_{d,s} \to \mu^+\mu^-)$ *considering only the HI solution for* $\Delta C_7^{\rm eff}$. *Dark (light) areas correspond to the* 68% *(*95%*) probability region.*

of this negative-interference solution for ΔC, which is responsible for the peaks around zero for all the rare decays in Figure 2.9.

We also note that eliminating $\Delta C < 0$ by means of $K^+ \to \pi^+\nu\bar{\nu}$ would basically also eliminate the HI solution for $\Delta C_7^{\rm eff}$. We therefore conclude that finding $Br(K^+ \to \pi^+\nu\bar{\nu})$ larger than the SM value would help in eliminating the positive sign of $C_7^{\rm eff}$. To our knowledge this triple correlation between $K^+ \to \pi^+\nu\bar{\nu}$, $B \to X_s\gamma$ and $B \to X_s l^+ l^-$ has not been discussed in the literature so far. It is very peculiar to MFV and is generally not present in models with new flavour violating contributions.

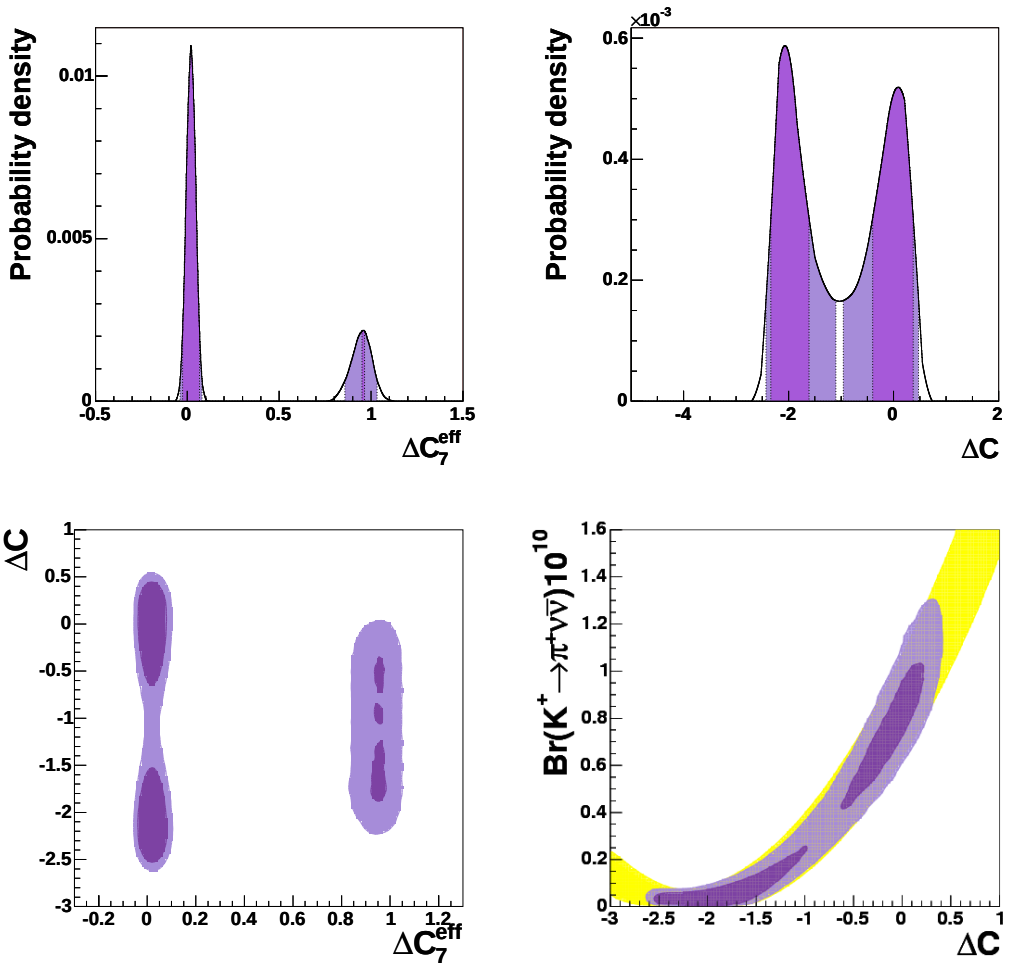

Figure 2.14: *P.d.f.'s for* $\Delta C_7^{\rm eff}$ *(top-left),* ΔC *(top-right),* ΔC *vs.* $\Delta C_7^{\rm eff}$ *(bottom-left) and* $Br(K^+ \to \pi^+ \nu\bar{\nu})$ *vs* ΔC *(bottom-right) obtained without using* $Br(K^+ \to \pi^+ \nu\bar{\nu})$ *as a constraint. Dark (light) areas correspond to the* 68% *(*95%*) probability region.*

The upper bound on $Br(K^+ \to \pi^+ \nu\bar{\nu})$ in Table 2.5 has been obtained using the experimental information on this decay. It corresponds to the following 95% probabilty ranges:

$$\begin{aligned} Br(K^+ \to \pi^+ \nu\bar{\nu}) &= [0, 0.17] \cup [0.24, 1.19] \\ &\quad (\text{LOW}: \ [0, 0.12] \cup [0.39, 1.26], \ \text{HI}: \ [0, 0.81]) \times 10^{-10} \end{aligned} \tag{2.25}$$

If we do not use the experimental result on $Br(K^+ \to \pi^+ \nu\bar{\nu})$, we obtain instead:

$$Br(K^+ \to \pi^+ \nu\bar{\nu}) = [0, 0.15] \cup [0.28, 1.12] \times 10^{-10}\,, \tag{2.26}$$

Function	MFV (68%)	MFV (95%)
X	$[-0.71,-0.55]\cup[0.86,1.90]$	$[-0.86,0.10]\cup[0.30,1.95]$
Y	$[-1.23,-1.06]\cup[0.33,1.37]$	$[-1.38,-0.44]\cup[-0.24,1.43]$
Z	$[-1.51,-1.40]\cup[-0.25,1.31]$	$[-1.74,-1.05]\cup[-0.92,1.46]$

Table 2.6: *Values at* 68% *and* 95% *probability for the functions* X, Y *and* Z. *See the text for details.*

corresponding to an upper bound of 11.2×10^{-11} at 95% probability.

We have also analyzed the decays $K_L\to\pi^0e^+e^-$ and $K_L\to\pi^0\mu^+\mu^-$ using the formulae of [50, 51]. In the models with MFV these decays are dominated by the contribution from the indirect CP violation that is basically fixed by the measured values of ϵ_K and $K_S\to\pi^0l^+l^-$. The dependence on $C(v)$ enters only in the subdominant direct CP-violating component and the interference of indirect and direct CP-violating contributions. We find that $Br(K_L\to\pi^0e^+e^-)$ and $Br(K_L\to\pi^0\mu^+\mu^-)$ can be enhanced with respect to the SM value by at most 8% and 10%, respectively. In view of theoretical uncertainties in these decays that are larger than these enhancements, a clear signal of new physics within the MFV scenario is rather unlikely from the present perspective. Therefore we do not show the corresponding p.d.f.s.

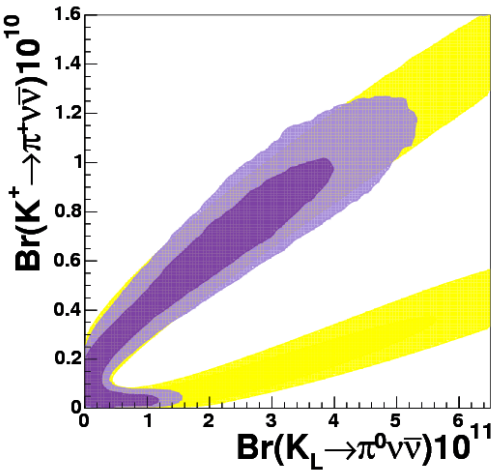

Figure 2.15: *P.d.f. for the branching ratios of the rare decays* $Br(K_{\rm L}\to\pi^0\nu\bar\nu)$ *vs* $Br(K^+\to\pi^+\nu\bar\nu)$. *Dark (light) areas correspond to the* 68% *(*95%*) probability region. Very light areas correspond to the range obtained without using the experimental information.*

Concerning $Br(K_{\rm L}\to\pi^0\nu\bar\nu)$, its 95% probability ranges are given by

$$Br(K_{\rm L}\to\pi^0\nu\bar\nu) \;=\; [0,4.59]\ (\text{LOW}:\ [0,4.83],\ \text{HI}:\ [0,2.84])\times 10^{-11} \qquad (2.27)$$

(see Figures 2.9, 2.12 and 2.13). In Figure 2.15 we see explicitly the correlation between the charged and neutral Kaon decay modes. We observe a very strong correlation, a peculiarity of models with MFV [64]. In particular, a large enhancement of $Br(K_{\rm L}\to\pi^0\nu\bar\nu)$ characteristic of models with new complex phases is not possible [65, 66]. An observation of $Br(K_{\rm L}\to\pi^0\nu\bar\nu)$ larger than $6\cdot 10^{-11}$ would be a clear signal of new complex phases or new flavour changing contributions that violate the correlations between B and K decays.

The 95% probability ranges for $Br(K_{\rm L}\to\mu^+\mu^-)_{\rm SD}$ are

$$Br(K_{\rm L}\to\mu^+\mu^-)_{\rm SD} \;=\; [0,1.36]\ (\text{LOW}:\ [0,1.44],\ \text{HI}:\ [0,0.74])\times 10^{-9} \qquad (2.28)$$

As in the previous cases, the HI solution corresponds to a much lower upper bound.

Let us now consider B decays:

$$\begin{aligned}
Br(B\to X_s\nu\bar\nu) &= [0,5.17]\ (\text{LOW}:\ [0,1.56]\cup[1.59,5.4],\ \text{HI}:\ [0,3.22])\times 10^{-5}\,,\\
Br(B\to X_d\nu\bar\nu) &= [0,2.17]\ (\text{LOW}:\ [0,2.26],\ \text{HI}:\ [0,1.34])\times 10^{-6}\,,\\
Br(B_s\to\mu\bar\mu) &= [0,7.42]\ (\text{LOW}:\ [0,7.91],\ \text{HI}:\ [0,3.94])\times 10^{-9}\,,\\
Br(B_d\to\mu\bar\mu) &= [0,2.20]\ (\text{LOW}:\ [0,2.37],\ \text{HI}:\ [0,1.15])\times 10^{-10}\,. \qquad (2.29)
\end{aligned}$$

The reader may wonder whether other observables could help improving the constraints on ΔC and testing MFV models. In particular, the Forward-Backward asymmetry in $B\to X_s l^+l^-$ is known to be a very sensitive probe of $C_7^{\rm eff}$ and of C [67]. Indeed, the HI and LOW solutions for $\Delta C_7^{\rm eff}$ and corresponding possible values of ΔC give rise to different profiles of the normalized $\bar A_{\rm FB}$, defined as

$$\bar A_{\rm FB}(\hat s)=\frac{\int_{-1}^{1} d\cos\theta_l \frac{d^2\Gamma(b\to s\mu^+\mu^-)}{d\hat s\, d\cos\theta_l}\,\mathrm{sgn}(\cos\theta_l)}{\int_{-1}^{1} d\cos\theta_l \frac{d^2\Gamma(b\to s\mu^+\mu^-)}{d\hat s\, d\cos\theta_l}}\,. \qquad (2.30)$$

This can be seen explicitly in Figure 2.16. Therefore, a measurement of $\bar A_{\rm FB}(\hat s)$ at a Super B factory will be extremely helpful in distinguishing the various scenarios discussed above [68]. On the other hand, concerning the CP asymmetry in $B\to X_s\gamma$ decays [69], it turns out that in MFV models its value is reduced with respect to the SM, once the constraint on the branching ratio is taken into account, so that it is not expected to play a significant role in present and future analyses [70].

In Figure 2.12 we show the p.d.f.'s for the branching ratios of rare decays for the LOW solution. The corresponding result for the HI solution is given in Figure 2.13. Clearly the branching ratios of various decays are larger in the case of the LOW solution.

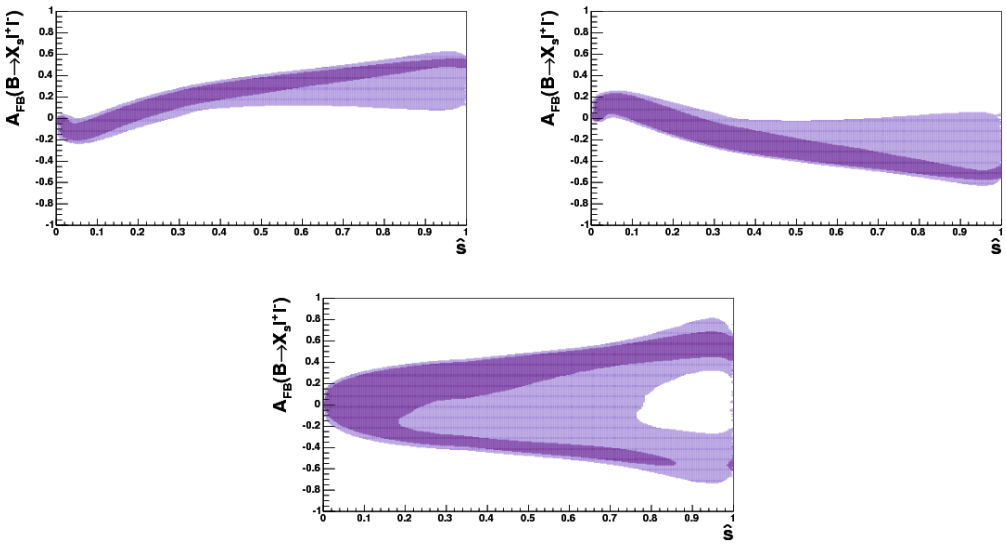

Figure 2.16: *P.d.f.'s for the normalized forward-backward asymmetry in* $B \to X_s l^+ l^-$ *for the LOW solution for* $\Delta C_7^{\rm eff}$ *with* $\Delta C > -1$ *(left), for the LOW solution with* $\Delta C < -1$ *(center) and for the HI solution for* $\Delta C_7^{\rm eff}$ *(right). Dark (light) areas correspond to the* 68% *(*95%*) probability region.*

Before concluding this section, let us make a few steps towards the future and consider a realistic scenario for the projected integrated luminosities of Belle and BaBar, plus a 10% measurement of $Br(K^+ \to \pi^+ \nu\bar{\nu})$. For concreteness, let us assume the following 2010 experimental data:

$$
\begin{aligned}
Br(B \to X_s l^+ l^-)_{0.04<q^2({\rm GeV})<1} &= (1.13 \pm 0.25) \times 10^{-6}\,, \\
Br(B \to X_s l^+ l^-)_{1<q^2({\rm GeV})<6} &= \begin{cases} (1.49 \pm 0.21) \times 10^{-6} ({\rm Belle}) \\ (1.80 \pm 0.18) \times 10^{-6} ({\rm BaBar}) \end{cases} \\
Br(B \to X_s l^+ l^-)_{14.4<q^2({\rm GeV})<25} &= \begin{cases} (4.18 \pm 0.48) \times 10^{-7} ({\rm Belle}) \\ (5.00 \pm 0.93) \times 10^{-7} ({\rm BaBar}) \end{cases} \\
Br(B \to X_s \gamma) &= \begin{cases} (3.51 \pm 0.16) \times 10^{-4} ({\rm Belle}) \\ (3.67 \pm 0.16) \times 10^{-4} ({\rm BaBar\ incl.}) \\ (3.29 \pm 0.16) \times 10^{-4} ({\rm BaBar\ semincl.}) \end{cases} \quad (2.31)
\end{aligned}
$$

corresponding to an integrated luminosity of 1 ab^{-1} and 700 fb^{-1} for Belle and BaBar, respectively. Additionally a reduction to 5% of the theoretical uncertainty in $Br(B \to X_s \gamma)$ thanks to a complete NNLO computation is assumed [71]. [11]

We can see the dramatic effect of these improvements in Figures 2.17-2.19. B-factory data will completely eliminate the non-standard solution for $\Delta C_7^{\rm eff}$,

[11] The future results for $Br(B \to X_s \gamma)$ are referred to the same kinematic ranges as the present results.

while they cannot distinguish the two solutions for ΔC (considering only branching ratio measurements), see Figure 2.19. However, this ambiguity is perfectly resolved by $Br(K^+ \to \pi^+ \nu\bar{\nu})$, leading to the impressive results in Figures 2.17 and 2.18.

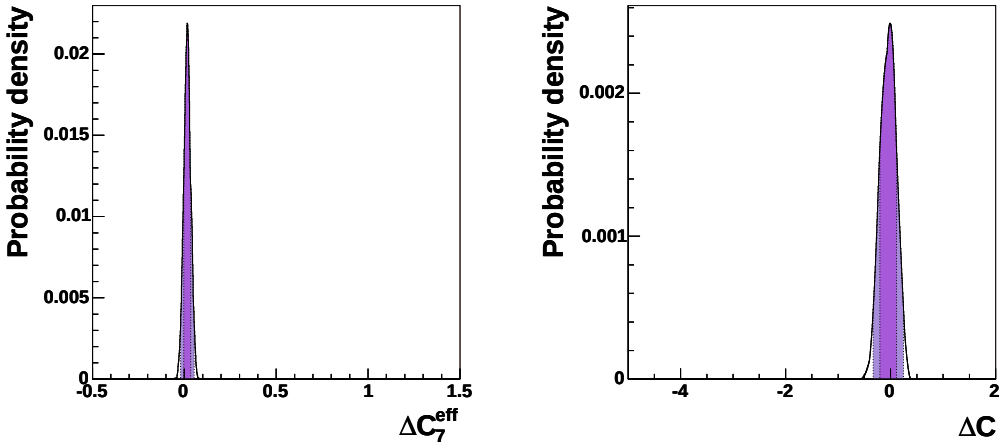

Figure 2.17: *P.d.f.'s for $\Delta C_7^{\rm eff}$ (left) and ΔC (right) in the future scenario specified by eq. (2.31). Dark (light) areas correspond to the 68% (95%) probability region.*

With so powerful experimental data, one can even think of generalizing our analysis by allowing for substantial deviations from the SM in box diagrams. If the size of new physics contributions to box diagrams is comparable to the SM ones, the results of our "future" analysis would not change sizably. On the other hand, a dramatic modification could occur for contributions to box diagrams much larger than the SM ones; however, it is very difficult to conceive new-physics models in which this possibility can be realized.

2.4.3 Messages

The main message here is the following one:

The existing constraints coming from $K^+ \to \pi^+ \nu\bar{\nu}$, $B \to X_s\gamma$ and $B \to X_s l^+ l^-$ do not allow within the MFV scenario of [10] for substantial departures of the branching ratios for all rare K and B decays from the SM estimates. This is evident from Table 2.5.

There are other messages signalled by our analysis. These are:

- The decays $B \to X_{s,d} l^+ l^-$ will not offer a precise value for the function C even in the presence of precise measurements of their branching ratios,

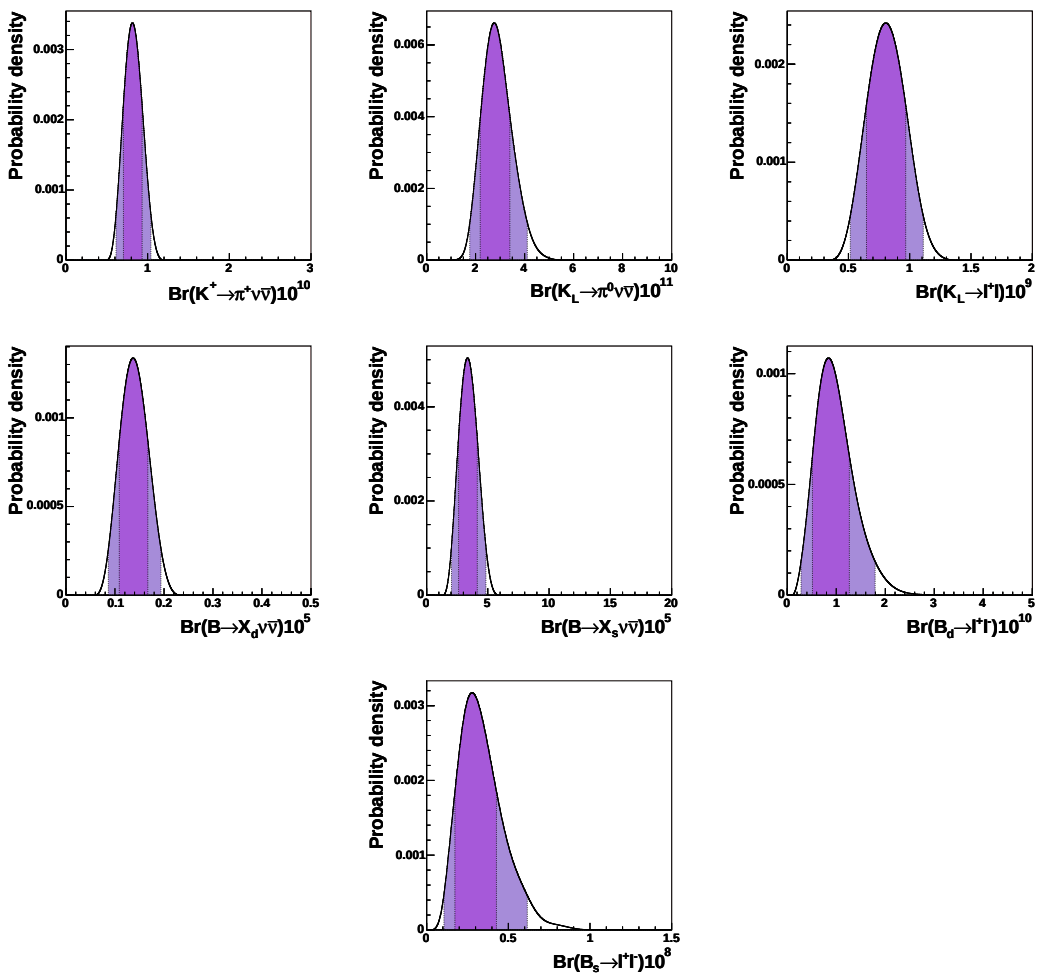

Figure 2.18: *P.d.f.'s for the branching ratios of the rare decays* $Br(K^+ \to \pi^+\nu\bar{\nu})$, $Br(K_{\rm L} \to \pi^0\nu\bar{\nu})$, $Br(K_{\rm L} \to \mu^+\mu^-)_{\rm SD}$, $Br(B \to X_{d,s}\nu\bar{\nu})$, *and* $Br(B_{d,s} \to \mu^+\mu^-)$ *in the future scenario specified by eq. (2.31). Dark (light) areas correspond to the* 68% *(*95%*) probability region.*

unless the theoretical errors in these decays and $B \to X_s\gamma$ and the experimental error on the branching ratio of the latter decay are reduced substantially. This is clearly seen in Figure 2.10.

- The situation is considerably better in the case of $B_{d,s} \to \mu^+\mu^-$ but as seen in Figure 2.11, for a given value of $Br(B_{d,s} \to \mu^+\mu^-)$ there are generally two solutions for ΔC and C, that cannot be disentangled on the basis of these decays alone.

- The great potential of the decays $K^+ \to \pi^+\nu\bar{\nu}$ and $K_L \to \pi^0\nu\bar{\nu}$ in measuring

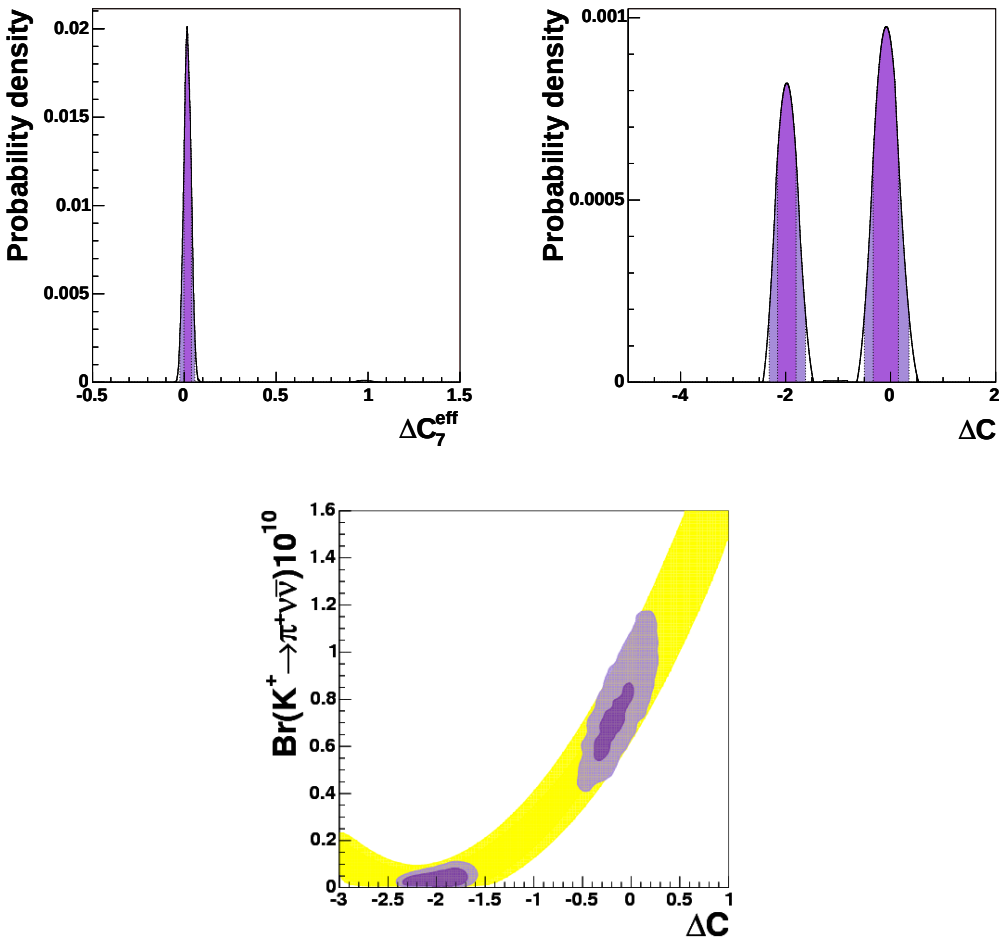

Figure 2.19: *P.d.f.'s for* $\Delta C_7^{\rm eff}$ *(top-left),* ΔC *(top-right) and* $Br(K^+ \to \pi^+ \nu\bar{\nu})$ *vs* ΔC *(bottom) obtained without using* $Br(K^+ \to \pi^+ \nu\bar{\nu})$ *as a constraint, in the future scenario specified by eq. (2.31). Dark (light) areas correspond to the* 68% *(*95%*) probability region.*

the function C is clearly visible in Figures 2.10 and 2.11, with the unique value obtained in the case of $K^+ \to \pi^+ \nu\bar{\nu}$ in the full allowed range of C. In the case of $K_L \to \pi^0 \nu\bar{\nu}$ the two solutions are only present for $Br(K_L \to \pi^0 \nu\bar{\nu})$ significant smaller that the SM value. Similar comment applies to $B \to X_{s,d} \nu\bar{\nu}$.

- Assuming that future more precise measurements of the $K \to \pi\nu\bar{\nu}$ branching ratios will be consistent with the MFV upper bounds presented here, the determination of C through these decays will imply much sharper predictions for various branching ratios that could confirm or rule out the MFV

scenario. In this context the correlations between various branching ratios discussed in [11] will play the crucial role.

- One of such correlations predicts that the measurement of $\sin 2\beta$ and of $Br(K^+ \to \pi^+\nu\bar{\nu})$ implies only two values of $Br(K_L \to \pi^0\nu\bar{\nu})$ in the full class of MFV models that correspond to two signs of the function X [64]. Figure 2.15 demonstrates that the solution with $X < 0$, corresponding to the values in the left lower corner, is practically ruled out so that a unique prediction for $Br(K_L \to \pi^0\nu\bar{\nu})$ can in the future be obtained.

- A strong violation of any of the 95% probability upper bounds on the branching ratios considered here by future measurements will imply a failure of MFV as defined in [10], unless an explicit MFV scenario can be found in which the contributions of box diagrams are significantly larger than assumed here. Dimensional arguments [65] and explicit calculations indicate that such a possibility is rather remote.

- If the only violation of the upper bounds in Table 2.5 occurs in $B_s \to \mu^+\mu^-$ and $B_d \to \mu^+\mu^-$, it will be most likely due to new operators beyond the SM ones. For example, the scalar operators which arise in MFV SUSY models at large $\tan\beta$ can enhance $Br(B_s \to \mu^+\mu^-)$ up to the present experimental upper bound [17, 20, 72].

- Conversely, a violation of the upper bounds for the other channels in Table 2.5 would signal the presence of new sources of flavour and in particular of CP violation. This can be confirmed observing a violation of the correlations between K and B decays discussed above.

- In particular, recalling that in most extensions of the SM the decays $K \to \pi\nu\bar{\nu}$ are governed by the single $(V-A)\otimes(V-A)$ operator, the violation of the upper bounds on at least one of the $K \to \pi\nu\bar{\nu}$ branching ratios, will either signal the presence of new complex weak phases at work or new contributions that violate the correlations between the B decays and K decays.

Assuming that the MFV scenario will survive future tests, the next step will be to identify the correct model in this class. Clearly, direct searches at high energy colliders can rule out or identify specific extensions of the SM. But also FCNC processes can play an important role in this context, provided the theoretical and experimental uncertainties in some of them will be sufficiently decreased. In this case, by studying simultaneously several branching ratios it should be in principle possible to select the correct MFV models by just identifying the pattern of enhancements and suppressions relative to the SM that is specific to a given model. If this pattern is independent of the values of the parameters defining the model, no detailed quantitative analysis of the enhancements and suppressions

is required in order to rule it out. As an example the distinction between the MSSM with MFV and the models with one universal extra dimension should be straightforward:

- In the MSSM with MFV the branching ratios for $K^+ \to \pi^+\nu\bar{\nu}$, $K_{\rm L} \to \pi^0\nu\bar{\nu}$, $B \to X_d\nu\bar{\nu}$ and $B_d \to \mu^+\mu^-$ are generally suppressed relative to the SM expectations, while those governed by V_{ts} like $B \to X_s\nu\bar{\nu}$, $B_s \to \mu^+\mu^-$ and $B \to X_s\gamma$ can be enhanced or suppressed depending on the values of parameters involved [73].

- In the model with one universal extra dimension discussed in Section 2.3, the branching ratios for essentially all rare decays are enhanced, the enhancement being stronger for the decays governed by V_{ts} than for those where V_{td} is involved. A prominent exception is the suppression of $B \to X_{s,d}\gamma$ [13, 74].

Finally, if MFV will be confirmed, and some new particles will be observed, the rare processes discussed in this work will constitute a most powerful tool to probe the spectrum of the NP model, which might not be entirely accessible via direct studies at the LHC.

Chapter 3

Minimal Flavour Violation in the lepton sector

3.1 Motivation

In the previous chapters we have encountered the framework of MFV applied to the quark sector. It proved to be a solution to the quark flavour problem: all new physics models which implement this idea are in a good shape and avoid fine-tuning in the flavour sector. At the same time these models can maintain a relatively low new physics scale at around a TeV. This is important if we want to stabilize the Higgs sector in a natural way (as in the MFV-MSSM or in little Higgs theories) and if these models are to be tested at the LHC.

If MFV really is nature's answer to the flavour problem in the quark sector two questions naturally arise:

- Can we extend the MFV framework to describe lepton flavour violation?
- MFV implies that the only CPV phase in the quark sector is the CKM phase, which is not enough CPV in order to generate the baryon asymmetry of the universe (BAU) via electroweak baryogenesis (see e.g. the review [75]), extending MFV to the lepton sector, can we generate the BAU using the mechanism of leptogenesis implemented in a MFV framework?

The following chapter tries to answer these two questions. The first drawback we find is, that we cannot extend the MFV framework in a straightforward way by just replacing Y_U by Y_ν and repeating the construction. The reason is that the best explanation for the smallness of the observed neutrino masses is the so called see-saw mechanism, which complicates matters as we shall see. Extending the SM to include right-handed neutrinos, their quantum numbers tell us, that they are sterile. Nothing prevents us to include a Majorana mass term for them. Contrary to a Dirac or Yukawa mass term, no chiral symmetry or Higgs-vev, respectively, sets the natural scale. This possibly large scale, the so-called see-saw

scale, in turn leads to an elegant explanation of the smallness of the observed neutrino masses: after integrating out the heavy neutrinos the effective mass of the light neutrinos is suppressed by this large scale and of the order of v^2/M_ν. The Majorana mass term is only a mixed blessing in that it generically introduces new flavour violation at a high-scale. An attempt to extend MFV to the lepton sector and to deal with this problem has first been given by [76]. In the following chapters[1] we will first introduce MFV in the lepton sector (MLFV) and describe its basic assumptions and parameters. We will then discuss two specific realisations. Then we will discuss radiative corrections and their implications for the low-scale flavour violation and the see-saw scale CPV relevant for leptogenesis. Finally we will discuss leptogenesis and possible implications for lepton FCNC.

3.2 Basic Framework

3.2.1 Preliminaries

The discovery of neutrino oscillations provides evidence for non-vanishing neutrino masses and leptonic mixing, leading to lepton-flavour violation. In the SM, neutrinos are strictly massless, since Dirac masses cannot be constructed due to the absence of right-handed neutrinos, and left-handed Majorana masses are not generated due to exact $(B - L)$ conservation.

The simplest extension of the SM which allows for non-vanishing but naturally small neutrino masses, consists of the addition of right-handed neutrinos to the spectrum of the SM. This extension has the nice feature of establishing on the one hand a lepton quark symmetry and on the other hand being naturally embedded in a grand unified theory like $SO(10)$. Since right-handed neutrinos are singlets under $U(1) \times SU(2) \times SU(3)$, Majorana neutrino masses M_R should be included, with a mass scale M_ν which can be much larger than the scale v of the electroweak symmetry breaking. Apart from M_R, Dirac neutrino mass terms m_D are generated through leptonic Yukawa couplings upon gauge symmetry breaking. The presence of these two neutrino mass terms leads, through the seesaw mechanism [78], to three light neutrinos with masses of order v^2/M_ν and three heavy neutrinos with mass of order M_ν. The decay of these heavy neutrinos can play a crucial role in the creation of a baryon asymmetry of the universe (BAU) through the elegant mechanism of baryogenesis through leptogenesis [79, 80]. In the presence of neutrino masses and mixing, one has, in general, both CP violation at low energies which can be detected through neutrino oscillations and CP violation at high energies which is an essential ingredient of leptogenesis. The connection between these two manifestations of CP violation can be established in the framework of specific lepton flavour models.

[1] This chapter is based on our paper [77].

In this chapter, we study lepton-flavour violation in this extension of the SM, assuming minimal lepton flavour violation (MLFV) but allowing for CP violation both at low and high energies. The case of no leptonic CP violation either at low or high energies, was considered in [76] where the suggestion of MLFV was first presented.

3.2.2 Yukawa Couplings and Majorana Mass Terms

We add then three right-handed neutrinos to the spectrum of the SM and consider the following leptonic Yukawa couplings and right-handed Majorana mass terms:

$$\mathcal{L}_Y = -\bar{e}_R Y_E \phi^\dagger L_L - \bar{\nu}_R Y_\nu \tilde{\phi} L_L + h.c. \tag{3.1}$$

$$\mathcal{L}_M = -\frac{1}{2}\bar{\nu}_R^c M_R \nu_R + h.c.\ , \tag{3.2}$$

where Y_E, Y_ν and M_R are 3×3 matrices in the lepton flavour space. In the limit $\mathcal{L}_Y = \mathcal{L}_M = 0$ the Lagrangian of this minimal extension of the SM has a large flavour symmetry

$$SU(3)_L \times SU(3)_E \times SU(3)_{\nu_R} \times U(1)_L \times U(1)_E \times U(1)_{\nu_R}, \tag{3.3}$$

which reflects the fact that gauge interactions treat all flavours on equal footing. This large global symmetry is broken by the Yukawa couplings Y_E, Y_ν and by the Majorana mass terms M_R. A transformation of the lepton fields:

$$L_L \to V_L L_L, \quad e_R \to V_E e_R, \quad \nu_R \to V_{\nu_R} \nu_R \tag{3.4}$$

leaves the full Lagrangian invariant, provided the Yukawa couplings and the Majorana mass terms transform as:

$$Y_\nu \ \to \ Y_\nu^{'} = V_{\nu_R} Y_\nu V_L^\dagger, \tag{3.5}$$
$$Y_E \ \to \ Y_E^{'} = V_E Y_E V_L^\dagger, \tag{3.6}$$
$$M_R \ \to \ M_R^{'} = V_{\nu_R}^* M_R V_{\nu_R}^T, \tag{3.7}$$

which means that there is a large equivalent class of Yukawa coupling matrices and Majorana mass terms, related through (3.5)-(3.7), which have the same physical content. The MLFV proposal [76] consists of the assumption that the physics which generates lepton number violation, leading to M_R, is lepton flavour blind, thus leading to an exactly degenerate eigenvalue spectrum for M_R, at a high-energy scale. As a result, in the MLFV framework, the Majorana mass terms break $SU(3)_{\nu_R}$ into $O(3)_{\nu_R}$.

3.2.3 An Useful Parametrisation

In order to analyse in a systematic way the above phenomena and study the implied relations among low-energy lepton mixing data, lepton flavour violation and leptogenesis in different scenarios classified below, it is convenient to choose an appropriate parametrisation for Y_ν. Since we are working in the basis where the charged lepton mass matrix is diagonal and real, leptonic mixing and CP violation at low energies are controlled by the PMNS matrix U_ν [81], which diagonalizes the effective low energy neutrino mass matrix:

$$U_\nu^T (m_\nu)_{eff} U_\nu = d_\nu, \tag{3.8}$$

where $d_\nu \equiv \mathrm{diag}(m_1, m_2, m_3)$, with m_i being the masses of the light neutrinos and [78]

$$(m_\nu)_{eff} = -v^2 Y_\nu^T D_R^{-1} Y_\nu, \tag{3.9}$$

where D_R denotes the diagonal matrix M_R and $v = 174$ GeV. In the case of MLFV, $D_R = M_\nu \mathbb{1}$ and one obtains at $M_\nu \approx \Lambda_{\rm LN}$

$$(m_\nu)_{eff} = -\frac{v^2}{M_\nu} Y_\nu^T Y_\nu. \tag{3.10}$$

We use the following parametrisation [82] of the neutrino Yukawa couplings:

$$(\sqrt{D_R})^{-1}\, Y_\nu = \frac{i}{v}\, R\, \sqrt{d_\nu}\, U_\nu^\dagger, \tag{3.11}$$

where R is an orthogonal complex matrix ($R^T R = R\, R^T = \mathbb{1}$), $d_\nu = \mathrm{diag}(m_1, m_2, m_3)$ and $D_R = \mathrm{diag}(M_1, M_2, M_3)$.

It is instructive to count next the number of independent parameters on both sides of (3.11). The left-hand side of (3.11) is an arbitrary 3×3 complex matrix with nine real parameters and six phases, since three of the initial nine phases can be removed by rephasing L_L. It is clear that the right-hand side of (3.11) also has nine real parameters and six phases. Indeed, R, d_ν and U_ν have each three real parameters and moreover R and U_ν have in addition each three phases. We consider now the case where the right-handed neutrinos are exactly degenerate, i.e. $D_R = M_\nu \mathbb{1}$. We will show that three of the real parameters of R can be rotated away. Note that any complex orthogonal matrix can be parameterised as

$$R = e^{A_1} e^{iA_2}, \tag{3.12}$$

with $A_{1,2}$ real and skew symmetric. Now in the degenerate case an orthogonal rotation of $\nu_R \to O_R \nu_R$ leaves the Majorana mass proportional to the unit matrix and defines a physically equivalent reparametrization of the fields ν_R. Choosing $O_R = e^{A_1}$ we see immediately that

$$Y_\nu \to O_R^\dagger Y_\nu = \frac{\sqrt{M_\nu}}{v}\, e^{-A_1}\, R\, \sqrt{d_\nu}\, U_\nu^\dagger = \frac{\sqrt{M_\nu}}{v}\, e^{iA_2}\, \sqrt{d_\nu}\, U_\nu^\dagger, \tag{3.13}$$

which shows that the physically relevant parameterization is given by $R_{deg} = e^{iA_2}$.

Using the parameterization in (3.11) one finds that the matrix $Y_\nu^T Y_\nu$ which controls low-energy CP-Violation and mixing can be written as follows

$$Y_\nu^T Y_\nu = -\frac{1}{v^2} (U_\nu^\dagger)^T \sqrt{d_\nu}\, R^{\mathrm{T}}\, D_R\, R \sqrt{d_\nu}\, U_\nu^\dagger = -\frac{M_\nu}{v^2} (U_\nu^\dagger)^T d_\nu U_\nu^\dagger, \tag{3.14}$$

where in the last step we have set $D_R = M_\nu \mathbb{1}$.

On the other hand, the matrix $Y_\nu^\dagger Y_\nu$ which controls charged LFV, can be written as follows (see also [83])

$$Y_\nu^\dagger Y_\nu = \frac{1}{v^2}\, U_\nu \sqrt{d_\nu}\, R^\dagger\, D_R\, R \sqrt{d_\nu}\, U_\nu^\dagger = \frac{M_\nu}{v^2}\, U_\nu \sqrt{d_\nu}\, R^\dagger R \sqrt{d_\nu}\, U_\nu^\dagger\,. \tag{3.15}$$

Finally, the matrix $Y_\nu Y_\nu^\dagger$ which enters in leptogenesis when flavor effects are not relevant is given by (see also [83]):

$$Y_\nu Y_\nu^\dagger = \frac{1}{v^2} \sqrt{D_R}\, R\, d_\nu\, R^\dagger \sqrt{D_R} = \frac{M_\nu}{v^2}\, R\, d_\nu\, R^\dagger. \tag{3.16}$$

We note that $Y_\nu^T Y_\nu$ depends only on U_ν and d_ν, while $Y_\nu Y_\nu^\dagger$ relevant for the leptogenesis only on d_ν and R. This means that CP violation at low energy originating in the complex U_ν and the CP violation relevant for leptogenesis are decoupled from each other and only the mass spectrum of light neutrinos summarized by d_ν enters both phenomena in a universal way. Here we would like to emphasize that within the RRL this common wisdom has to be modified as through RGE $Y_\nu Y_\nu^\dagger$ at $\mu = M_\nu$ will eventually depend on the elements of the PMNS matrix, in particular on its complex phase. In this manner some correlation between low and high energy CP violation could in principle be possible.

In this respect the charged LFV, represented by (3.15), appears also interesting as it depends on d_ν, U_ν and R and consequently can also provide an indirect link between low energy and high energy CP violations and generally a link between low and high energy phenomena.

3.3 Radiative corrections in MLFV

3.3.1 Preliminaries

Our MLFV scenario defined in the previous section contains no free parameters beyond the neutrino masses, the PMNS matrix, a matrix of form R_{deg}, an initial, universal heavy Majorana neutrino mass, and perhaps additional flavour-blind parameters that depend on the MLFV model. The rates for charged lepton flavour violation thus follow upon computing radiative corrections due to the degrees of freedom between the scales M_Z and Λ_{GUT}, and with suitable washout factors also the baryon asymmetry η_B.

In this section we investigate how the CP- and flavour-violating quantities relevant to leptogenesis and charged lepton flavour violation, respectively, are radiatively generated. Since leptogenesis in the present framework can be considered as a generalization of the setup with two heavy singlets in [84] to the case of three degenerate flavours, we will also clarify what novelties arise in this case. This will be important in comparing our results to the existing literature.

An important point will be that, due to the hierarchy between the GUT/flavour-breaking scale $\mathbf{\Lambda_{GUT}}$ and the neutrino mass scale M_ν, large logarithms appear such that the parameter counting for the coefficients c_i of flavour structures that has been recently presented in [85] should be modified. Rather than being independent, the coefficients of structures containing different powers of Yukawa matrices are related by the renormalization group, while any additional independent effects are suppressed. Although this fact in principle increases the predictivity of MLFV, in our phenomenological sections it will still turn out insufficient to have correlations between high-scale and weak-scale observables.

3.3.2 MLFV with a degeneracy scale

We have defined our MLFV scenario to have a scale at which the masses of the right-handed neutrinos are exactly degenerate, such that the matrix M_R has no flavour structure at all. In general, there will be additional flavoured particles in the theory. As a specific example, we consider the MSSM. Here the N_i are accompanied by heavy sneutrinos $\tilde{N}_i^c$, and there are also SU(2) doublet sleptons $\tilde{l}_i$, transforming as

$$\tilde{l} \to V_L \tilde{l}, \qquad \tilde{N}^c \to V_{\nu_R}^* \tilde{N}^c \tag{3.17}$$

under the transformation (3.4). The Lagrangian then contains soft SUSY breaking terms

$$\mathcal{L}_{soft} = -\tilde{N}_i^{c*} \tilde{m}^2_{\nu ij} \tilde{N}_j^c - \tilde{l}_i^* \tilde{m}^2_{lij} \tilde{l}_j + \ldots, \tag{3.18}$$

where the ellipsis denotes further scalar mass matrices and trilinear scalar interactions. In general all matrices in $\mathcal{L}_{soft}$ have nonminimal flavour structure. The simplest generalization of our degenerate scenario is then to extend the requirement of exact degeneracy to all mass matrices, similar to minimal supergravity. To be specific, we require all scalar masses to have the same value m_0 at the high scale and also require the A-terms to have the mSUGRA form $A = aY$ with Y the corresponding Yukawa matrix and a a universal, real parameter of the theory. This example also provides us with a concrete value for the scale $\Lambda_{\rm LFV}$: LFV processes such as $l_i \to l_j \gamma$ are mediated by loop diagrams involving sleptons and higgsinos or (weak) gauginos, and unless gaugino masses are very large, the scalar particles such as $\tilde{l}_i$ decouple at a scale $\Lambda \sim m_0$. Hence the operators governing charged LFV are suppressed by powers of $m_0 \equiv \Lambda_{\rm LFV}$. As in the case of the heavy Majorana masses, the generalized degeneracy requirement is not sta-

ble under radiative corrections, and for the same reason it is not renormalization scheme independent.

3.3.3 Radiatively generated flavour structure and large logarithms

As will be discussed in detail in the following section, the CP asymmetries necessary for leptogenesis require mass splittings between the decaying particles. The decaying particles are on their mass shell[2], but the degenerate initial conditions are usually specified in a massless scheme[3] ($\overline{\text{MS}}$ to be definite [89]).

At one loop, the two mass definitions are related by a formula of the structure

$$M_i^{os} = M_i^{\overline{\text{MS}}}(\mu) + c_i M_i^{\overline{\text{MS}}}(\mu) \ln \frac{M_i}{\mu} + \text{nonlogarithmic corrections}, \tag{3.19}$$

where $\mu \sim \Lambda_{\text{GUT}}$ is the $\overline{\text{MS}}$ renormalization scale, $c_i = 2(Y_\nu Y_\nu^\dagger)_{ii}/(16\pi^2)$ in the standard-model seesaw, and the nonlogarithmic corrections depend on our choice of massless (or any other) renormalization scheme. The resulting scheme dependence cannot be present in physical observables such as the BAU. Since this issue is usually not discussed in the literature on lepton flavour violation, let us elaborate on how it may be resolved.

First, notice that while the nonlogarithmic terms in (3.19) are scheme dependent, the logarithmic corrections proportional to c_i are actually scheme independent. If $\ln \Lambda_{\text{GUT}}/M_\nu \gg 1$, the logarithmic terms must be considered $\mathcal{O}(1)$ and summed to all orders. This is achieved in practice by solving renormalization group equations. Similar resummations must be performed for all other parameters in the theory (such as Yukawa couplings). Correspondingly, the dominant higher-loop corrections to LFV observables and leptogenesis are approximated by using leading-order expressions with one-loop RGE-improved Yukawa couplings and masses. This is the leading-logarithmic approximation. Nonlogarithmic corrections such as those indicated in (3.19) are then subleading and should be dropped.

What happens when the logarithms are not large is the following. If the MLFV framework is an effective theory for some fundamental theory where the degeneracy is enforced by a flavour symmetry, for instance the group (3.3), then the degeneracy holds in *any* scheme (that respects the symmetry) in the full theory and the scheme dependence observed in (3.19) must be due to unknown threshold corrections in matching the underlying and effective theories. Since the flavour symmetry in MLFV, by definition, is broken precisely by the Yukawa

[2] We follow the treatment of [86, 87] (see also [88]), where sometimes the on-shell masses are replaced by thermal masses. (We will employ zero-temperature masses.)

[3] This is likely appropriate if the degeneracy is true to some flavour symmetry of an underlying theory, relating high-energy Lagrangian parameters and broken at the scale Λ_{GUT}.

matrices, this matching introduces all possible terms that are invariant under transformations (3.4,3.5,3.6,3.7). A list of such structures has recently been given in [85], for instance,

$$M_R = M_\nu \Big[1 + c_1 (Y_\nu Y_\nu^\dagger + (Y_\nu Y_\nu^\dagger)^T) + c_2 (Y_\nu Y_\nu^\dagger Y_\nu Y_\nu^\dagger + (Y_\nu Y_\nu^\dagger Y_\nu Y_\nu^\dagger)^T) + \dots \Big]. \quad (3.20)$$

The coefficients c_1 and c_2 have been claimed by these authors to be independent $\mathcal{O}(1)$ coefficients. Indeed these terms contain only nonlogarithmic terms and (small) decoupling logs when M_R is taken in the $\overline{\rm MS}$ scheme, renormalized near the GUT (matching) scale.

However, when computing the (physically relevant) on-shell M_R in the case of $\Lambda_{\rm GUT} \gg M_\nu$, large logarithms dominate both c_1 and c_2. The leading logarithmic contributions are not independent, but are related by the renormalization group. c_2 is quadratic in $L \equiv \ln \Lambda_{\rm GUT}/M_\nu$, while c_1 is linear, and the RGE for M_R implies $c_2|_{L^2} = \frac{1}{2}[c_1|_L]^2$. These logs are summed by RG-evolving $M_R^{\overline{\rm MS}}$ to a scale $\mu \sim M_\nu$. The additional conversion to on-shell masses is then again a subleading correction.

Finally, we note that if there is no underlying symmetry, the degeneracy condition can again be true at most for special choices of scheme/scale, and must be fine-tuned.

Numerically, the logarithms dominate already for mild hierarchies $\Lambda_{\rm GUT}/M_\nu > 10^2$, as then $2 \ln \Lambda_{\rm GUT}/M_\nu \approx 10$. Let us now restrict ourselves to hierarchies of at least two orders of magnitude and work consistently in the leading-logarithmic approximation. As explained above, in this case nonlogarithmic corrections both of the threshold type (in the coefficients c_i in (3.20) and in physical quantities (on-shell masses, CP asymmetries, etc.) are subleading and should be dropped. In this regard our apparently "special" framework of initially degenerate heavy neutrinos turns out to be the correct choice at leading-logarithmic order.

Finally we recall that the positions of the poles of the N_i two-point functions contain an imaginary part related to the widths of these particles. While not logarithmically enhanced, these are also scheme-independent at one loop (as the widths are physical), and it is unambiguous to include them in applications. In fact, these widths effects are often numerically important for the CP asymmetries in N_i decay [86, 87], and we will keep them in our numerical analysis.

3.3.4 Renormalization-group evolution: high scales

For the running above the seesaw scale the relevant renormalization-group equations have been given in in [90] for the SM and MSSM seesaw models. As the physical quantities studied below, such as leptonic CP asymmetries, involve mass eigenstates, it is convenient to keep the singlet mass matrix diagonal during evolution (see, e.g., appendix B of [90]):

$$M_R(\mu) = \mathrm{diag}(M_1(\mu), M_2(\mu), M_3(\mu)).$$

Defining

$$H = Y_\nu Y_\nu^\dagger, \tag{3.21}$$

and

$$t = \frac{1}{16\pi^2} \ln\left(\mu/\Lambda_{\rm GUT}\right), \tag{3.22}$$

one obtains for the mass eigenvalues in the SM with right handed neutrinos:

$$\frac{dM_i}{dt} = 2H_{ii}\, M_i \qquad \text{(no sum)}. \tag{3.23}$$

Note that due to the positivity of the right-hand side of (3.23), the running will always decrease the masses when running from the GUT to the seesaw scale.

The matrix H satisfies the RGEs

$$\frac{dH}{dt} = [T,H] + 3\,H^2 - 3\,Y_\nu Y_E^\dagger Y_E Y_\nu^\dagger + 2\alpha H \qquad \text{(SM)}, \tag{3.24}$$

$$\frac{dH}{dt} = [T,H] + 6\,H^2 + 2\,Y_\nu Y_E^\dagger Y_E Y_\nu^\dagger + 2\alpha H \qquad \text{(MSSM)}, \tag{3.25}$$

where

$$\begin{aligned}
\alpha &= Tr(Y_\nu^\dagger Y_\nu) + Tr(Y_e^\dagger Y_e) + 3\,Tr(Y_u^\dagger Y_u) + 3\,Tr(Y_d^\dagger Y_d) - \frac{9}{20}g_1^2 - \frac{9}{4}g_2^2 \quad \text{(SM)},\\
\alpha &= Tr(Y_\nu^\dagger Y_\nu) + 3\,Tr(Y_u^\dagger Y_u) - \frac{3}{5}g_1^2 - 3g_2^2 \quad \text{(MSSM)},\\
T_{ij} &= \begin{cases} -\frac{M_j+M_i}{M_j-M_i}{\rm Re}H_{ij} - i\frac{M_j-M_i}{M_j+M_i}{\rm Im}H_{ij} & (i\neq j),\\ 0 & (i=j),\end{cases}
\end{aligned} \tag{3.26}$$

and GUT normalization has been employed for g_1. The matrix T satisfies $\dot U = TU$, where $M_R^{(0)}(\mu) = U(\mu)^T M_R(\mu) U(\mu)$ and $M_R^{(0)}$ satisfies the unconstrained RGEs given in [90]. Note that α is real and has trivial flavour structure. Note the different relative signs in (3.24) and (3.25); we will return to this point below.

We now turn to a qualitative analysis of these equations and their impact on leptogenesis and flavour violation. Ignoring flavour effects in the Boltzmann evolution of charged leptons, the baryon asymmetry η_B is approximately proportional to the combinations ${\rm Im}((H_{ij})^2) = 2\,{\rm Re}H_{ij}\,{\rm Im}H_{ij}$ $(i\neq j)$, evaluated in the mass eigenbasis. At the scale $\Lambda_{\rm GUT}$, degeneracy of M_R allows the use of an $SO(3)$ transformation to make the off-diagonal elements of ReH vanish.[4] As explained above, we should RG-evolve all parameters to the scale $\mu \sim M_\nu$ to avoid large

[4] To see this, notice that H is hermitian, so ReH is real symmetric. That is, it can be diagonalized by a real orthogonal (and hence unitary) transformation of the right-handed neutrinos. Now if all three neutrinos are degenerate, such a rotation affects no term in the Lagrangian besides Y_ν. By inspecting the unconstrained RGEs, one finds furthermore that the matrix T is actually zero at the initial scale, and consequently the commutator $[T,H]$ absent from (3.24), (3.25), (3.27), and (3.28).

logarithms. Let us first consider the formal limit of vanishing charged lepton Yukawa couplings Y_E for the SM case. It is instructive to split (3.24) into real and imaginary parts. The former satisifes

$$\frac{d\mathrm{Re}H}{dt} = [\mathrm{Re}T, \mathrm{Re}H] - [\mathrm{Im}T, \mathrm{Im}H] + 3\Big\{(\mathrm{Re}H)^2 - (\mathrm{Im}H)^2\Big\} + 2\alpha\mathrm{Re}H. \quad (3.27)$$

To investigate how ReH can be generated radiatively, assume that it is zero at some scale (initial or lower). Then (3.27) reduces to

$$\frac{d\mathrm{Re}H}{dt} = -[\mathrm{Im}T, \mathrm{Im}H] - 3(\mathrm{Im}H)^2. \quad (3.28)$$

Now evaluate this for the $(2,1)$ element and notice that $T_{ij} = 0$ and $\mathrm{Im}H_{ij} = 0$ for $i = j$. If there were only two heavy singlets in the theory, each term in each matrix product would require one $(2,1)$ element and one $(1,1)$ or $(2,2)$ element from the two matrix factors. For example,

$$(\mathrm{Im}T\,\mathrm{Im}H)_{21} = \mathrm{Im}T_{21}\underbrace{\mathrm{Im}H_{11}}_{0} + \underbrace{\mathrm{Im}T_{22}}_{0}\mathrm{Im}H_{21} = 0, \quad (3.29)$$

and similarly for the other terms. Consequently,

$$\mathrm{Re}H_{21} = 0 \Rightarrow \frac{d\mathrm{Re}H_{21}}{dt} = 0. \quad (3.30)$$

We see that there is no radiative leptogenesis in the two-flavour case when $Y_E = 0$. This is consistent with the approximate equation (12) in [84], where ReH_{21} was found to be proportional to y_τ^2. It is easy to see that the argument breaks down in the three-flavour case. For instance,

$$((\mathrm{Im}H)^2)_{21} = \mathrm{Im}H_{21}\mathrm{Im}H_{11} + \mathrm{Im}H_{22}\mathrm{Im}H_{21} + \mathrm{Im}H_{23}\mathrm{Im}H_{31} = \mathrm{Im}H_{23}\mathrm{Im}H_{31}, \quad (3.31)$$

which is in general not zero. The other terms in (3.28) are also proportional to $\mathrm{Im}H_{23}\mathrm{Im}H_{31}$. We see that three generations of heavy neutrinos are necessary and sufficient to generate leptogenesis without help from charged lepton Yukawas.

Once we restore the charged lepton Yukawas, they will also contribute. The important qualitative difference is that, whereas the contribution involving the charged-lepton Yukawas is only logarithmically dependent of the seesaw scale (as seen in eqs.(3.55)–(3.57) below for the two-flavour case, or from [87] for the three-flavour case), the pure Y_ν contribution to the radiatively generated ReH_{ij} scales with M_ν because it contains two extra powers of Y_ν as observed in the three flavour scenario studied in [85].

In summary, we expect the following qualitative behaviour for the BAU as a function of M_ν:

- For small Y_ν (small M_ν), the dominant contribution to ReH_{ij} and hence to η_B should be due to Y_E. η_B turns out to be weakly dependent on M_ν.

- For large Y_ν (large M_ν), in the three-flavour case there is a relevant contribution proportional to $((\mathrm{Im}H)^2)_{ij}$. Since it contains two extra powers of Y_ν with respect to the contribution proportional to y_τ^2, η_B scales linearly with M_ν.

- In the case of only two heavy flavours, η_B is weakly dependent on M_ν over the whole range of M_ν. We will therefore include an "effective" two-flavour scenario in our numerical analysis.

Let us stress that we reached these qualitative conclusions only upon neglecting flavour effects in the Boltzmann evolution of the products of the N_i decays. We will return to these points in Section 3.4 and in Section 3.5, where we perform a detailed quantitative analysis.

Finally, let us briefly discuss $l_i \to l_j\gamma$. In MLFV these radiative lepton decays are governed by $\Delta_{ij} \equiv Y_\nu^\dagger Y_\nu$ (and structures involving more powers of Yukawa matrices). In the case of the SM, the rates are known to be essentially zero due to a near perfect GIM cancellation among the tiny neutrino masses. From the point of view of MLFV, this smallness can be traced to the fact that, in the SM, the LFV scale is equal to the LNV scale $\sim M_\nu$.

On the other hand, in the more generic case of the MSSM, there are additional contributions mediated by slepton-higgsino or slepton-gaugino loops suppressed only by a scale $\Lambda_{\mathrm{LFV}} \sim m_{\tilde{l}}$, of order TeV, as discussed in Section 3.3.2. Linearizing the RG evolution, the charged slepton soft mass matrix acquires the form[91]

$$\tilde{m}_l^2(M_\nu) = m_0^2\mathbf{1} - L\frac{Y_\nu^\dagger Y_\nu}{16\pi^2}(6m_0^2 + 2a_0^2) + \ldots, \tag{3.32}$$

where the dots denote terms governed by charged lepton Yukawa couplings Y_E or conserving lepton flavour. Note that the flavour structure in the soft terms is generated at a high scale and that, unlike the case of CP asymmetries in N_i decay, the necessary flavour structure Δ is already present at the initial scale Λ_{GUT}. Hence the RGE running of Δ merely gives a correction. Note also that there is dependence on the MLFV model beyond the choice of LFV scale due to the (in general unknown) RGE coefficients in (the relevant analog of) (3.32).

3.3.5 RGE evolution below M_ν: PMNS matrix and Δ_{ij}

So far we have ignored renormalization effects in equations such as (3.11), identifying d_ν and U_ν with the physical (light) neutrino masses and mixing matrix, while the objects Y_ν and D_R are defined at a high scale. However, to be orthogonal the matrix R has to be defined with all objects given at the same scale. Now it is well known that using low-energy inputs in d_ν can be a bad approximation because there are significant radiative corrections between the weak and GUT scales. However, as investigated in [92], both in the SM and in the MSSM with

small $\tan\beta$ the main effect below M_ν is an approximately universal rescaling of the light neutrino masses. This results in larger magnitudes of the elements of Y_ν extracted by means of (3.11) but in a weak running of the matrix U_ν. Above the scale M_ν, even though the heavy singlets are now dynamical, one can still *define* an effective neutrino mass matrix through the seesaw relation (3.9). However, the evolution becomes more involved, as in the presence of heavy singlets there are additional contributions to the running involving Y_ν. To deal with this situation, where some of our inputs are specified at the weak scale, while the matrix $R_{\rm deg}$ is defined at the scale $\Lambda_{\rm GUT}$, we employ an iterative procedure detailed in our paper [77]. As was the case for the evolution above M_ν, also the RGE effects below M_ν, and consequently the relation of e.g $Y_\nu^\dagger Y_\nu$ to the input parameters necessarily depends on the details of the MLFV model.

3.4 Numerical Analysis: $B(l_i \to l_j\gamma)$ and CP asymmetries in ν_R decay

3.4.1 Preliminaries

For our numerical analysis we take our input parameters at the weak scale, except for the matrix $R_{\rm deg}$, which has to be defined at the scale $\Lambda_{\rm GUT}$. From these inputs we find a consistent set of parameters at the seesaw scale M_ν, where the CP asymmetries as well as $B(l_i \to l_j\gamma)$ are calculated, through an iterative procedure. For the running we use the package REAP [93].
For the PMNS matrix we use the convention:

$$U_\nu = \begin{pmatrix} c_{12}c_{13} & s_{12}c_{13} & s_{13}e^{-i\delta} \\ -s_{12}c_{23} - c_{12}s_{23}s_{13}e^{i\delta} & c_{12}c_{23} - s_{12}s_{23}s_{13}e^{i\delta} & s_{23}c_{13} \\ s_{12}s_{23} - c_{12}c_{23}s_{13}e^{i\delta} & -s_{23}c_{12} - s_{12}c_{23}s_{13}e^{i\delta} & c_{23}c_{13} \end{pmatrix} \cdot V \qquad (3.33)$$

and $V = \mathrm{Diag}(e^{i\alpha/2}, e^{i\beta/2}, 1)$ where α and β denote the Majorana phases and δ denotes the Dirac phase. We parameterize the complex orthogonal matrix R as follows:

$$R = \begin{pmatrix} \hat{c}_{12} & \hat{s}_{12} & 0 \\ -\hat{s}_{12} & \hat{c}_{12} & 0 \\ 0 & 0 & 1 \end{pmatrix} \begin{pmatrix} 1 & 0 & 0 \\ 0 & \hat{c}_{23} & \hat{s}_{23} \\ 0 & -\hat{s}_{23} & \hat{c}_{23} \end{pmatrix} \begin{pmatrix} \hat{c}_{13} & & \hat{s}_{13} \\ 0 & 1 & 0 \\ -\hat{s}_{13} & 0 & \hat{c}_{13} \end{pmatrix}, \qquad (3.34)$$

with $\hat{s}_{ij} \equiv \sin\hat{\theta}_{ij}$, with $\hat{\theta}_{ij}$ in general complex:

$$\hat{\theta}_{ij} = x_{ij} + i\, y_{ij}. \qquad (3.35)$$

In the degenerate case, the angles x_{ij} can be made to vanish by a redefinition of the right-handed neutrinos, i.e. a matrix of the form R_{deg} is parameterized by three real numbers y_{ij}.

In the following, we use maximal atmospheric mixing $c_{23} = s_{23} = 1/\sqrt{2}$ and a solar mixing angle $\theta_{\rm sol} = 33^\circ$, with corresponding values for its sine $s \equiv s_{12}$ and cosine $c \equiv c_{12}$. For the sine of the CHOOZ angle s_{13} and the phases we allow the ranges

$$0 \leq s_{13} \leq 0.25, \qquad 0 < \alpha, \beta, \delta < 2\pi, \tag{3.36}$$

and for the light neutrinos we use the low energy values

$$\Delta m^2_{\rm sol} = m_2^2 - m_1^2 = 8.0 \cdot 10^{-5}\ \text{eV}^2 \tag{3.37}$$

$$\Delta m^2_{\rm atm} = |m_3^2 - m_2^2| = 2.5 \cdot 10^{-3}\ \text{eV}^2 \tag{3.38}$$

$$0 \leq m_\nu^{\rm lightest} \leq 0.2\ \text{eV} \tag{3.39}$$

with $m_\nu^{\rm lightest} = m_1(m_3)$ for normal (inverted) hierarchy, respectively. See [94] for a detailed discussion of the neutrino masses and mixing. For the heavy neutrino mass scale, we consider a wide range

$$10^6\,\text{GeV} < M_\nu < 10^{14}\,\text{GeV}, \tag{3.40}$$

and the CP violating parameters y_{ij} are all taken in the range $[-1, 1]$ if not otherwise stated.

3.4.2 Perturbativity bounds

In the MLFV framework the magnitudes of the Yukawa couplings Y_ν are very sensitive to the choice of M_ν, $m_\nu^{\rm lightest}$ and the angles in the matrix $R_{\rm deg}$, as is evident from (3.11). To render the framework perturbative, we impose the constraint

$$\frac{y^2_{\rm max}}{4\pi} < 0.3, \tag{3.41}$$

where $y^2_{\rm max}$ is the largest eigenvalue of $Y_\nu^\dagger Y_\nu$. By means of (3.15), it translates into a bound on $R^\dagger R = R^2$ and the angles y_{ij} that scales with M_ν^{-1} and hence is most severe for a large lepton-number-violating scale. Analogous bounds apply to other dimensionless couplings whose number depends on the precise MLFV model. For instance, in the SM there is also the Higgs self coupling λ_H, whereas in the MSSM there is no such additional coupling.

3.4.3 Lepton Flavour Violation and $l_i \to l_j\gamma$

Following Cirigliano *et al.* [76] we consider the normalized branching fractions defined as

$$B(l_i \to l_j\gamma) = \frac{\Gamma(l_i \to l_j\gamma)}{\Gamma(l_i \to l_j\nu_i\bar{\nu}_j)} \equiv r_{ij}\hat{B}(l_i \to l_j\gamma), \tag{3.42}$$

where $\hat{B}(l_i \to l_j\gamma)$ is the true branching ratio and $r_{\mu e} = 1.0$, $r_{\tau e} = 5.61$ and $r_{\tau\mu} = 5.76$. Assuming first the heavy right-handed neutrinos to be degenerate but not making the assumptions of $R = \mathbb{1}$ and U_ν being real as done in [76], the straightforward generalization of (29) in [76] is

$$B(l_i \to l_j\gamma) = 384\pi^2 e^2 \frac{v^4}{\Lambda_{\rm LFV}^4} |\Delta_{ij}|^2 |C|^2. \tag{3.43}$$

Here $v = 174$ GeV is the vacuum expectation value of the SM Higgs doublet,[5] $\Lambda_{\rm LFV}$ is the scale of charged lepton flavour violation, and C summarizes the Wilson coefficients of the relevant operators that can be calculated in a given specific model. They are naturally of $\mathcal{O}(1)$ but can be different in different MLFV models. As we would like to keep our presentation as simple as possible, we will set $|C| = 1$ in what follows, bearing in mind that in certain scenarios C may differ significantly from unity. Thus the true $B(l_i \to l_j\gamma)$ can be different from our estimate in a given MLFV model, but as C is, within MLFV, independent of external lepton flavours, the ratios of branching ratios take a very simple form

$$\frac{B(l_i \to l_j\gamma)}{B(l_m \to l_n\gamma)} = \frac{|\Delta_{ij}|^2}{|\Delta_{mn}|^2}. \tag{3.44}$$

The most important objects in (3.43) and (3.44) are

$$\Delta_{ij} \equiv (Y_\nu^\dagger Y_\nu)_{ij} = \frac{1}{v^2}(U_\nu \sqrt{d_\nu} R^\dagger D_R R \sqrt{d_\nu} U_\nu^\dagger)_{ij}, \tag{3.45}$$

which in the limit of $R = \mathbb{1}$, $D_R = M_\nu \mathbb{1}$, and U_ν being real reduce to Δ_{ij} as given in (14) of [76].

With the formula (3.45) at hand we can generalize the expressions for Δ_{ij} in (24) of [76] to the general case of complex R and U_ν. To this end we will use the standard parametrization of the PMNS matrix U_ν in (3.33) and the parametrization of R in (3.34). We will discuss in our numerical analysis also the cases for which y_{13} and y_{23} are non-vanishing. As mentioned above, setting $x_{ij} = 0$ is in accord with the degeneracy of the right-handed neutrinos. Once this degeneracy is broken by RG effects, the x_{ij} become non-zero.

Recall from Section 3.3 that Δ_{ij} evolves above the scale M_ν and the flavour structures it affects, such as the slepton mass matrix $m_{\tilde{l}}^2$, also evolve between M_ν and $\Lambda_{\rm LFV}$ (and the resulting effective operators below $\Lambda_{\rm LFV}$ also evolve). Moreover, the flavour-violating piece in, for example, $m_{\tilde{l}}^2$ is not exactly proportional to Δ at the scale M_ν beyond leading order because these objects satisfy different RGEs between M_ν and $\Lambda_{\rm GUT}$. All this running depends, beyond the operator, also on the details of the model. Below the seesaw scale the flavour-nonuniversal

[5] $v = \sqrt{v_1^2 + v_2^2}$ for two-Higgs-doublet models such as the MSSM. Powers of $\sin\beta$ can be absorbed into C or into a redefinition $\Lambda_{\rm LFV} \to \Lambda_{\rm LFV}^{\rm eff}$

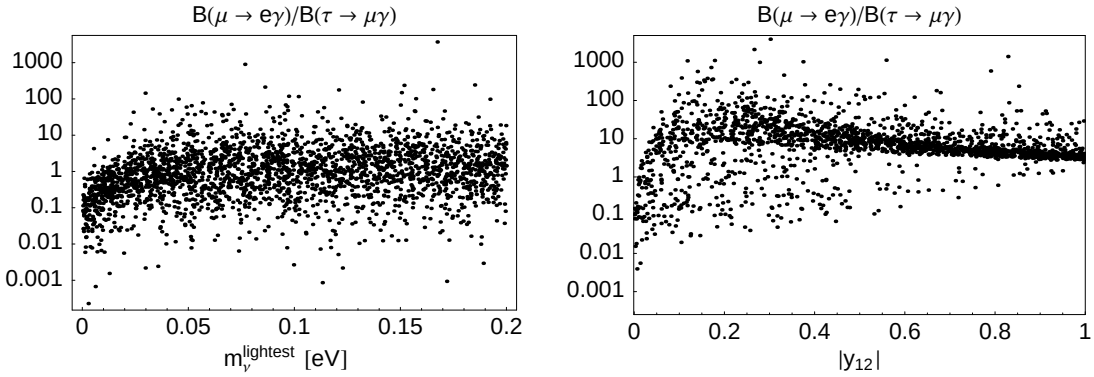

Figure 3.1: Double ratios of $l_i \to l_j\gamma$ for the MSSM with $\tan\beta = 2$. Left plot: All parameters varied, right plot: no phases and only $y_{12} \neq 0$. For a discussion, see the text.

contributions are governed by Y_E (although trilinear couplings such as the A-terms in the MSSM can also contribute), which is analogous to the case of the PMNS matrix. Based on the experience that the running of the PMNS angles is weak in the SM and the MSSM unless $\tan\beta$ (and hende y_τ) is large, we ignore all these details and evaluate Δ_{ij} at the scale M_ν.

That Δ_{ij} has to be evaluated at the high energy scale M_ν, and hence U_ν and d_ν have to be evaluated at M_ν by means of renormalization group equations with the initial conditions given by their values at M_Z, has recently been stressed in particular in [83]. The dominant contributions to the flavour-violating pieces in the charged slepton masses matrix in the MSSM that is relevant for $l_i \to l_j\gamma$ are proportional to $Y_\nu^\dagger Y_\nu$ and come from scales above M_ν, as seen for instance in equation (30) of [95] (where charged lepton Yukawas and A-terms have been dropped and only contribute at higher orders) and the fact that right-handed neutrinos and their Yukawa couplings are absent below that scale.

All other parameters of a given MLFV model, hidden in the Wilson coefficient C in (3.43), like slepton and chargino masses in the MSSM, would have to be evaluated at the electroweak scale and lower scales if a concrete value for C was desired.

The ratio $B(\mu \to e\gamma)/B(\tau \to \mu\gamma)$ is shown for the case of the MSSM with $\tan\beta = 2$ in Fig. 3.1 (left). All other parameters are varied in the ranges given above. We see that this ratio varies over about six orders of magnitude and $B(\mu \to e\gamma)$ can be a factor 10^3 larger than $B(\tau \to \mu\gamma)$ in qualitative agreement with [96, 97]. We have checked that the leptogenesis constraint, as discussed in Section 3.5, has no significant impact. This contradicts the findings of [85]. Even when constraining the Dirac and Majorana phases in the PMNS matrix to zero and allowing only for a single nonvanishing angle y_{12} at the scale $\Lambda_{\rm GUT}$, we can still have $B(\mu \to e\gamma) \gg B(\tau \to \mu\gamma)$. This is again in agreement with [96, 97]. We will consider the single ratio $B(\mu \to e\gamma)$ together with the leptogenesis constraint

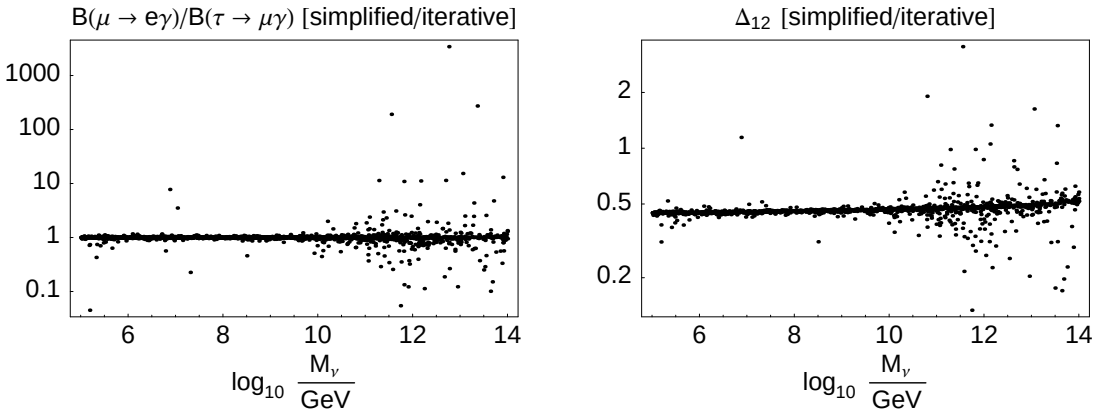

Figure 3.2: Impact of iterative vs simplified procedure. Left plot: Simplified result for the ratio of branching ratios $B(\mu \to e\gamma)/B(\tau \to \mu\gamma)$, normalized to the one obtained with the iterative procedure. Right plot: Similarly for Δ_{12}.

in Section 3.5.

It is also interesting to compare our elaborate iterative procedure of matching high- and low-energy parameters to a simpler procedure where we simply impose the weak-scale PMNS and neutrino mass parameters at the scale $\Lambda_{\rm GUT}$ (Fig. 3.2 (left), corresponding to the MSSM with $\tan\beta = 2$). It turns out that both procedures agree well for small scales M_ν. (This agreement is slightly worse for $\tan\beta = 10$.) For large values $M_\nu > 10^{11}$ GeV, deviations up to a few orders of magnitude can occur for some choices of parameters. It appears that this is usually due accidentally small branching ratios in one of the approaches. This is supported by the right plot in the Fig. 3.2, which shows a good agreement for the more fundamental flavour-violating quantity Δ_{12} up to the (expected) different overall normalization.

3.4.4 CP asymmetries

We are also in a position to illustrate and check numerically our qualitative discussion in Section 3.3 of the CP asymmetries relevant for leptogenesis. A thorough investigation of the baryon asymmetry follows in the next section. Fig. 3.3 shows the sum of the three CP asymmetries $|\sum_i \epsilon_i|$ defined below (3.47), for the generic three-flavour case (left plot) and the CP asymmetry ϵ_1 for the effective two-flavour case where only $y_{12} \neq 0$ (right plot). One can see clearly that in the latter case the dependence on M_ν is weak and slightly reciprocal. In fact this dependence is approximately proportional to $\ln^2 \Lambda_{\rm GUT}/M_\nu$ (black solid line) in agreement with expectations. The generic case is shown in the left plot for the SM (black solid) as well as the MSSM for $\tan\beta = 2$ (red dot-dashed) and $\tan\beta = 10$ (blue dotted), with the remaining parameters given in the Figure caption. In contrast to the two-flavour case, there is strong dependence on M_ν

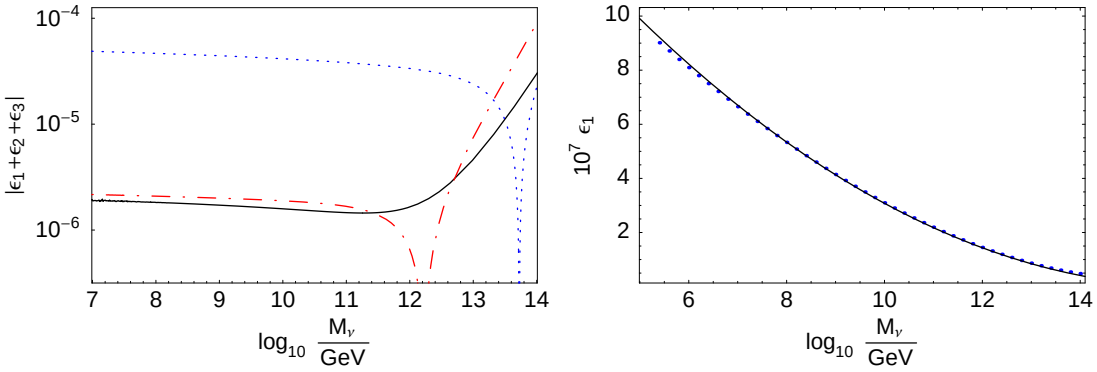

Figure 3.3: Left plot: M_ν dependence of $|\sum_i \epsilon_i|$ for the generic (3-flavour) case. Right plot: effective 2-flavour case. Normal hierarchy, $m_\nu^{\text{lightest}} = 0.02$ eV ; $y_{12} = 0.8$, $y_{13} = 0.2$, $y_{23} = 0.6$ (3-flavour case), $y_{12} = 1$ and $y_{13} = y_{23} = 0$ (effective 2-flavour case). The PMNS phases have been taken to be $\delta = \alpha = \beta = \pi/10$. Right plot: Effective two-flavour case; only ϵ_1 is shown, on a linear scale.

for $M_\nu > 10^{12}$ GeV, when the contribution due to Y_ν alone starts to dominate the RGEs (3.24),(3.25). The precise form of the M_ν dependence is quite sensitive to the "angles" y_{ij}, but the roughly linear growth of $|\sum_i \epsilon_i|$ in the regime of large M_ν appears to be general. However, the figure also clearly shows a strong dependence on the MSSM parameter $\tan\beta$ particularly for small M_ν. Indeed already for relatively small $\tan\beta = 10$ the CP asymmetries can be more than an order of magnitude larger than in the SM. Moreover, in the case of the MSSM we observe a sign change at some scale $M_\nu \gtrsim 10^{12}$ GeV, which can be traced to the different relative signs between the terms on the right-hand sides of (3.24) and (3.25). This example clearly demonstrates a rather dramatic dependence on details of the model. Finally, as in the case of the double ratios above, we investigated the impact of the iterative procedure compared to the simplified approach and found it to be generically small. Hence we feel justified to use the simplified procedure in Section 3.5 in order to save computer time.

3.5 Leptogenesis in the extended MLFV Framework

3.5.1 Preliminaries

One of the most plausible mechanisms for creating the observed matter–antimatter asymmetry in the universe is leptogenesis, where a CP asymmetry generated through the out-of-equilibrium L-violating decays of the heavy Majorana neutrinos leads to a lepton asymmetry which is subsequently transformed into a baryon asymmetry by $(B + L)$-violating sphaleron processes [79, 80, 98].

Unfortunately, even in its simplest realization through the well-known seesaw mechanism [78], the theory has too many parameters. Indeed, as recalled in Section 2.4 in the framework of the standard model (SM) extended with three heavy Majorana neutrinos $N_i\,(i = 1, 2, 3)$, the high-energy neutrino sector, characterized by the Dirac neutrino (m_D) and the heavy Majorana neutrino (M_R) mass matrices, has eighteen parameters. Of these, only nine combinations enter into the seesaw effective neutrino mass matrix $m_D^T\, M_R^{-1}\, m_D$, thus making difficult to establish a direct link between leptogenesis and low-energy phenomenology [99]. Furthermore, there are six CP-violating phases which are physically relevant at high energies, while only three combinations of them are potentially observable at low energies. Therefore, no direct link between the sign of the baryon asymmetry and low-energy leptonic CP violation can be established, unless extra assumptions are introduced.

Furthermore, additional assumptions are usually required to completely determine the high-energy neutrino sector from low-energy observables. Typical examples are the introduction of texture zeros in the Yukawa matrices or the imposition of symmetries to constrain their structure [100]. On the other hand, the heavy Majorana neutrino masses can range from the TeV region to the GUT scale, and the spectrum can be hierarchical, quasi-degenerate or even exactly degenerate [101]. Despite this arbitrariness, the heavy Majorana neutrino mass scale turns out to be crucial for a successful implementation of the leptogenesis mechanism. In particular, the standard thermal leptogenesis scenario with hierarchical heavy Majorana neutrino masses ($M_1 \ll M_2 < M_3$) requires $M_1 \gtrsim 4 \times 10^8$ GeV [102], if N_1 is in thermal equilibrium before it decays, or the more restrictive lower bound $M_1 \gtrsim 2 \times 10^9$ GeV [103] for a zero initial N_1 abundance. Since this bound also determines the lowest reheating temperature allowed after inflation, it could be problematic in supersymmetric theories due to the overproduction of light particles like the gravitino [104].

It should be emphasized, that the above bounds are model dependent in the sense that they can be avoided, if the heavy Majorana neutrino spectrum is no longer hierarchical. For example, if at least two of the N_i are quasi-degenerate in mass, *i.e.* $M_1 \simeq M_2$, then the leptonic CP asymmetry relevant for leptogenesis exhibits the resonant behaviour $\varepsilon_1 \sim M_1/(M_2 - M_1)$ [86, 87]. In this case, it is possible to show that the upper bound on the CP asymmetry is independent of the light neutrino masses and successful leptogenesis simply requires $M_{1,2}$ to be above the electroweak scale for the sphaleron interactions to be effective. The quasi-degeneracy may also be achieved in soft leptogenesis where a small splitting is induced by the soft supersymmetry breaking terms [88].

Another possibility which has been recently explored [105, 106] relies on the fact that radiative effects, induced by the renormalization group (RG) running from high to low energies, can naturally lead to a sufficiently small neutrino mass splitting at the leptogenesis scale. In the latter case, sufficiently large CP asymmetries are generated.

In the minimal seesaw scenario with only two heavy neutrinos the resulting baryon asymmetry in the SM turns out to be below the observed value [105]. On the other hand, this mechanism can be successfully implemented in its minimal supersymmetric extension (MSSM) [106].

It has been shown [84] that the above problems in the SM can be overcome in a more realistic scenario where the effects of a third heavy neutrino are also taken into account. In [84], leptogenesis was studied in the framework of a model where there are three right-handed neutrinos, with masses $M_1 \approx M_2 \ll M_3$. We will discuss this scenario below as a special limit of the MLFV framework.

In view of the above, it is important to analyze leptogenesis in the extended MLFV framework, where CP violation is allowed both at high and low energies. In the MLFV scenario, right-handed neutrinos are assumed to be *exactly* degenerate at a high energy scale. In the limit of exact degeneracy, no lepton-asymmetries can be generated. However, as previously emphasized, even if exact degeneracy is assumed at a high energy scale, renormalization group effects lead to a splitting of right-handed neutrino masses at the scale of leptogenesis, thus offering the possibility of viable leptogenesis in the extended MLFV framework.

3.5.2 BAU in the RRL and Flavour Effects

In leptogenesis scenarios the baryon asymmetry of the universe η_B arises due to non-perturbative sphaleron interactions that turn a lepton asymmetry into a baryon asymmetry. The predicted value of η_B has to match the results of WMAP and the BBN analysis for the primordial deuterium abundance [107]

$$\eta_B = \frac{n_B}{n_\gamma} = (6.3 \pm 0.3) \times 10^{-10}. \tag{3.46}$$

The lepton asymmetry is generated by out-of-equilibrium decays of heavy right-handed Majorana neutrinos N_i and is proportional to the CP asymmetry ε_i^l with

$$\varepsilon_i^l = \frac{\Gamma(N_i \to L_l\,\phi) - \Gamma(N_i \to \bar{L}_l\,\bar{\phi})}{\sum_l \left[\Gamma(N_i \to L_l\,\phi) + \Gamma(N_i \to \bar{L}_l\,\bar{\phi})\right]}\,, \tag{3.47}$$

and l denoting the lepton flavour, that arises at one-loop order due to the interference of the tree level amplitude with vertex and self-energy corrections.
A characteristic of the MLFV framework is that only admissable BAU with the help of leptogenesis is radiative and thereby resonant leptogenesis. The mass splittings of the right-handed neutrinos induced by the RGE are of similar size $\Delta M \sim \mathcal{O}(M_\nu\, Y_\nu Y_\nu^\dagger)$ as the decay widths $\Gamma \sim \mathcal{O}(M_\nu\, Y_\nu Y_\nu^\dagger)$. This is the condition of resonant leptogenesis. The CP asymmetry is for the lepton flavour l given by

$$\varepsilon_i^l = \frac{1}{(Y_\nu Y_\nu^\dagger)_{ii}} \sum_j \Im((Y_\nu Y_\nu^\dagger)_{ij}(Y_\nu)_{il}(Y_\nu^\dagger)_{lj})\, g(M_i^2, M_j^2, \Gamma_j^2) \tag{3.48}$$

where $g(M_i^2, M_j^2, \Gamma_j^2)$ is an abbreviation for the full result given in [87]. The total CP asymmetries ε_i are obtained summing over the lepton flavours l.
The baryon to photon number ratio η_B can then be calculated solving the Boltzmann equations for the lepton asymmetry and converting it into η_B using suitable dilution and sphaleron conversion factors. Which Boltzmann equation to use depends on the temperature scale at which leptogenesis takes place. We will follow a simplistic approach ignoring all subtleties generically coming into play in the intermediate regime between different mechanisms at work. Our main conclusions, however, will not be affected by this omission. We will simply divide the temperature scale into a region up to which all three lepton flavours have to be taken into account and a region above which the single flavour approximation works.

Below some temperature $T_{\rm eq}^{\mu} \simeq 10^9$ GeV muon and tau charged lepton Yukawa interactions are much faster than the expansion H rendering the μ and τ Yukawa couplings in equilibrium. The correct treatment in this regime requires the solution of lepton flavour specific Boltzman equations. In the strong washout regime η_B is independent of the initial abundances and an estimate including flavour effects is given by [108]

$$\eta_B \simeq -10^{-2} \sum_{i=1}^{3} \sum_{l=e,\mu,\tau} e^{-(M_i-M_1)/M_1}\, \varepsilon_i^l \frac{K_i^l}{K^l K_i}, \tag{3.49}$$

with

$$K_i^l = \frac{\Gamma(N_i \to L_l \phi) + \Gamma(N_i \to \bar{L}_l \bar{\phi})}{H(T = M_i)} \tag{3.50}$$

$$K_i = \sum_{l=e,\mu,\tau} K_i^l, \qquad K^l = \sum_{i=1}^{3} K_i^l, \qquad H(T = M_i) \simeq 17 \frac{M_i^2}{M_{\rm Pl}} \tag{3.51}$$

where $M_{\rm Pl} = 1.22 \times 10^{19}$ GeV and K_i^l is the washout factor due to the inverse decay of the Majorana neutrino N_i into the lepton flavour l. The impact of lepton flavour effects on η_B is discussed in [109, 108, 110, 111, 112]. As we shall also see below, the inclusion of flavour effects generally leads to an enhancement of the resulting η_B. This is due to two effects: (1) the washout gets reduced since the interaction with the Higgs is with the flavour eigenstates only and (2) an additional source of CP violation arises due to lepton flavour specific CP asymmetries.

For higher values of $T \gtrsim 10^{12}$ GeV the charged lepton Yukawa couplings do not break the coherent evolution of the lepton doublets produced in heavy neutrino decays anymore. In this regime flavour effects can be ignored and an order of magnitude estimate is given by

$$\eta_B \simeq -10^{-2} \sum_{i=1}^{3} e^{-(M_i-M_1)/M_1}\, \frac{1}{K} \sum_{l=e,\mu,\tau} \varepsilon_i^l, \tag{3.52}$$

with $K = \sum_i K_i$. This agrees with a recent analytical estimate by [113] up to factors of $\mathcal{O}(1)$ for the region of interest in parameter space, where the estimate of [113] generally leads to a smaller efficiency and smaller η_B. We have also compared the analytical estimate of [113] and (3.52) with the numerical solution of the Boltzman equations using the LeptoGen code [108][6]. For the relevant ranges of the input parameters the analytical estimate of (3.52) and the full numerical solution agree quite well, whereas the estimate of [113] leads to an efficiency and η_B generally smaller by a factor of 5 to 10. This is shown in Fig. 3.8. These estimates, however, do not take into account the potentially large lepton flavour effects included in (3.49).

Let us remark in passing that in the flavour independent region we are always in the strong washout regime, since

$$K = K_1 + K_2 + K_3 = \frac{1}{m^*} \operatorname{tr}\left(R d_\nu R^\dagger\right) \geq \frac{(\Delta m^2_{\text{atm}})^{1/2}}{m^*} \simeq 50, \tag{3.53}$$

where $m^* = \mathcal{O}(10^{-3})$. This inequality holds since the trace is linear function of the neutrino masses with positive coefficents, which reaches its minimum for $y_{ij} = 0$. We also made sure that the estimate (3.49) including flavour effects is applicable [108] and checked that the inequality

$$K_i^l \gtrsim 1 \tag{3.54}$$

is always satisfied for the points considered in the plots. Since both (3.53) and (3.54) are satisfied, a simple decay-plus-inverse decay picture is a good description and the estimates (3.49) and (3.52) independent of the initial abundances give a good approximation of the numerical solution of the full Boltzman equations.

We have performed the leptogenesis analysis specifically for the SM. We do not expect large deviations in the MSSM from the SM if the same $Y_\nu(M_\nu)$ and $M_\nu^i(M_\nu)$ are given. The main differences come (1) from the CP-asymmetries, which now include contributions from the supersymmetric particles, (2) from the washout, and (3) from conversion and dilution factors. The supersymmetric CP asymmetries have the same flavour structure as in the SM and using [114] one can show that $\epsilon^{MSSM} \simeq 2\,\epsilon^{SM}$ for quasi-degenerate heavy neutrinos. We also expect the correction by the decay widths to be similar in size. Next, the washout in the strong washout regime is about a factor of $\sqrt{2}$ larger [115] in the MSSM, whereas the dilution and sphaleron conversion factors stay almost unchanged. Concluding, we find that in the scenario considered the predicted values roughly satisfy $\eta_B^{\text{MSSM}} \simeq 1.5\,\eta_B^{\text{SM}}$ for the same set of input parameters $Y_\nu(M_\nu)$ and $M_\nu^i(M_\nu)$. The RGE induced values of $Y_\nu(M_\nu)$ and $M_\nu^i(M_\nu)$, however, are model dependent and lead to in general different $Y_\nu(M_\nu)$ and $M_\nu^i(M_\nu)$ for the same boundary conditions at the GUT and low-energy scale, as discussed in Section 3.3.4. Especially

[6] http://www.ippp.dur.ac.uk/∼teju/leptogen/

sensitive is the region $M_\nu \lesssim 10^{12}$ GeV where the CP asymmetries are dominantly generated by the tau Yukawa coupling, which is enhanced by a factor of $\tan\beta$ in the MSSM.

3.5.3

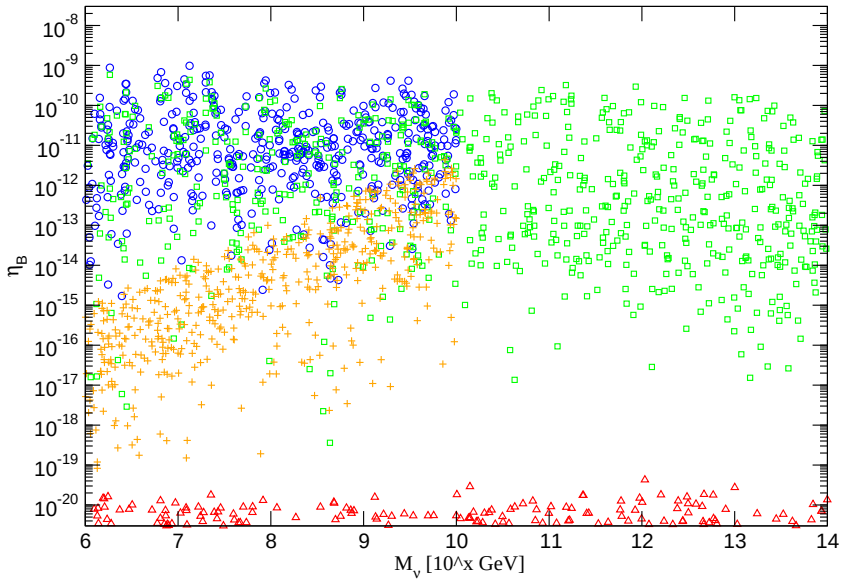

Figure 3.4: Resulting η_B for the case in which only $y_{12} \neq 0$ (effective two flavour case) as a function of M_ν for the normal hierarchy of light neutrinos: the *orange crosses* and *red triangles* show the unphysical limit setting the charged lepton yukawas $Y_e = 0$ in the renormalization group evolution with and without including lepton flavour effects in the calculation of η_B, respectively. Setting the charged lepton Yukawas to their physical values, the *blue circles* and the *green squares* correspond to including and ignoring lepton flavour effects in the calculation, respectively.

As a first step we discuss the special case of y_{12} being non-vanishing at the GUT scale and all other $y_{ij} = 0$. This corresponds approximately to one of the scenarios considered in a recent study of radiative leptogenesis [84] with two right-handed neutrinos quasi-degenerate and a third right-handed neutrino decoupled $M_1 \simeq M_2 \ll M_3$. If only $y_{12} \neq 0$ the calculation of η_B proceeds in the same way since to a good approximation only ν_R^1 and ν_R^2 contribute to the CP asymmetry. The only difference comes from the enhanced wash-out. Since the third heavy neutrino is now also contributing, the lower bound on the washout K in (3.53) is in our case relatively enhanced by a factor $(\Delta m^2_{\rm atm})^{1/2}/(\Delta m^2_{\rm sol})^{1/2} \simeq 4-5$. We have checked this correspondence for η_B also numerically. Ignoring flavour

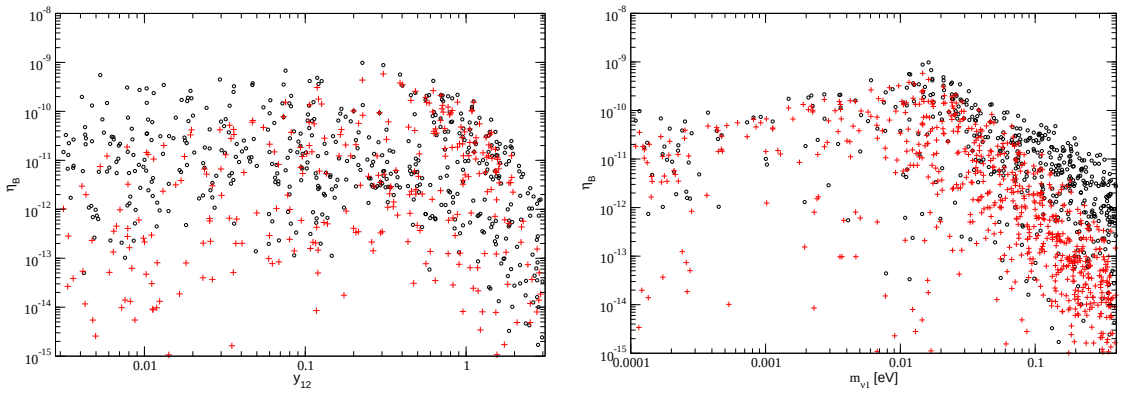

Figure 3.5: η_B for the case in which only $y_{12} \neq 0$ (effective two flavour case) as a function of y_{12} (left) and $m_{\nu 1}$ (right) for the normal hierarchy. The *black circles* are obtained including lepton flavour effects and the *red crosses* are calculated ignoring them.

subtleties in leptogenesis for a moment, the CP violating effects due to renormalization group effects are induced only by the charged lepton yukawa couplings, see Section 3.3.4, and the total CP asymmetries for each heavy Majorana neutrino take the form [84]

$$\varepsilon_{1,2} \simeq \frac{\bar{\varepsilon}_{1,2}}{1+D_{2,1}}, \qquad \varepsilon_3 \simeq 0, \tag{3.55}$$

and

$$\bar{\varepsilon}_j \simeq \frac{3y_\tau^2}{32\,\pi}\frac{\mathrm{Im}(H_{21})\,\mathrm{Re}\left[(Y_\nu)^*_{23}\,(Y_\nu)_{13}\right]}{H_{jj}(H_{22}-H_{11})} = \frac{3\,y_\tau^2}{64\,\pi}\,\frac{m_j(m_1+m_2)\,\sqrt{m_1\,m_2}\,\sinh(2\,y_{12})\,\mathrm{Re}\,(U^*_{\tau 2}\,U_{\tau 1})}{(m_1-m_2)(m_j^2\,\cosh^2 y_{12}+m_1 m_2\,\sinh^2 y_{12})}\,, \tag{3.56}$$

$$D_j \simeq \frac{\pi^2}{4}\frac{H_{jj}^2}{(H_{22}-H_{11})^2\,\ln^2\left(M_\nu/M_{\mathrm{GUT}}\right)} = \left[\frac{\pi}{2}\,\frac{m_j^2\,\cosh^2 y_{12}+m_2 m_1\,\sinh^2 y_{12}}{m_j(m_2-m_1)\,\ln\left(M_\nu/M_{\mathrm{GUT}}\right)}\right]^2. \tag{3.57}$$

where D_j are regularisation factors coming from the heavy Majorana decay widths. We immediately see that the total CP asymmetries only bare a very mild dependence on the heavy Majorana scale. The almost negligible dependence on M_ν has to be compared with the power-suppression in M_ν in the hierarchical case ($M_1 \ll M_2 < M_3$). We find this expectation confirmed in Fig. 3.4, where the resulting η_B is shown as a function of M_ν.
Fig. 3.4 also nicely illustrates the relative importance of flavour effects in leptogenesis. If no cancellations occur, we find, that flavour effects generate an η_B which is of the same order of magnitude (blue circles), however almost always larger than the one calculated ignoring flavour effects (green squares).

If we now consider the unphysical limit of setting $Y_e = 0$ in the renormalization group running only, we find that the *total* CP asymmetries and η_B should vanish since no CP violation effects are induced by the RGE, see Section 3.3.4. We confirm this behaviour in Fig. 3.4 (red triangles). A very different picture emerges once we include flavour effects. The relevant quantity for leptogenesis is then $\Im((Y_\nu Y_\nu^\dagger)_{ij}(Y_\nu)_{il}(Y_\nu^\dagger)_{lj})$ with no summation over the charged lepton index l. Although no *total* CP asymmetries are generated via the RG evolution in the limit $Y_e = 0$, the CP asymmetries for a specific lepton flavour are non-vanishing. Additionally, the resulting η_B now shows a M_ν dependence which stems from the RGE contributions due to Y_ν only, which are absent in the total CP asymmetries in the two flavour limit (orange crosses).
All plots have been generated assuming a normal hierarchy of the light neutrino masses. We have checked that the results for the inverted hierarchy are similar, although η_B turns out to be generally smaller and below the observed value, in accordance with the findings of [84]. Including flavour effects it is however still possible to generate a η_B of the correct order of magnitude. In Fig. 3.5 we additionally show the dependence of η_B on y_{12} and $m_{\nu 1}$. We find that flavour effects enlarge the y_{12} range where successful baryogenesis is possible and slightly soften the upper bound on the light neutrino mass scale. The left panel even demonstrates that leptogenesis in the MLFV scenario is possible for a real R matrix. Then lepton flavour effects are essential [110, 111].

3.5.4 General case

Now we consider the general case with all three phases y_{ij} non-vanishing. We have varied the parameters as described in Section 3.4. The regularisation of the resonant CP asymmetry by the D_i turns out to be important for values of $\epsilon_i \gtrsim 10^{-6}$, see Fig. 3.6. As seen there, in the regime where flavour effects are important we find an upper bound on the light neutrino mass of $m_{\nu 1} \lesssim 0.2$ eV in order to generate the right amount of η_B. Beyond the temperature scale where flavour effects play a role, no relevant bound can be found. This is due to the enhancement of the CP asymmetry which approximately grow linearly for values of $M_\nu \gtrsim 10^{12}$ GeV, see the discussion in Section 3.4.4

In Fig. 3.8, we compare different calculations of η_B:

- the flavour independent estimate of [113] used in Cirigliano et al. [85] (red boxes),
- the numerical solution of the flavour independent Boltzmann equations using the LeptoGen package (black circles),
- the recent estimate by Blanchet and Di Bari [112] that includes flavour effects (green triangles),

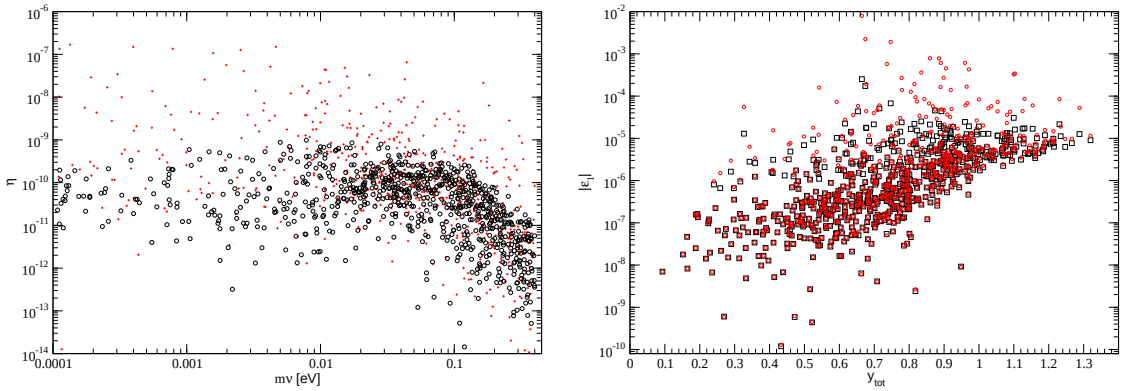

Figure 3.6: (left) η_B for the general case with $0.01 < |y_{ij}| < 1$ as a function of $m_{\nu 1}$ (right). The *black circles* are obtained including lepton flavour effects whereas the *red crosses* are calculated ignoring them. The flavour blind results (*red crosses*) reach higher values due to the CP asymmetries growing as M_ν gets bigger in this regime. (right) The total CP asymmetry $|\epsilon_1|$ for the general case with $0.01 < |y_{ij}| < 0.8$ as a function of $y_{tot} = (y_{12}^2 + y_{13}^2 + y_{23}^2)^{\frac{1}{2}}$ for input values that result in the right oder of magnitude of η_B. The *red circles* are obtained using the uncorrected CP asymmetries and the *black squares* include the corrections by the decay widths

- the approximate expression of [108] given in (3.49) that also includes flavour effects (brown crosses).

We find that

- the flavour blind estimate of [113] used in Cirigliano et. al. [85] lies consistently below the numerical solution of the flavour independent Boltzmann equations. For $M_\nu \geq 10^{12}\,\text{GeV}$ this turns out to be unimportant as flavour effects in this region are small and we confirm the increase of η_B with M_ν in this region found by these authors.

- Potentially large flavour effects that have been left out in [85] generally enhance the predicted η_B, in particular for $M_\nu \leq 10^{12}\,\text{GeV}$, in accordance with the existing literature.

- Both flavour estimates and the numerical solution of the flavour independent Boltzmann equations show solutions with η_B of the measured order of magnitude without imposing a stringent lower bound on the value of M_ν.

The last finding is in contrast to the analysis of Cirigliano et. al. [85] which using the flavour independent estimate of [113] finds a lower bound on M_ν of $\mathcal{O}(10^{12}\text{GeV})$ as clearly represented by the red boxes in Fig. 3.8. The same qualitative conclusion holds for η_B using the RGE induced CP asymmetries in the

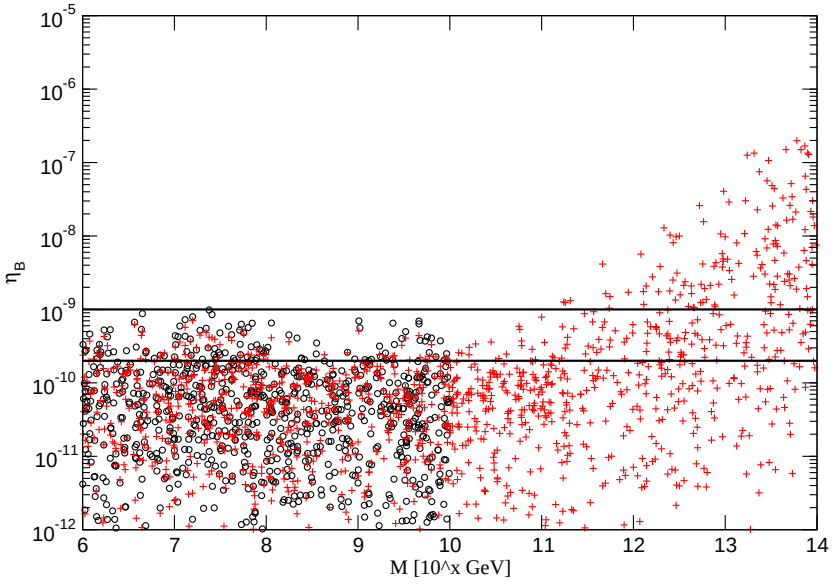

Figure 3.7: η_B for the general case with $0.01 < |y_{ij}| < 1$ as a function of M_ν. The *circles* are obtained including lepton flavour effects and the *red crosses* are calculated ignoring them.

MSSM. The $\tan\beta$ enhancement of the CP asymmetries as discussed in Section 3.4.4 even facilitates the generation of an η_B of the right size.

Our analysis that includes flavour effects demonstrates that baryogenesis through leptogenesis in the framework of MLFV is a stable mechanism and allows a successful generation of η_B over a wide range of parameters. The absence of a lower bound on M_ν found here has of course an impact on the LFV processes, which we will discuss next.

In Fig. 3.9 we show $\mathrm{Br}(\mu \to e\gamma)$ vs. M_ν for the parameter ranges described above and a lepton flavor violation scale of 1 TeV. We highlighted the points where successful baryogenesis is possible (black squares). We find that $\mathrm{Br}(\mu \to e\gamma)$ can be made small enough to evade bounds from current and future experiments and one can have successful baryogenesis through leptogenesis at the same time. This is another finding which is in contrast to a recent analysis [85]. We will summarize the differences to [85] in the next paragraph.

3.5.5 Comparison with [85]

Recently in an independent analysis Cirigliano, Isidori and Porretti [85] generalized MLFV formulation in [76] to include CP violation at low and high energy. Similarly to us they found it convenient to use for Y_ν the parametrization of Casas

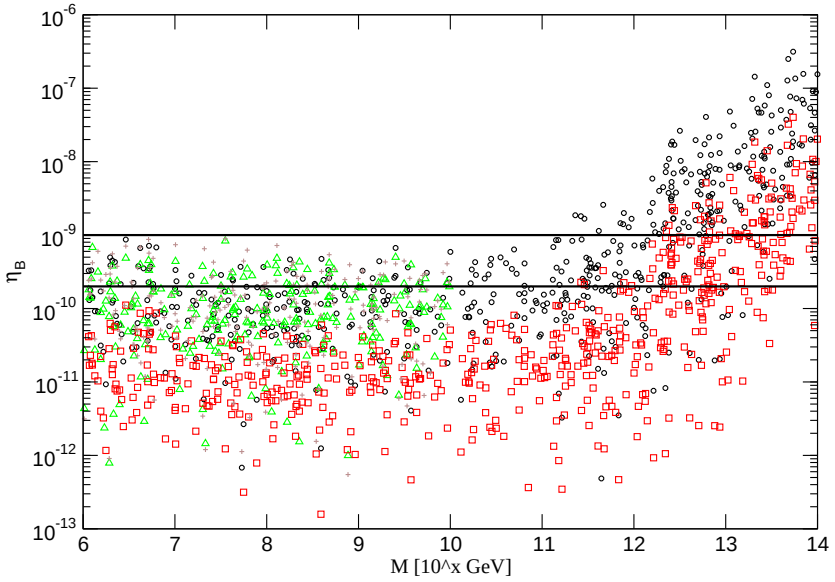

Figure 3.8: Different determinations of η_B for the general case with $0.01 < |y_{ij}| < 1$ as a function of M_ν. The *black circles* are obtained numerically solving the flavour independent Boltzmann equations using the LeptoGen package, the *green triangles* and the *brown crosses* show estimates including flavour effects of [112] and (3.49), respectively. Finally the *red boxes* show the estimate of [113] used in Cirigliano et. al [85] which ignores flavour effects.

and Ibarra. They have also pointed out that in the MFLV framework the most natural is the resonant leptogenesis.

On the other hand, these authors neglected flavour dependent effects in the evaluation of η_B, that we find in agreement with other authors to be important [109, 108, 110, 111, 112]. This has important consequences already at the qualitative level. Their qualitative discussion of the splittings of the M_ν^i at the see-saw scale is similar to ours and we agree with the main physical points made by these authors in this context. On the other hand, while we have demonstrated explicitely by means of a renormalization group analysis that a successful RRL can be achieved, Cirigliano et al confined their analysis to parametrizing possible radiative effects in terms of a few parameters. In this context a new point made by us (see discussion Section 3.3.3) is that the coefficients c_i in (3.19) are in fact not independent of each other. Indeed the leading logarithmic contribution to c_i are related by the renormalization group. This can in principle increase the predictivity of MLFV.
The three most interesting messages of [85] are

- A successful resonant leptogenesis within the MLFV framework implies a lower bound $M_\nu \geq 10^{12}\,\mathrm{GeV}$,

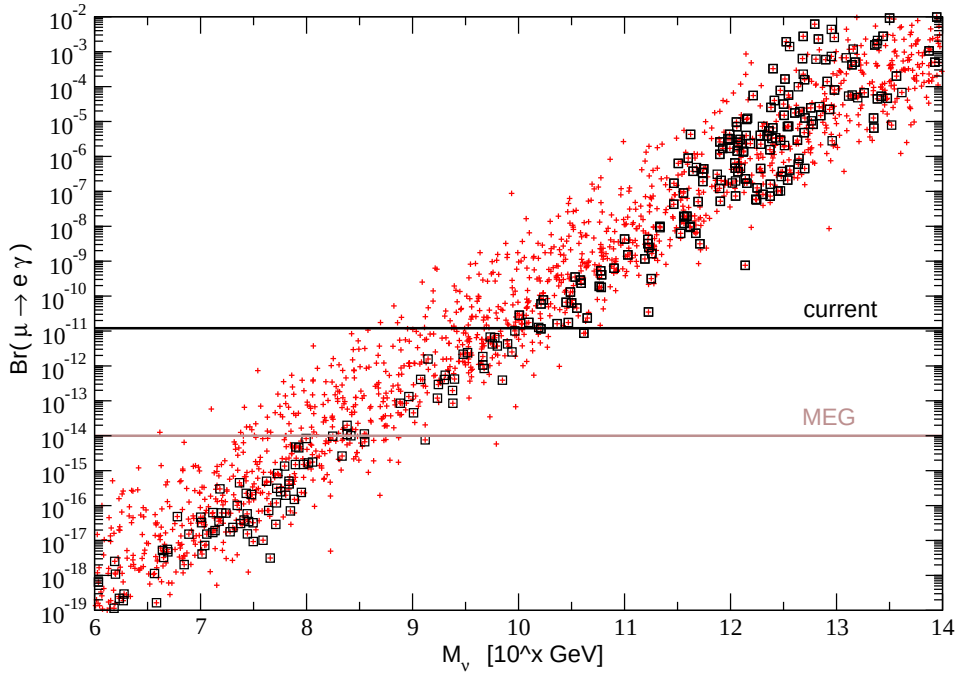

Figure 3.9: B($\mu \to e\gamma$) as a function of M_ν for $\Lambda_{\rm LFV} = 1$ TeV. The *black squares* show points where a baryon asymmetry in the range $2 \cdot 10^{-10} < \eta_B < 10 \cdot 10^{-10}$ is possible.

- With $\Lambda_{\rm LFV} = \mathcal{O}(1\,\text{TeV})$, this lower bound implies the rate for $\mu \to e\gamma$ close to the present exclusion limit,

- MLFV implies a specific pattern of charged LFV rates: $B(\mu \to e\gamma) < B(\tau \to \mu\gamma)$.

For $M_\nu \geq 10^{12}\,\text{GeV}$, in spite of some differences in the numerics as discussed above, we basically confirm these findings. Unfortunately, for lower values of M_ν our results differ from theirs. In particular, as we have demonstrated in Fig. 3.8, the observed value of η_B can be obtained for M_ν by several orders of magnitude below the bound in [85], in accordance with other analyses of leptogenesis. Once M_ν is allowed to be far below $10^{12}\,\text{GeV}$, $\Lambda_{LFV} = \mathcal{O}(1\,\text{TeV})$ does not imply necessarily $B(\mu \to e\gamma)$ close to the inclusion limit as clearly seen in Fig. 3.9.

One of the reasons for the descrepancy between our result with regard to M_ν and the one of [85] is the neglect of flavour effects in leptogenesis in the latter paper. Fig. 3.8 illustrates that flavour effects in leptogenesis matter.

Concerning $B(\mu \to e\gamma) < B(\tau \to \mu\gamma)$, we confirm the result of [85] in the limit of very small y_{12}, but as shown in Fig. 3.1, this is not true in general, as also found in [96, 97]. Consequently, this hierarchy of charged LFV rates cannot be used as model independent signature of MLFV.

3.6 Summary and Conclusions

In this chapter we have generalized the proposal of minimal flavour violation in the lepton sector of [76] to include CP Violation at low and high energy. While the definition proposed in [76] could be considered to be truly minimal, it appears to us too restrictive and not as general as the one in the quark sector (MFV) in which CP violation at low energy is automatically included [10] and in fact all flavour violating effects proceeding through SM Yukawa couplings are taken into account [17]. The new aspect of MLFV in the presence of right-handed neutrinos, when compared with MFV, is that the driving source of flavour violation, the neutrino Yukawa matrix Y_ν, depends generally also on physics at very high scales. This means also on CP violating sources relevant for the generation of baryon-antibaryon asymmetry with the help of leptogenesis. The first discussion of CP violation at low and high energy has been presented in [85]. Our conclusions for $M_\nu \geq 10^{12}$ agree basically with these authors. However, they differ in an essential manner for lower values of M_ν.

Let us conclude this chapter with the following messages:

- A new aspect is the realization that in the context of MLFV the only admissable BAU with the help of leptogenesis is the one through radiative resonant leptogenesis (RRL). Similar observations have been made in [85]. In this context our analysis benefited from the ones in [105, 106, 86, 87]. The numerous analyses of leptogenesis with hierarchical right-handed neutrinos present in the literature are therefore outside the MLFV framework and the differences between the results presented here and the ones found in the literature for $M_1 \ll M_2 \ll M_3$ can be used to distinguish MLFV from these analyses that could be affected by new flavour violating interactions responsible for hierarchical right-handed neutrinos.

- We have demonstrated explicitely within the SM and the MSSM at low $\tan\beta$ that within a general MLFV scenario the right size of η_B can indeed be obtained by means of RRL. The important property of this type of leptogenesis is the very weak sensitivity of η_B to the see-saw scale M_ν so that for scales as low as 10^6 GeV but also as high as 10^{13} GeV, the observed η_B can be found.

- Flavor effects, as addressed by several authors recently in the literature [109, 108, 110, 111, 112], play an important role for $M_\nu \lesssim 10^{10}$ GeV as they generally enhance η_B.

- As charged LFV processes, like $\mu \to e\gamma$ are sensitive functions of M_ν, while η_B is not in the RRL scenario considered here, strong correlations between the rates for these processes and η_B, found in new physics scenarios with other types of leptogenesis can be avoided.

- Except for this important message, several of the observations made by us with regard to the dependence of charged LFV processes on the complex phases in the matrix R and the Majorana phases have been already made by other authors in the rich literature on LFV and leptogenesis. But most of these analyses were done in the context of supersymmetry. Here we would like to emphasize that various effects and several patterns identified there are valid also beyond low energy supersymmetry, even if supersymmetry allows a definite realization of MLFV provided right-handed neutrinos are degenerate in mass at the GUT scale.

- One of the important consequences of the messages above is the realization that the relations between the flavour violating processes in the charged lepton sector, the low energy parameters in the neutrino sector, the LHC physics and the size of η_B are much richer in a general MLFV framework than suggested by [76, 85]. Without a specific MLFV model no general clear cut conclusions about the scale Λ_{LFV} on the basis of a future observation or non-observation of $\mu \to e\gamma$ with the rate $\mathcal{O}(10^{-13})$ can be made in this framework.

- On the other hand we fully agree with the point made in [76] that the observation of $\mu \to e\gamma$ with the rate at the level of 10^{-13}, is much easier to obtain within the MLFV scenario if the scales $\Lambda_{\rm LFV}$ and M_ν are sufficiently separated from each other. We want only to add that the necessary size of this separation is sensitive to the physics between M_Z and $\Lambda_{\rm GUT}$, Majorana phases and CP violation at high energy. In this manner the lepton flavour violating processes, even in the MLFV framework, probe scales well above the scales attainable at LHC, which is not necessarily the case within MFV in the quark sector.

- Finally, but very importantly, MLFV being very sensitive to new physics at high energy scales, does not generally solve possible CP and flavour problems. This should be contrasted with the MFV in the quark sector, where the sensitivity to new physics at scales larger than 1 TeV is suppressed by GIM mechanism.

Chapter 4

Warped Wilson Line Phases

4.1 Introduction

Electroweak symmetry breaking and the hierarchy problem are the central issues of high-energy physics in the remaining years until the start of the measurements at the Large Hadron Collider (LHC) at CERN. The leading candidate to stabilize the Higgs mass is the minimal supersymmetric standard model (MSSM). Direct and indirect measurements, however, have led to a ever-rising scale of the supersymmetric particle masses to considerable fine-tuning of the parameters, especially if one wants to reproduce the electroweak symmetry breaking scale. Within the most popular supersymmetric models experimental constraints have already excluded large portions of the parameter space ($\approx 99\%$ in the case of universal soft masses [116]). Alternatives to the MSSM have therefore gained increasing attention. Gauge-Higgs unification (GHU) models are interesting contenders which allow, when embedded in a warped space-time, to dynamically break the electroweak symmetry and solve the hierarchy problem at the same time.

The recent years have led to remarkable results in the framework of GHU. It could be shown that the instability of the electroweak scale under radiative corrections, the hierarchy problem, can be resolved, if one breaks the electroweak symmetry by means of new mechanisms in extra-dimensions. It has been known for a long time [117] that identifying the Higgs as the zero-mode of the fifth component of a 5 dimensional gauge field renders the effective potential stable and the Higgs mass is not sensitive to the UV scale anymore. This idea has been re-inspected in the recent years and has led to realizations in the framework of higher-dimensional orbifold models. A somewhat minimal model has been given in [118]. Here, the gauge symmetry is broken by a combination of Z_2 projection and Scherk-Schwarz (SS) twists. Electroweak symmetry breaking then happens dynamically and non-locally by the so-called Hosotani mechanism [119]. All properties of the electroweak sector can be derived from the effective potential

and allow a direct test of the models.

Very recently these constructions have been extended to warped extra dimensions and have for the first time resulted in completely realistic predictions[120]. Using the duality between five-dimensional Anti-deSitter space and strongly coupled conformal field theory in 4 dimensions, these models even allow an interpretation reminding of 'walking technicolor' constructions.

As we will see, GHU in flat extra dimensions is not completely realistic at the moment. One has to put a lot of effort in raising the scale of the Higgs mass beyond the weak gauge-bosons scale. Only when adding large kinetic terms on the branes one can generate a realistic Higgs mass. Large kinetic terms on the branes, however, are a dynamical consequence of the Randall-Sundrum model in warped extra-dimensions. This motivates a calculation of the effective potential in warped extra-dimensions which will be one of the main results of this section.

We will first discuss the minimal model of [118] in flat extra dimensions and work out the problems. In Section 4.2.2, we briefly review the Hosotani mechanism on the orbifold S^1/Z_2. In Section 4.3.1, we obtain the Kaluza-Klein (KK) expansions of the five dimensional gauge and ghost fields with most general twists in the presence of a gauge field background. Then we will discuss the properties of the so-called Wilson line phase (WLP) in warped extra dimensions. [1]

In Section 4.3.2, we calculate the effective potential for the extra dimensional component of the background gauge field.

In the last section we summarize and discuss our result and we will give an outlook and show how it helps to avoid the problems of flat space constructions.

4.2 Flat extra dimensions

4.2.1 Gauge Higgs unification in flat extra dimensions

The simplest possibility allowing an embedding of the Higgs field as an internal component of a gauge field is a 5D gauge theory with the gauge group $G = SU(3)$ on the orbifold S^1/Z_2. The orbifold S^1/Z_2 has two fixed points and we have to specify the boundary conditions. Equivalently we can fix the behaviour under a reflection $y \to -y$ (P) and translation $y \to y + 2\pi R$ (T) along the internal coordinate y. Since we want to preserve a $SU(2)$ symmetry we will choose the following Z_2 orbifold projection

$$P = e^{i\pi\lambda_3} = \begin{pmatrix} -1 & 0 & 0 \\ 0 & -1 & 0 \\ 0 & 0 & 1 \end{pmatrix} , \tag{4.1}$$

where λ_a are the $SU(3)$ Gell-Mann matrices, normalized as $\mathrm{Tr}\,\lambda_a\lambda_b = 2\delta_{ab}$, so that $A_M = A_M^a\lambda_a/2$.

[1] The results of this chapter are based on our paper [121],

In the low-energy 4 D limit the group G is broken to the subgroup $H = SU(2)$ that commutes with P. The massless degrees of freedom are the 4D gauge bosons and a charged scalar doublet which stems from the internal components A_5^a of the gauge field. A VEV for A_5 leads to additional spontaneous symmetry breaking to $E = \hat{U}(1)$. The generators of E are given by $\hat{A}_\mu = (A_\mu^8 + \sqrt{3}A_\mu^3)/2$. Since a $SU(2)$ symmetry remains after orbifolding we can always choose $\langle A_5 \rangle$ along the λ_7 component, corresponding to the down component of the doublet, and take

$$\langle A_5^a \rangle = \frac{2\theta}{g_5 \pi R}\, \delta^{a7} \,. \tag{4.2}$$

The above is a description of electroweak symmetry breaking once we identify H with the electroweak gauge group, E with the electromagnetic group, and the zero-mode of A_5 with the Higgs field H.

Since we embedded the SM gauge group in a simple gauge-group $G = SU(3)$ we will get a prediction for the weak mixing angle θ_W which however turns out to be too large, $\theta_W = \pi/3$. In a more realistic construction this would be avoided by starting with a different unified group G, namely by adding a $U(1)$ factor to G and taking the electro-magnetic $U(1)$ as the diagonal of E and the additional $U(1)$ factor. We will not discuss this further since it does not impact our discussion of issues related to the effective potential and the extension to include the extra $U(1)$ is straightforward.

Taking into account the normalization of the zero-mode, (4.2) corresponds to a VEV for the neutral component of the Higgs doublet H equal to $2\theta/(g_4 \pi R)$, where we have used the relation between the 4 D and 5 D coupling constant

$$g_4 = \frac{g_5}{\sqrt{2\pi R}} \,. \tag{4.3}$$

It has been known for some time [122] that a VEV for A_5 induces a Wilson line which is equivalent to a Scherk–Schwarz twist, the two situations being related through a non-periodic gauge transformation. We will discuss this relation further in the following paragraph for general $SU(N)$ gauge groups. The twist matrix $T(\theta)$ satisfies the consistency condition $TPT = P$; for the choice (4.2), it is given in our simple model by

$$T(\theta) = e^{2i\theta\lambda_7} = \begin{pmatrix} 1 & 0 & 0 \\ 0 & \cos 2\theta & \sin 2\theta \\ 0 & -\sin 2\theta & \cos 2\theta \end{pmatrix} . \tag{4.4}$$

The orbifold projection is a soft symmetry breaking of G to H, the masses of the fields in G/H being of order $1/R$, with all the UV Ward identities intact, whereas the Scherk-Schwarz twist corresponds to a spontaneous symmetry breaking of H to E, the masses of the fields in H/E being of order $\theta/(\pi R)$.

After spontaneous symmetry breaking induced by (4.2), we have to define a new basis for the gauge-field modes to diagonalize their mass terms. We will

choose the complex gauge field $A_\mu^{(1)}$ with charge $q^{(1)} = 1$ ($\Psi_0^{+(1)}$) and identify it with the W boson, the real field $A_\mu^{(2)}$ with $q^{(2)} = 2$ ($\Psi_0^{+(2)}$) is identified with the Z boson and the neutral field $A_\mu^{(0)}$ ($\Psi_0^{+(3)}$) with the photon. Similarly, the scalar field $A_5^{(0)}$ ($\Psi_0^{-(4)}$) is identified with the physical component of the Higgs field H that is left over after the spontaneous symmetry breaking. Due to $\sec\theta_W = 2$, we find for the masses of the W and Z fields

$$m_W = \frac{\theta}{\pi R}\ , \quad m_Z = 2\frac{\theta}{\pi R}\ . \tag{4.5}$$

The Higgs mass is radiatively induced after electroweak symmetry breaking and as in the case of the SM Higgs mechanism depends on the second derivative of the potential evaluated at the minimum:

$$m_H = \frac{g_4 \pi R}{2}\sqrt{V''(\theta)}\ . \tag{4.6}$$

This potential, however, is now radiatively generated and flat on tree level. Its shape and potential minimum will depend on the exact matter content contributing to the radiative corrections.

4.2.2 Wilson lines on flat S^1/Z_2

We briefly review how twists and background gauge field configurations are related by large gauge transformations. We consider a five dimensional $SU(N)$ gauge theory compactified on the orbifold S^1/Z_2, which is obtained from the simply-connected space $R^1 : -\infty < y < \infty$ by modding with S^1 and Z_2 identifications $y \sim y + 2\pi R$ and $y \sim -y$, where R is the compactification radius.

Under these identifications, the gauge fields A_M ($M = 0, \ldots, 3; 4$) are in general twisted by global $SU(N)$ transformations

$$\begin{aligned} A_M(-y) &= \pm P_0 A_M(y) P_0^{-1}, \\ A_M(\pi R + y) &= \pm P_1 A_M(\pi R - y) P_1^{-1}, \qquad (4.7) \\ A_M(y + 2\pi R) &= U A_M(y) U^{-1}, \qquad (4.8) \end{aligned}$$

where the extra $\pm$ sign is positive for four dimensions and negative for the extra dimension.[2] We use μ for $0, \ldots, 3$ and y for both x^4 and index "4" such as $A_y = A_4$.

Note that the consistency conditions $U = P_1 P_0$ and $P_0^2 = P_1^2 = 1$ are imposed.

Starting from the most general twists we can always choose the following basis [123]

[2] In principle local identifications are possible but we assume them global for simplicity here.

$$\begin{array}{rcl} P_0 & = & \text{blockdiag}\,(\sigma_3, \quad \ldots, \quad \sigma_3, \quad I_r, \quad I_s, \quad -I_t, \quad -I_u), \\ P_1 & = & \text{blockdiag}\,(\sigma_{\theta_1}, \quad \ldots, \quad \sigma_{\theta_q}, \quad I_r, \quad -I_s, \quad I_t, \quad -I_u), \end{array} \tag{4.9}$$

where I_r is $r \times r$ unit matrix, σ_a $(a = 1, 2, 3)$ are Pauli matrices, and

$$\sigma_\theta = \sigma_3 \cos\theta + \sigma_1 \sin\theta = e^{-i\theta\sigma_2}\sigma_3 = \sigma_3 e^{i\theta\sigma_2}. \tag{4.10}$$

with $2q + r + s + t + u = N$. The A_y^a either within a block of $\pm I$ or connecting different blocks does not have a zero-mode, a mode having vanishing KK mass, and the dynamics of the corresponding Wilson line is trivial [124].[3] Therefore we can concentrate on a $SU(2)$ subblock with twists

$$P_0 = \sigma_3, \tag{4.11}$$

$$P_1 = \sigma_\theta, \tag{4.12}$$

without loss of generality. In general, only $A_y^{(2)}$ ($A_M = A_M^{(a)}\sigma_a/2$) has even Z_2 parities, hence a zero mode background: $gA_y^{(2)c} \equiv v$. The KK expansions are given by

$$A_\mu^{(2)}(x, y) = \sum_{n=1}^{\infty} A_{\mu n}^{(2)}(x) \frac{\sin\frac{ny}{R}}{\sqrt{\pi R}}, \tag{4.13}$$

$$A_y^{(2)}(x, y) = A_{y0}^{(2)}(x) \frac{1}{\sqrt{2\pi R}} + \sum_{n=1}^{\infty} A_{yn}^{(2)}(x) \frac{\cos\frac{ny}{R}}{\sqrt{\pi R}}, \tag{4.14}$$

$$A_\mu^{\pm}(x, y) = \sum_{n=-\infty}^{\infty} A_{\mu n}(x) \frac{e^{\pm i(m_n + v)y}}{N_n}, \tag{4.15}$$

$$A_y^{\pm}(x, y) = \pm i \sum_{n=-\infty}^{\infty} A_{yn}(x) \frac{e^{\pm i(m_n + v)y}}{N_n}, \tag{4.16}$$

where $A_M^{\pm} = \frac{A_M^{(3)} \pm i A_M^{(1)}}{\sqrt{2}}$, $A_{Mn}(x)$ are real fields,

$$m_n = \frac{n}{R} + \frac{\theta}{\pi R} - v \tag{4.17}$$

are KK masses, and

$$N_n = \sqrt{2\pi R}\, m_n \tag{4.18}$$

are normalization constants. Here we present a different form as in the literature in Eq. (4.16) to make the orthogonality of the wave functions transparent.

[3] Of course when, say, $r < u$, we can combine I_r and a part of $-I_u$ to form r additional σ_θ blocks with $\theta = 0$.

Consider the following large gauge transformation that is non-periodic on the covering space R^1:

$$igA_M(y) \to ig\widetilde{A}_M(y) = \left[\Omega\left(igA_M - \overleftarrow{\partial_M}\right)\Omega^{-1}\right](y) \tag{4.19}$$

with

$$\Omega(y) = \exp\left[i\varphi y\frac{\sigma_2}{2}\right], \tag{4.20}$$

which results in

$$g\widetilde{A}_y^{(2)c} = v - \varphi/\pi R. \tag{4.21}$$

We find that the shift of the background is canceled by the transformation of

$$A_M^{\pm} \to \widetilde{A}_M^{\pm} = e^{\mp i\varphi y/\pi R}A_M^{\pm} \tag{4.22}$$

leaving its KK masses invariant: $\widetilde{m}_n = m_n$. Now the new fields are twisted by matrices

$$\widetilde{P}_0 = \sigma_3, \tag{4.23}$$

$$\widetilde{P}_1 = \sigma_{\theta-\varphi} \equiv \sigma_{\tilde{\theta}}. \tag{4.24}$$

Above, the two sets of twists P_i and $\widetilde{P}_i$ with the corresponding backgrounds are equivalent under the large gauge transformation, by which one may e.g. diagonalize the twist $\tilde{\theta} = 0$ or remove the background $\widetilde{A}_y^{(2)c} = 0$, but not both.

If we choose to take the former (or latter) gauge, different values of $\widetilde{A}_y^{(2)c}$ (or $\tilde{\theta}$) correspond to physically different vacua which are degenerate at the classical level. Quantum corrections determine whether the symmetry is dynamically broken or restored, depending on the matter content [122, 123].

4.2.3 Problems of gauge-Higgs unification in flat space

Given the field content one can compute the one-loop Higgs effective potential $V(H)$. Since the symmetry is broken in a non-local way, it is necessarily finite. One finds in flat extra dimensions that an EWSB occurs with values of the Wilson line phase at the minimum which is about $\theta \sim 1/2$. Qualitatively we can reproduce all the features of the SM. Quantitatively, flat extra dimensional models run into problems. These problems are a general characteristic of the models considered so far and can even be predicted to occur on rather general grounds.

- The one-loop Higgs effective potential $V(H)$ is radiatively generated and one would expect a small quartic self-coupling, leading to a small Higgs mass

$$m_H \sim \sqrt{\frac{\alpha_W}{30}}\,\frac{1}{R} \sim \sqrt{\frac{\alpha_W}{30}}\,\frac{\pi m_W}{|\sin\theta|} \tag{4.25}$$

which typically gives a too small $m_H \sim 10\,\text{GeV}$. Of course, θ can be small as a result of cancellations among contributions from various matter fields. However, it requires tuning of the matter content. We will argue that natural resolution of the problem can be found once gauge-Higgs unification is embedded in Randall-Sundrum space-time.

- The strict relation between the Wilson line phase at the minimum, the mass of the EW gauge bosons and the compactification scale $1/R$ given by $M_W = \theta/(\pi R)$ leads to Kaluza-Klein excitations of the SM gauge bosons of mass

$$1/R = \pi M_W/\theta, \tag{4.26}$$

which are excluded by current bounds for non-finetuned values of θ, see e.g. [125].

There are various solutions to these problems. One way is to increase the 5D gauge coupling constant g_5 which is responsible for the size of the Yukawa couplings and the Higgs effective potential. In flat extra dimensions the simple relation

$$g_5 = g_4\sqrt{2\pi R} \tag{4.27}$$

holds. Since $1/R$ and g_4 are determined by the experimental values of M_W and the SM gauge coupling constant, the only possibility to increase g_5 is to introduce modifications which affect the relation between g_5 and g_4. Adding kinetic terms for the 4D gauge fields on the branes is a possibility. One can tune those terms and make them large enough to increase the Higgs mass to phenomenologically acceptable values, see e.g. [118]. As an additional benefit, the masses of the KK excitations get shifted above the current bounds. However, one also pays a price due to the induced mixing between the Kaluza Klein states by these terms. Two devastating results are the violation of universality of 4D gauge couplings and a contribution to the ρ parameter which exceeds the current limit [118].

Motivated by this partial solution in flat space by adding large kinetic terms to the brane one is lead to consider curved space extra dimensions. In these so called warped set-ups, localized kinetic terms are dynamically generated and could offer a solution to the above mentioned problems.

4.3 Warped extra dimensions

4.3.1 Kaluza-Klein expansion in warped space

Warped compactification not only provides a beautiful explanation how the large hierarchy $m_{\text{weak}}/M_{\text{Planck}}$ is generated from the exponential profile of its metric [9] but also is itself a quite general consequence of string theory due to the fact

that D-branes generically provide sources for warping (See [126] and references therein).

In the original Randall-Sundrum model [9], five dimensional spacetime is compactified on the orbifold S^1/Z_2, along which the normalization of the four dimensional metric is exponentially scaled.[4]

Eventually, the vacuum expectation value (vev) of the $SU(2)$ gauge field that is related to the Scherk-Schwarz twist must be determined dynamically by quantum corrections to the effective potential.

To that end, it is important to solve the dynamics of Wilson lines in warped space, which has not been explored so far.[5]

We consider a $SU(N)$ gauge theory in the bulk of the Randall-Sundrum geometry [9], which is a five dimensional Anti de Sitter (AdS) space compactified on S^1/Z_2 with the metric:

$$G_{MN}dx^M dx^N = e^{-2\sigma(y)}\eta_{\mu\nu}dx^\mu dx^\nu + dy^2, \tag{4.28}$$

where $\eta_{\mu\nu}$ is the Lorentzian metric and $\sigma(y)$ is defined by

$$\sigma(y) = k|y| \tag{4.29}$$

in $-\pi R < y \leq \pi R$, with k being the inverse AdS curvature radius. Elsewhere on the covering space R^1, we define σ by the periodicity condition $\sigma(y+2\pi R) = \sigma(y)$. For later use we also define

$$\epsilon(y) = \sigma'(y)/k \tag{4.30}$$

and

$$z(y) = e^{\sigma(y)}. \tag{4.31}$$

When there arises an ambiguity at the orbifold fixed point, say, around $y = 0$, we can use the regularized form $\sigma(y) = k\delta \log\cosh(y/\delta)$ with an infinitesimal $\delta = +0$ to check the expression. For our purpose we can use

$$\epsilon(y) = \theta(y) - \theta(-y), \tag{4.32}$$

$$\epsilon'(y) = 2\left[\delta(y) - \delta(y - \pi R)\right], \tag{4.33}$$

$$\epsilon(y)^2 = 1, \tag{4.34}$$

at $-\pi R < y \leq \pi R$. We call the orbifold fixed points at $y = 0$ and $y = \pi R$ ultraviolet (UV) and infrared (IR) branes, respectively, and write

$$z_0 = z(0) = 1 \tag{4.35}$$

[4]For a pedagogical introduction to warped extra dimensions, see e.g. [127]. In Appendix B, we collect the most useful formulae for calculations in warped extra-dimensions.

[5] In Ref. [128] a Wilson line in warped space is considered in the context of the AdS/Conformal Field Theory (CFT) correspondence, where the analysis is confined to a (potentially false) vacuum that corresponds to imposing both diagonal twists and vanishing background field configurations. See Ref. [129] for further discussions.

and

$$z_1 = z(\pi R) = e^{\pi k R}. \tag{4.36}$$

Here we assume that the radion is already stabilized e.g. by the Goldberger-Wise mechanism [130].

We employ the background field method, separating the gauge field into classical and quantum parts

$$A_M = A^c_M + A'_M, \tag{4.37}$$

and take the following gauge fixing[6]

$$S_f = -\frac{1}{\xi}\int d^4x \int_{-\pi R}^{\pi R} dy \sqrt{-G}\,\mathrm{tr}\,[ff]\,, \tag{4.38}$$

with

$$f = z^2 \eta^{\mu\nu} D^c_\mu A'_\nu + \xi z^t D^c_y z^{-t} A'_y, \tag{4.39}$$

where D_M is the gauge covariant derivative and the superscript c indicates that the gauge field is replaced by its classical part, e.g.

$$D^c_M A'_N = \partial_M A'_N + ig[A^c_M, A'_N]. \tag{4.40}$$

We consider the pure gauge background $F^c_{MN} = 0$, being a classical potential minimum, and assume $A^c_\mu = 0$ since it can be gauged away towards spatial infinity.

When we choose $\xi = 1$ and $t = 2$, the quadratic terms for the gauge and ghost fields simplify:

$$S = \int d^4x \int_{-\pi R}^{\pi R} dy\,\mathrm{tr}\left[\eta^{\mu\nu} A'_\mu(\Box + \mathcal{P}_4)A'_\nu + A'_y z^{-2}(\Box + \mathcal{P}_y)A'_y + 2z^{-2}\overline{\omega}'(\Box + \mathcal{P}_4)\omega'\right], \tag{4.41}$$

where

$$\mathcal{P}_4 = D^c_y z^{-2} D^c_y, \tag{4.42}$$

$$\mathcal{P}_y = D^c_y D^c_y z^{-2}, \tag{4.43}$$

and we have put $\omega^c = \overline{\omega}^c = 0$. The surface terms vanish consistently for the given boundary conditions below.

Following the same argument as in the flat case, we concentrate on a $SU(2)$ subblock with twists $P_0 = \sigma_3$ and $P_1 = \sigma_\theta$, without loss of generality. Again a

[6] The choice $t = 4$ and $\xi = 1$ makes f manifestly invariant under five dimensional diffeomorphisms.

zero mode resides only in $A_y^{(2)}$ and we can write $gA_y^{(2)c}(y) = vz^2$. (The derivation of the form of zero mode z^2 is given below.)

To obtain the KK expansions, we follow the strategy of Ref. [131].

First, we solve the bulk KK equations at $0 < y < \pi R$ in terms of z neglecting all the boundary effects. Second, we put the boundary conditions at $z = z_0$ and z_1 on the obtained "downstairs" solution to make it consistent with the Z_2 twists so that the "upstairs" field on the covering space is well-defined, i.e. continuous everywhere.

Let us start with $A_\mu^{(2)}$ and $A_y^{(2)}$ which have definite odd and even Z_2 parities. We obtain the following KK expansions

$$A_\mu^{(2)}(x,y) = \sum_{n=1}^{\infty} A_{\mu n}^{(2)}(x)\epsilon\frac{z[J_1(\hat{M}_n z) + B_n Y_1(\hat{M}_n z)]}{N_n}, \tag{4.44}$$

$$A_y^{(2)}(x,y) = \sum_{n=0}^{\infty} A_{yn}^{(2)}(x)\frac{f_n(z)}{\mathcal{N}_n}, \tag{4.45}$$

where $N_n, \mathcal{N}_n$ are normalization constants,

$$B_n = -\frac{J_1(\hat{M}_n z_0)}{Y_1(\hat{M}_n z_0)} = -\frac{J_1(\hat{M}_n z_1)}{Y_1(\hat{M}_n z_1)}, \tag{4.46}$$

and the downstairs KK wave functions for vectoscalar

$$f_n(z) = z^2[J_0(\hat{M}_n z) + B_n Y_0(\hat{M}_n z)] \tag{4.47}$$

are defined for later use.

The KK masses

$$M_n = k\hat{M}_n \tag{4.48}$$

are determined by zeros of the KK mass function:

$$J_1(\hat{M}z_1)Y_1(\hat{M}z_0) - Y_1(\hat{M}z_1)J_1(\hat{M}z_0), \tag{4.49}$$

which we find is exactly the same for both $A_\mu^{(2)}$ and $A_y^{(2)}$.

In order to get the KK expansions of $A_M^{\pm}$, it is convenient to perform the large (background) gauge transformation (4.20), which again results in the new twists $\widetilde{P}_0 = \sigma_3$, $\widetilde{P}_1 = \sigma_{\theta-\varphi} \equiv \sigma_{\tilde{\theta}}$ and the background

$$g\widetilde{A}_y^{(2)c} = vz^2 - \frac{\varphi}{\pi R} = \left(v - \frac{2ka^2\varphi}{1-a^2}\right)z^2 - \frac{\varphi}{\pi R}\sum_{n=1}^{\infty}\frac{(1,f_n)}{\mathcal{N}_n^2}f_n(z), \tag{4.50}$$

where $a = z_0/z_1 = e^{-k\pi R} \ll 1$ and

$$(1, f_n) = \int_{z_0}^{z_1} 2\frac{dz}{kz}z^{-2}f_n(z). \tag{4.51}$$

Unlike in the flat case, all the higher KK modes are generated, as can be seen in the last step of Eq. (4.50).

However, these higher modes all vanish when integrated along the extra dimension in the Wilson line due to the orthogonality conditions of KK wave functions and one would expect that these modes can be gauged away.

To see this, consider the following background gauge transformation

$$\check{\Omega}(y) = \exp\left[i\mathcal{F}(y)\frac{\sigma_2}{2}\right], \tag{4.52}$$

which we require to be normal in the sense that $\mathcal{F}(y)$ is continuous everywhere and periodic $\mathcal{F}(y+2\pi R) = \mathcal{F}(y)$. When $\mathcal{F}(y)$ is odd $\mathcal{F}(-y) = -\mathcal{F}(y)$, twists P_i are left invariant under this transformation, while gauge fields transform as

$$gA_y^{(2)} \to g\widetilde{A}_y^{(2)} = gA_y^{(2)} - \mathcal{F}'(y). \tag{4.53}$$

Again, this shift is canceled by the transformation of $A_M^{\pm}$ in its KK mass. Let us take

$$\mathcal{F}(y) = k\sum_{n=1}^{\infty}\varphi_n F_n(y), \tag{4.54}$$

with

$$F_n(y) = \int_0^y dy' f_n\left(z(y')\right), \tag{4.55}$$

where the summation is over all the non-zero modes.

By definition, $F_n(y)$ is odd and its derivative is $f_n(y)$. Due to the downstairs boundary conditions, we find that $F_n(y)$ vanishes at both boundaries, i.e., the transformation $\check{\Omega}(y)$ is continuous everywhere on the covering space as well as periodic, as promised. To summarize, all the non-zero mode can always be removed by taking φ_n appropriately, without changing the twists P_i.

Now we choose $\varphi = \theta$ to diagonalize the twist $\tilde{\theta} = 0$ and gauge away all the resulting non-zero mode background. We then have definite Z_2 parity for all $\widetilde{A}_M^{(a)}$. Hereafter we omit the tilde for notational simplicity. The KK expansions are obtained as[7]

$$A_\mu^{\pm}(x,y) = \sum_{n=0}^{\infty} A_{\mu n}(x)E^{\pm i\epsilon\hat{v}z^2/2}\frac{\chi_{1,n}^{\pm}(z)}{N_n}, \tag{4.56}$$

$$A_y^{\pm}(x,y) = \sum_{n=0}^{\infty} A_{yn}(x)\epsilon E^{\pm i\epsilon\hat{v}z^2/2}\frac{\chi_{0,n}^{\pm}(z)}{\mathcal{N}_n}, \tag{4.57}$$

[7] To derive Eq. (4.57) we have used $\epsilon^2 = 1$ in $A_y^{(1)}$, which can be justified similarly as above.

where $A_{Mn}(x)$ are real fields,

$$\hat{v} = v/k - 2\theta a^2/(1-a^2) \tag{4.58}$$

is the dimensionless vev,

$$E^{\pm i\epsilon w} \equiv \cos w \pm i\epsilon \sin w, \tag{4.59}$$

N_n and $\mathcal{N}_n$ are normalization constants, and

$$\chi^{\pm}_{\nu,n}(z) = z^{2-\nu}[\alpha^{\pm}_n J_\nu(\hat{m}_n z) + \beta^{\pm}_n Y_\nu(\hat{m}_n z)] \tag{4.60}$$

are the downstairs KK wave functions with $\hat{m}_n \equiv m_n/k$ and $\alpha^{\pm}_n, \beta^{\pm}_n$ being dimensionless KK masses and complex constants, respectively. Note that

$$\alpha^{\pm}_n = \frac{\alpha^{(3)}_n \pm i\alpha^{(1)}_n}{\sqrt{2}}. \tag{4.61}$$

The boundary conditions on the downstairs fields can be summarized as

$$M(\hat{m}_n)\vec{V} = 0, \tag{4.62}$$

with $\vec{V} = (\alpha^{(3)}_n\ \beta^{(3)}_n\ \alpha^{(1)}_n\ \beta^{(1)}_n)^T$ for A_μ, $\vec{V} = (\alpha^{(1)}_n\ \beta^{(1)}_n\ \alpha^{(3)}_n\ \beta^{(3)}_n)^T$ for A_y, and

$$M(\hat{m}_n) = \begin{pmatrix} \mathcal{J}_C(1) & \mathcal{Y}_C(1) & \mp\mathcal{J}_S(1) & \mp\mathcal{Y}_S(1) \\ \mathcal{J}_C(0) & \mathcal{Y}_C(0) & \mp\mathcal{J}_S(0) & \mp\mathcal{Y}_S(0) \\ \pm\sin\frac{\hat{v}z_1^2}{2} J_\nu(\hat{m}_n z_1) & \pm\sin\frac{\hat{v}z_1^2}{2} Y_\nu(\hat{m}_n z_1) & \cos\frac{\hat{v}z_1^2}{2} J_\nu(\hat{m}_n z_1) & \cos\frac{\hat{v}z_1^2}{2} Y_\nu(\hat{m}_n z_1) \\ \pm\sin\frac{\hat{v}z_0^2}{2} J_\nu(\hat{m}_n z_0) & \pm\sin\frac{\hat{v}z_0^2}{2} Y_\nu(\hat{m}_n z_0) & \cos\frac{\hat{v}z_0^2}{2} J_\nu(\hat{m}_n z_0) & \cos\frac{\hat{v}z_0^2}{2} Y_\nu(\hat{m}_n z_0) \end{pmatrix},$$

where upper and lower signs as well as $\nu = 1$ and 0 are for A_μ and A_y, respectively, and

$$\begin{pmatrix} \mathcal{J}_C(i) \\ \mathcal{J}_S(i) \end{pmatrix} = \begin{pmatrix} \cos\frac{\hat{v}z_i^2}{2} & -\sin\frac{\hat{v}z_i^2}{2} \\ \sin\frac{\hat{v}z_i^2}{2} & \cos\frac{\hat{v}z_i^2}{2} \end{pmatrix} \begin{pmatrix} \nu J_\nu(\hat{m}z_i) + \hat{m}_n z_i J'_\nu(\hat{m}z_i) \\ \hat{v}z_i^2 J_\nu(\hat{m}z_i) \end{pmatrix},$$

and the $\mathcal{Y}_C$ and $\mathcal{Y}_S$ are defined similarly to $\mathcal{J}_C$ and $\mathcal{J}_S$ with J replaced by Y. [8] The KK mass function for $A^{\pm}$ is obtained from the determinant of the boundary condition matrix:

$$N(\hat{m}) = \det M(\hat{m}), \tag{4.63}$$

and $N(\hat{m}) = 0$ determines the KK masses. We find that the N's are exactly the same for A_μ and A_y and that its dependence on $\hat{v}$ is only through the term

$$\frac{2}{\pi^2}\cos[\hat{v}(z_1^2 - z_0^2)]. \tag{4.64}$$

[8] J_ν and Y_ν are Bessel functions of order ν.

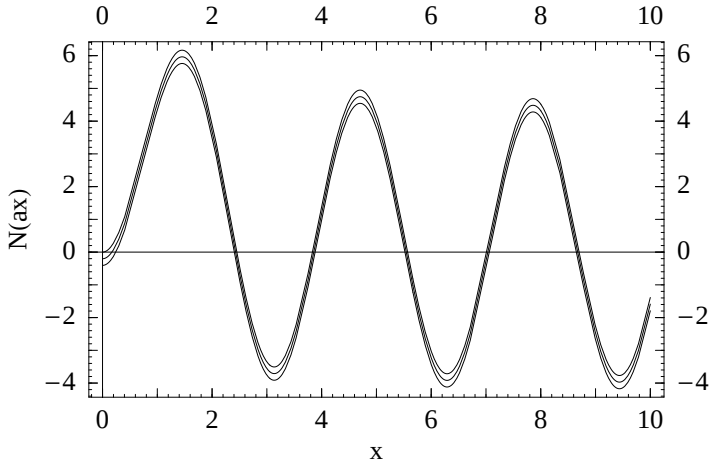

Figure 4.1: KK mass function $N(ax)$ vs x with $a = 10^{-15}$ for $\hat{v}/a^2 = 0, \frac{\pi}{2}, \pi$. The zeros of N correspond to the KK masses. Note that a massless mode appears only for $\hat{v} = 0 \bmod 2\pi$.

The KK expansions for the ghost field is obtained similarly to A_μ. Recall that the antighost field $\overline{\omega}$ is not necessarily the complex conjugate of the ghost field ω.

In Fig. 4.1 we plot $N(ax)$ as a function of $x = \hat{m}/a$ within half a period of $\hat{v}$, i.e. for $\hat{v}(z_1^2 - z_0^2) = 0, \pi/2, \pi$ from above to below when $a = 10^{-15}$. The points where the curve crosses the x-axis give the values of the corresponding KK masses, with even and odd modes appearing in alternating order. We can see that there appears an extra massless mode for $\hat{v} = 0$, as expected, and that the dependence on the variation of $\hat{v}$ is strongest for this would-be zero mode, whose mass can be easily determined from Eq. (4.63) to be

$$m_0 = ka\sqrt{\frac{1 - \cos(\hat{v}/a^2)}{k\pi R}}, \tag{4.65}$$

in the approximation $a \ll 1$. For the maximal breaking with $\cos(\hat{v}/a^2) = -1$, we find $m_0 \approx 0.24\, ka$ for $a = 10^{-15}$.

4.3.2 One loop effective potential

We perform the dimensional reduction in the coordinate frame where the warp factor is unity at the UV brane.[9] The contribution of a pair of Z_2 even and odd

[9] The physical effective potential from the point of view of the IR brane will be enhanced by a^{-4} [132].

gauge fields $A_M^{(3)}$ and $A_M^{(1)}$ is

$$V_{\rm eff} = \frac{\mu^{4-d}}{2}\int\frac{d^dp}{(2\pi)^d}\sum_{n=0}^{\infty}\log(p^2+m_n^2) = -\frac{1}{2}\frac{(ka)^4}{(4\pi)^2}\left(\frac{4\pi\mu^2}{k^2a^2}\right)^{\varepsilon/2}\Gamma\left(-2+\frac{\varepsilon}{2}\right)\sum_{n=0}^{\infty}x_n^{4-\varepsilon}, \tag{4.66}$$

per degree of freedom, where $d = 4-\varepsilon$ is the number of dimensions with ε being infinitesimal, μ is an arbitrary scale, and $x_n = m_n/ka$ is the dimensionless KK mass. The infinite sum over KK masses can be evaluated utilizing zeta function regularization techniques [132, 133, 134]

$$v_{\rm eff}(\hat{v}) \equiv -\Gamma\left(-2+\frac{\varepsilon}{2}\right)\sum_{n=0}^{\infty}x_n^{4-\varepsilon} = -\Gamma\left(-2+\frac{\varepsilon}{2}\right)\int_C\frac{dx}{2\pi i}x^{4-\varepsilon}\frac{N'(ax)}{N(ax)}, \tag{4.67}$$

where C is a contour encircling all the poles on the positive real axis counter-clockwise. Note that these are the only poles in the right half plane since there is a one-to-one correspondence between the zeros of the KK mass function (4.63) and the eigenvalues of the operators $\mathcal{P}_4$ and $\mathcal{P}_y$ in Eq. (4.41) which are Hermitian with respect to our boundary conditions.

After a few manipulations, we find

$$\begin{aligned} v_{\rm eff}(\hat{v}) &= I_{\rm IR} + \frac{I_{\rm UV}}{a^{4-\varepsilon}} + 2\int_0^\infty dx\, x^{3-\varepsilon}\log\Bigg[\\ &\quad 1-\frac{1}{2}\left(\frac{K_0(x)I_0(ax)}{I_0(x)K_0(ax)}+\frac{K_1(x)I_1(ax)}{I_1(x)K_1(ax)}-\frac{K_0(x)I_1(ax)}{I_0(x)K_1(ax)}-\frac{K_1(x)I_0(ax)}{I_1(x)K_0(ax)}\right) \\ &\quad +\frac{K_0(x)K_1(x)I_0(ax)I_1(ax)}{I_0(x)I_1(x)K_0(ax)K_1(ax)}-\frac{\cos\left(\frac{\hat{v}}{a^2}(1-a^2)\right)}{2ax^2I_0(x)I_1(x)K_0(ax)K_1(ax)}\Bigg], \\ &\simeq I_{\rm IR} + \frac{I_{\rm UV}}{a^{4-\varepsilon}} + 2\int_0^\infty dx\, x^{3-\varepsilon}\log\left[1-\frac{I_0(x)K_1(x)-K_0(x)I_1(x)-\frac{1}{x}\cos\frac{\hat{v}}{a^2}}{2I_0(x)I_1(x)\left(\gamma+\log\frac{ax}{2}\right)}\right], \end{aligned} \tag{4.68}$$

where divergent integrals $I_{\rm IR}$ and $I_{\rm UV}$ are independent of v and a and can be absorbed in the renormalization of the IR- and UV-brane tensions, respectively, as in Ref. [134]. I_ν and K_ν are the modified Bessel functions. We find that the effective potential is a periodic function of $\hat{v}$ with the period

$$2\pi a^2/(1-a^2) \tag{4.69}$$

as is expected from the shape of the KK mass function. In the last line of Eq. (4.68), the small a limit is taken, assuming that $\hat{v}$ is within the first period, i.e. $\hat{v}/a^2 = O(1)$, without loss of generality. We can expand in a with converging coefficients since for large x, the integrand goes to zero fast enough for the integral to be finite.

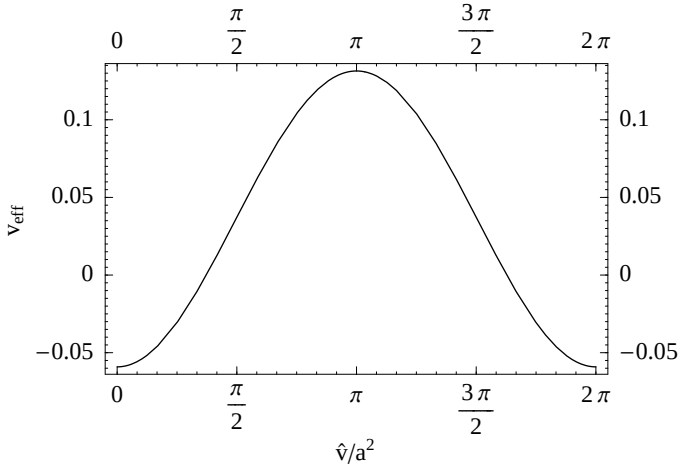

Figure 4.2: Normalized effective potential v_{eff} vs $\hat{v}/a^2$ with $a = 10^{-15}$.

In Fig. 4.2, we plot v_{eff} as a function of $\hat{v}/a^2$ when $a = 10^{-15}$. Contribution from the ghost loop is equal to Eq. (4.68) multiplied by -2. The final result including gauge and ghost field contributions is therefore:

$$V_{\text{eff}} = \frac{3}{32\pi^2}(ka)^4 v_{\text{eff}}. \tag{4.70}$$

Note that if we include extra adjoint bulk fermions, they would contribute with opposite signs to Eq. (4.68) and that if we add more than required to make the theory supersymmetric, the potential of Fig. 4.2 would be flipped upside down, realizing a dynamical symmetry breaking vacuum which corresponds to the maximal twist $\theta = \pi/2$ in the $A_y^c = 0$ gauge. This vacuum breaks $SU(2)$ completely and hence provides a rank reduction of the gauge symmetry. We find that the symmetry breaking scale is of the order of $ka \simeq$ TeV for this case.

4.3.3 Warped space gauge-Higgs unification

After having calculated the effective potential of the Wilson line phase in warped extra dimensions we are interested to see if some of the problems of gauge Higgs unification can be alleviated in the warped framework. The Higgs field corresponds to 4 D vacuum fluctuations of the Wilson line phase θ around the vacuum value. We can then infer its mass and self-coupling from the effective potential for θ. Since we would need the full effective potential including fermions in order arrive at a non-trivial vacuum value for θ, we will be able to just describe how the general relations are altered in the warped case.
As an example, let us discuss the $SO(5) \times U(1)_{B-L}$ model by Agashe et al. [120]. One finds that the phase θ in this particular embedding of the SM gauge group

is given by

$$\Theta = \theta \cdot \Lambda \quad , \quad \Lambda = \begin{pmatrix} 0 & & & & \\ & 0 & & & \\ & & 0 & & \\ & & & -i & \\ & & & i & \end{pmatrix} \tag{4.71}$$

which leads to a m_W mass of

$$m_W \sim \sqrt{\frac{k}{\pi R}}\, e^{-\pi k R \left| \sin\theta \right|} \ . \tag{4.72}$$

The relation between the mass of the first KK excitation and the m_W mass, which caused phenomenological problems in the flat case (4.26), because the KK mass was too low, is now changed to

$$m_{KK} \sim \frac{m_W}{\theta} \pi \sqrt{k\pi R} \tag{4.73}$$

where the extra factor of $\sqrt{k\pi R}$ comes from the warped geometry of the extra dimension. It is exactly this factor $\sqrt{k\pi R} \approx 6$ that makes the KK modes heavy enough to evade conflict with lower bounds for the KK masss from direct searches, see e.g. [125].
The second problem, namely the too light Higgs mass is also addressed. The relation between the Higgs field ϕ^0 and the corresponding extra-dimensional degrees of freedom of the gauge field A_5 is given by

$$A_y = \sqrt{\frac{k}{2e^{2\pi k R}}}\, e^{2ky}\ \phi^0(x) \cdot \Lambda \quad . \tag{4.74}$$

Finally, the Higgs mass and the self-coupling are given as the 2nd and 4th derivative of the effective potential, respectively:

$$m_H \ \sim \ \sqrt{\frac{3\alpha_W}{8\pi} v_{eff}^{(2)}(\theta_H)}\ \frac{\pi k R}{2}\ \frac{\sqrt{2}\, m_W}{\sin\theta_H} \quad , \tag{4.75}$$

$$\lambda \ \sim \ \frac{\alpha_W^2}{4}\ v_{eff}^{(4)}(\theta_H) \left(\frac{\pi k R}{2} \right)^2 \quad . \tag{4.76}$$

The presence of the enhancement factor $\pi kR/2 \sim 20$, which is a consequence of the warped geometry, together with typical values of $\theta_H = (0.1 \sim 0.3)\pi$ leads to a realistic Higgs mass of $m_H = (70 - 170)$ GeV. Note, that this is just an estimate which lacks a full calculation of the effective potential including fermions. However, a similar result has also been found in the full calculation of Agashe et. al [120]

4.4 Summary and discussions

We have studied the $SU(N)$ pure gauge theory in the bulk of the Randall-Sundrum geometry and have obtained Kaluza-Klein expansions of gauge and ghost fields under the presence of the gauge field background with most general twists P_i.

We find that four dimensional gauge, fifth component and ghost fields have exactly the same KK masses.

During the course of this calculation we have clarified the notion of a large gauge transformation that is non-periodic on the covering space and how it is consistently realized in the warped background.

The effective potential for the background A_y^c is obtained. We find that a gauge symmetry corresponding to a continuous Wilson line, i.e. a $SU(2)$ subgroup of Eq. (4.9), which is completely broken for finite θ at the classical level, is dynamically restored to $U(1)$.

It is straightforward to apply our method to include other fields with or without extra boundary masses and especially to supersymmetrize our setup, where the symmetry breaking scales due to continuous Wilson lines will be of the order of $ka \simeq$ TeV according to the analysis presented here.

It is also interesting to pursue the AdS/CFT correspondence generalizing the analysis of Ref. [128] to our setup, as the Wilson line on the AdS side will correspond to a quantity that is integrated all the way from UV to IR on the CFT side.

The techniques developed here can also be applied to the gauge-Higgs unification models in warped space and we have shown how the warped geometry solves many of the problems of flat-space gauge-Higgs unification.

Chapter 5

Summary and Conclusions

In the first part of this this dissertation we have studied hadronic and leptonic flavour violation in specific models and in a model independent approach.

In particular we have studied the impact of the universal extra dimensional model of Applequist, Cheng and Dobrescu on FCNC processes. First we investigated the impact on the unitarity triangle and on $\Delta F = 2$ processes. Here we found that in light of the still large hadronic uncertainties, the small deviation coming virtual KK excitations do not significantly constrain the parameter space of the model. Further we studied $\Delta F = 1$ processes and found that the constraint on the compactification scale from $B \to X_s\gamma$ employing the recently reported NNLO calculation for the SM prediction is stronger than electroweak precision tests and much stronger than direct searches. For the future, we found a very distinct signature of enhancements and suppressions of the various clean rare decay channels. Two very clean observables stand out to help to discriminate the model $K^+ \to \pi^+\nu\bar{\nu}$ is expected to be found enhanced compared to the SM and the zero ($\hat{s}_0$) in the $A_{\rm FB}$ asymmetry should be suppressed.

In the model independent framework of MFV we have derived upper bounds on rare K and B decays. Using the input of the UTfit collaboration for the universal unitarity triangle, we were able to constrain the Z penguin contribution using $B \to X_s\gamma$ and $B \to X_s l^+ l^-$. Due to the flavour universality of NP in MFV this constraint allowed us to give 95% C.L. upper-bounds on rare K and B decays. Any deviation from the SM violating these bounds would imply new sources of CP and flavour violation beyond the ones in the SM with the caveat that a MFV scenario would be found in which the contribution from box diagrams are much larger than assumed here. From dimensional arguments and calculations in specific models we consider this a remote possibility.

In the following chapter we extended the discussion of MFV to the lepton sector. Extending the original proposal of CIGW to include CP violation at high energies, we studied a realisation of MFV in the lepton sector in the SM and in the MSSM. First we showed how baryogenesis through leptogenesis is possible over large amount of parameter space. Specifically, we found that due to the inclusion

of flavour effects in the calculation of the Boltzmann equations no lower bound of the Majorana scale exits. Furthermore, we have discussed the implications for correlations between $\mu \to e\gamma$ and successful leptogenesis.

In the last part of the dissertation we have studied Wilson line phases and their dynamics in warped extra-dimensions. Motivated by models of gauge-Higgs unification we have discussed the Hosotani mechanism and calculated the effective potential of the Wilson line phase for the first time. In order to do this we first had to derived the KK expansion in the background of a Wilson line phase, then we calculated the effective potential resumming the KK contribution using a zeta-function technique for the pure-gauge case. We have found that the relation between the mass of the first KK mode is sufficiently high and does not lead to a phenomenologically excluded scenario. Furthermore, the dynamically generated Higgs mass is now large enough to allow for realistic models.

Appendix A

MFV Operator Basis

Here we list and classify all possible flavour changing operators up to dimension 6 which are compatible with the SM gauge symmetries. This has first been derived in [17], we have added one operator omitted in the construction.

Before electroweak symmetry breaking we find the following operators.
$\Delta F = 2$. After using Fiertz identities all possible structures turn out to be equivalent to a single independent term

$$\mathcal{O}_0 = \frac{1}{2}\left(\bar{Q}_L \lambda_{\rm FC} \gamma_\mu Q_L\right)^2 \ . \tag{A.1}$$

$\Delta F = 1$ Higgs field. Neglecting terms which are suppressed by quark masses via the equations of motion, we find

$$\mathcal{O}_{H1} = i\left(\bar{Q}_L \lambda_{\rm FC} \gamma_\mu Q_L\right) H^\dagger D_\mu H \ , \qquad \mathcal{O}_{H2} = i\left(\bar{Q}_L \lambda_{\rm FC} \tau^a \gamma_\mu Q_L\right) H^\dagger \tau^a D_\mu H \ . \tag{A.2}$$

$\Delta F = 1$ gauge fields. The couplings to the gluon field are

$$\mathcal{O}_{G1} = H^\dagger\left(\bar{D}_R \lambda_d \lambda_{\rm FC} \sigma_{\mu\nu} T^a Q_L\right) G^a_{\mu\nu} \ , \qquad \mathcal{O}_{G2} = \left(\bar{Q}_L \lambda_{\rm FC} \gamma_\mu T^a Q_L\right) D_\mu G^a_{\mu\nu} \ . \tag{A.3}$$

The only terms relevant for low-energy processes ($p^2 \ll v^2$) are only those involving the photon field and we can ignore the other electroweak bosons, namely

$$\mathcal{O}_{F1} = H^\dagger\left(\bar{D}_R \lambda_d \lambda_{\rm FC} \sigma_{\mu\nu} Q_L\right) F_{\mu\nu} \ , \qquad \mathcal{O}_{F2} = \left(\bar{Q}_L \lambda_{\rm FC} \gamma_\mu Q_L\right) D_\mu F_{\mu\nu} \ . \tag{A.4}$$

$\Delta F = 1$ four-fermion operators. The operators involving leptons are given as

$$\begin{aligned} &\mathcal{O}_{\ell 1} = \left(\bar{Q}_L \lambda_{\rm FC} \gamma_\mu Q_L\right)\left(\bar{L}_L \gamma_\mu L_L\right) \ , \qquad \mathcal{O}_{\ell 2} = \left(\bar{Q}_L \lambda_{\rm FC} \gamma_\mu \tau^a Q_L\right)\left(\bar{L}_L \gamma_\mu \tau^a L_L\right) \ , \\ &\mathcal{O}_{\ell 3} = \left(\bar{Q}_L \lambda_{\rm FC} \gamma_\mu Q_L\right)\left(\bar{E}_R \gamma_\mu E_R\right) \ . \end{aligned} \tag{A.5}$$

The operators involving only quarks are as follows

$$\begin{aligned}
&\mathcal{O}_{q1} = \left(\bar{Q}_L \lambda_{\rm FC} \gamma_\mu Q_L\right) \left(\bar{Q}_L \gamma_\mu Q_L\right) , && \mathcal{O}_{q2} = \left(\bar{Q}_L \lambda_{\rm FC} \gamma_\mu \tau^a Q_L\right) \left(\bar{Q}_L \gamma_\mu \tau^a Q_L\right) , \\
&\mathcal{O}_{q3} = \left(\bar{Q}_L \lambda_{\rm FC} \gamma_\mu T^a Q_L\right) \left(\bar{Q}_L \gamma_\mu T^a Q_L\right) , && \mathcal{O}_{q4} = \left(\bar{Q}_L \lambda_{\rm FC} \gamma_\mu T^a \tau^b Q_L\right) \left(\bar{Q}_L \gamma_\mu T^a \tau^b Q_L\right) , \\
&\mathcal{O}_{q5} = \left(\bar{Q}_L \lambda_{\rm FC} \gamma_\mu Q_L\right) \left(\bar{D}_R \gamma_\mu D_R\right) , && \mathcal{O}_{q6} = \left(\bar{Q}_L \lambda_{\rm FC} \gamma_\mu T^a Q_L\right) \left(\bar{D}_R \gamma_\mu T^a D_R\right) , \\
&\mathcal{O}_{q7} = \left(\bar{Q}_L \lambda_{\rm FC} \gamma_\mu Q_L\right) \left(\bar{U}_R \gamma_\mu U_R\right) , && \mathcal{O}_{q8} = \left(\bar{Q}_L \lambda_{\rm FC} \gamma_\mu T^a Q_L\right) \left(\bar{U}_R \gamma_\mu T^a U_R\right) .
\end{aligned} \tag{A.6}$$

A.1 Operator Basis relevant for Phenomenology

After the electroweak symmetry breakdown and after integrating out off-shell gauge fields, the relevant operators involving down quarks can be derived from the above using the projection

$$\mathcal{H}_{\rm eff}^{\Delta F=1} = \frac{1}{\Lambda^2} \sum_n a_n \mathcal{O}_n \ + \ \text{h.c.} \qquad \longrightarrow \qquad \frac{G_{\rm F} \alpha}{2\sqrt{2}\pi \sin^2\theta_{\rm W}} V_{3i}^* V_{3j} \sum_n C_n \mathcal{Q}_n \ + \ \text{h.c.} \tag{A.7}$$

The sum on the r.h.s. contains 13 terms, namely four QCD-penguin operators ($\mathcal{Q}_{3\ldots6}$), four electroweak-penguin operators ($\mathcal{Q}_{7\ldots10}$), magnetic and chromomagnetic dipole operators ($\mathcal{Q}_{7\gamma}$ and $\mathcal{Q}_{8G}$), and three quark-lepton operators ($\mathcal{Q}_{9V}$, $\mathcal{Q}_{10A}$ and $\mathcal{Q}_{\nu\bar{\nu}}$). 1) Quark-lepton currents:

$$\begin{aligned}
\mathcal{Q}_{\nu\bar{\nu}} &= \bar{d}_i \gamma_\mu (1-\gamma_5) d_j \ \bar{\nu} \gamma_\mu (1-\gamma_5) \nu \\
\mathcal{Q}_{10A} &= \bar{d}_i \gamma_\mu (1-\gamma_5) d_j \ \bar{\ell} \gamma_\mu \gamma_5 \ell \\
\mathcal{Q}_{9V} &= \bar{d}_i \gamma_\mu (1-\gamma_5) d_j \ \bar{\ell} \gamma_\mu \ell
\end{aligned} \tag{A.8}$$

2) Non-leptonic electroweak operators:

$$\begin{aligned}
\mathcal{Q}_7 &= \bar{d}_i^\alpha \gamma_\mu (1-\gamma_5) d_j^\alpha \ \sum_q e_q \bar{q}^\beta \gamma_\mu (1+\gamma_5) q^\beta \\
\mathcal{Q}_8 &= \bar{d}_i^\alpha \gamma_\mu (1-\gamma_5) d_j^\beta \ \sum_q e_q \bar{q}^\beta \gamma_\mu (1+\gamma_5) q^\alpha \\
\mathcal{Q}_9 &= \bar{d}_i^\alpha \gamma_\mu (1-\gamma_5) d_j^\alpha \ \sum_q e_q \bar{q}^\beta \gamma_\mu (1-\gamma_5) q^\beta \\
\mathcal{Q}_{10} &= \bar{d}_i^\alpha \gamma_\mu (1-\gamma_5) d_j^\beta \ \sum_q e_q \bar{q}^\beta \gamma_\mu (1-\gamma_5) q^\alpha
\end{aligned} \tag{A.9}$$

3) Dipole operators:

$$\begin{aligned}
\mathcal{Q}_{7\gamma} &= \frac{1}{g^2} m_{d_i} \bar{d}_i (1-\gamma_5) \sigma_{\mu\nu} d_j (e F_{\mu\nu}) \\
\mathcal{Q}_{8G} &= \frac{1}{g^2} m_{d_i} \bar{d}_i (1-\gamma_5) \sigma_{\mu\nu} T^a d_j (g_s G_{\mu\nu}^a)
\end{aligned} \tag{A.10}$$

The coefficients ϵ_i used in the text are given as

$$\epsilon_i = \left(\frac{\Lambda_0}{\Lambda}\right)^2 a_i \ , \qquad \Lambda_0 = \frac{\lambda_t \sin^2\theta_{\rm W} M_W}{\alpha} \approx 2.4 \text{ TeV} \ . \tag{A.11}$$

Appendix B

Warped Extra Dimensions

This is a collection of useful formulae when performing calculations in the Randall-Sundrum I model.

B.1 Setup

The total action is given as

$$S = S_G + S_m, \tag{B.1}$$

where

$$\begin{aligned} S_G &= -M^3 \int d^4x \int_{-\pi R}^{\pi R} dy \sqrt{-G} \left[\frac{\mathcal{R}}{2} - \Lambda - \delta(y)\Lambda_0 - \delta(y-\pi R)\Lambda_\pi \right], \\ S_m &= -\int d^4x \int_{-\pi R}^{\pi R} dy \sqrt{-G} \left[\frac{1}{2} \operatorname{tr}\left(F_{MN}F^{MN}\right) + \cdots \right], \end{aligned} \tag{B.2}$$

$x^M = (x^\mu, y) = (x^0, \ldots, x^3, x^5)$ and $y = x^5$.
The metric is

$$G_{MN}dx^M dx^N = e^{-2\sigma}\eta_{\mu\nu}dx^\mu dx^\nu + dy^2, \quad G^{MN}\partial_M\partial_N = e^{2\sigma}\eta^{\mu\nu}\partial_\mu\partial_\nu + \partial_y^2. \tag{B.3}$$

$$G = \det_{M,N} G_{MN} = -e^{-8\sigma}, \qquad \sqrt{-G} = e^{-4\sigma}. \tag{B.4}$$

B.1.1 Classical Gravity

The Christoffel and Riemann tensor satisfy the following relations

$$\Gamma^K_{MN} = \frac{G^{KL}}{2}\left(-\partial_L G_{MN} + \partial_M G_{NL} + \partial_N G_{LM}\right). \tag{B.5}$$

$$\begin{aligned}\mathcal{R}^J_{KLM} &= \partial_L\Gamma^J_{KM} - \partial_M\Gamma^J_{KL} + \Gamma^J_{NL}\Gamma^N_{KM} - \Gamma^J_{NM}\Gamma^N_{KL},\\ \mathcal{R}_{MN} &= \partial_K\Gamma^K_{MN} - \partial_N\Gamma^K_{MK} + \Gamma^K_{MN}\Gamma^L_{KL} - \Gamma^K_{ML}\Gamma^L_{NK},\\ \mathcal{R} &= G^{MN}\mathcal{R}_{MN}.\end{aligned} \tag{B.6}$$

$$\begin{aligned}\partial_y G_{\mu\nu} &= -2\sigma' e^{-2\sigma}\eta_{\mu\nu},\\ \text{other derivatives} &= 0.\end{aligned} \tag{B.7}$$

$$\begin{aligned}\Gamma^y_{\mu\nu} &= \sigma' e^{-2\sigma}\eta_{\mu\nu},\\ \Gamma^\mu_{y\nu} = \Gamma^\mu_{\nu y} &= -\sigma'\delta^\mu_\nu,\\ \text{others} &= 0.\end{aligned} \tag{B.8}$$

$$\begin{aligned}\partial_y\Gamma^y_{\mu\nu} &= \left(-2k^2 + \sigma''\right) e^{-2\sigma}\eta_{\mu\nu},\\ \partial_y\Gamma^\mu_{y\nu} = \partial_y\Gamma^\mu_{\nu y} &= -\sigma''\delta^\mu_\nu,\\ \text{other derivatives} &= 0.\end{aligned} \tag{B.9}$$

$$\begin{aligned}\mathcal{R}_{yy} &= -4k^2 + 4\sigma'',\\ \mathcal{R}_{\mu y} = \mathcal{R}_{y\mu} &= 0,\\ \mathcal{R}_{\mu\nu} &= (-4k^2 + \sigma'')e^{-2\sigma}\eta_{\mu\nu}.\end{aligned} \tag{B.10}$$

$$\mathcal{R} = -20k^2 + 8\sigma''. \tag{B.11}$$

$$\delta\sqrt{-G} = -\frac{1}{2}\sqrt{-G}G_{MN}\delta G^{MN}. \tag{B.12}$$

Solving the gravity part classically,

$$\begin{aligned}\delta S_G = -M^3 \int d^5x\sqrt{-G}\frac{\delta G^{MN}}{2}\\ \times\left[\mathcal{R}_{MN} - \frac{\mathcal{R}}{2}G_{MN} + \Lambda G_{MN} + \Big(\Lambda_0\delta(y) + \Lambda_\pi\delta(y-\pi R)\Big)G_{\mu\nu}\delta^\mu_M\delta^\nu_N\right],\end{aligned} \tag{B.13}$$

we obtain $\Lambda = -6k^2$, $\Lambda_0 = +6k$ and $\Lambda_\pi = -6k$.

B.1.1.1 vector field

Notation:

$$\boldsymbol{\mathcal{D}}_M A_N = \mathcal{D}_M A_N + ig[A_M, A_N] = D_M A_N - \Gamma^L_{MN} A_L, \tag{B.14}$$

where

$$\begin{aligned} D_M A_N &= \partial_M A_N + ig[A_M, A_N], \\ \mathcal{D}_M A_N &= \partial_M A_N - \Gamma^K_{MN} A_K. \end{aligned} \tag{B.15}$$

Note that

$$\mathcal{D}_K G_{MN} = \mathcal{D}_K G^{MN} = \mathcal{D}^K G_{MN} = \mathcal{D}^K G^{MN} = 0, \tag{B.16}$$

and

$$\begin{aligned} [\mathcal{D}_M, \mathcal{D}_N] V^K &= \mathcal{R}^K_{JMN} V^J, \\ [\mathcal{D}_M, \mathcal{D}_N] V_K &= -\mathcal{R}^J_{KMN} V_J. \end{aligned} \tag{B.17}$$

$$\begin{aligned} \mathcal{D}_M V_N &= \partial_M V_N - \Gamma^K_{MN} V_K, \\ \mathcal{D}_M V^N &= \partial_M V^N + \Gamma^N_{MK} V^K. \end{aligned} \tag{B.18}$$

$$\begin{aligned} \mathcal{D}_y V_y &= \partial_y V_y, \\ \mathcal{D}_y V_\mu &= \partial_y V_\mu + \sigma' V_\mu, \\ \mathcal{D}_\mu V_y &= \partial_\mu V_y + \sigma' V_\mu, \\ \mathcal{D}_\mu V_\nu &= \partial_\mu V_\nu - \sigma' e^{-2\sigma} \eta_{\mu\nu} V_y. \end{aligned} \tag{B.19}$$

$$V^y = V_y, \qquad V^\mu = e^{2\sigma} \eta^{\mu\nu} V_\nu, \qquad V_\mu = e^{-2\sigma} \eta_{\mu\nu} V^\nu, \tag{B.20}$$

$$\begin{aligned} F_{MN} &= \mathcal{D}_M A_N - \mathcal{D}_N A_M + ig[A_M, A_N] \\ &= \partial_M A_N - \partial_N A_M + ig[A_M, A_N]. \end{aligned} \tag{B.21}$$

$$\begin{aligned} F_{yy} &= 0, \\ F_{\mu y} &= \partial_\mu A_y - \partial_y A_\mu + ig[A_\mu, A_y], \\ F_{\mu\nu} &= \partial_\mu A_\nu - \partial_\nu A_\mu + ig[A_\mu, A_\nu]. \end{aligned} \tag{B.22}$$

B.1.1.2 Equation of motion for vector

$$\partial^M = e^{2\sigma}\eta^{M\nu}\partial_\nu + \delta^M_y\partial_y. \tag{B.23}$$

$$\begin{aligned} F^{y\nu} &= \partial_y A^\nu - e^{2\sigma}\eta^{\nu\mu}\partial_\mu A^y + ig[A^y, A^\nu], \\ F^{\mu\nu} &= e^{2\sigma}\left(\eta^{\mu\kappa}\partial_\kappa A^\nu - \eta^{\nu\kappa}\partial_\kappa A^\mu\right) + ig[A^\mu, A^\nu], \\ F^{yy} &= 0. \end{aligned} \tag{B.24}$$

$$0 = D_M\left(\sqrt{-G}F^{MN}\right). \tag{B.25}$$

$$\begin{aligned} \eta^{\mu\nu}D_\mu F_{\nu\lambda} + e^{-2\sigma}(D_y - 2\sigma')F_{y\lambda} &= 0, \\ \eta^{\mu\nu}D_\mu F_{\nu y} &= 0. \end{aligned} \tag{B.26}$$

$$\begin{aligned} \eta^{\mu\nu}D_\mu\left(\partial_\nu A_\lambda - \partial_\lambda A_\nu + ig[A_\nu, A_\lambda]\right) + e^{-2\sigma}(D_y - 2\sigma')\left(\partial_y A_\lambda - \partial_\lambda A_y + ig[A_y, A_\lambda]\right) &= 0, \\ \eta^{\mu\nu}D_\mu\left(\partial_\nu A_y - \partial_y A_\nu + ig[A_\nu, A_y]\right) &= 0. \end{aligned} \tag{B.27}$$

In the axial gauge $A_y = 0$,

$$\begin{aligned} \eta^{\mu\nu}D_\mu\left(\partial_\nu A_\lambda - \partial_\lambda A_\nu + ig[A_\nu, A_\lambda]\right) + e^{-2\sigma}(\partial_y - 2\sigma')\partial_y A_\lambda &= 0, \\ \eta^{\mu\nu}D_\mu\partial_y A_\nu &= 0. \end{aligned} \tag{B.28}$$

When $A^{c\mu} = 0$, the classical version of Eq. (B.27) becomes

$$0 = \eta^{\mu\nu}\partial_\mu\partial_\nu A^c_y, \qquad\qquad 0 = (D_y - 2\sigma')\partial_\mu A^c_y. \tag{B.29}$$

This is trivially satisfied when $\partial_\mu A^c_y = 0$.

B.1.2 Orbifolding

For $-\pi R < y \le \pi R$,

$$\sigma = k|y|, \qquad \sigma' = k\epsilon(y), \qquad \sigma'' = k\epsilon'(y) = 2k\big[\delta(y) - \delta(y - \pi R)\big], \tag{B.30}$$

where

$$\begin{aligned} \epsilon(y) = \frac{d|y|}{dy} = \theta(y) - \theta(-y) &= \begin{cases} +1 & 0 < y < \pi R, \\ -1 & -\pi R < y < 0, \end{cases} \qquad \epsilon(y)^2 = 1, \\ \epsilon'(y) &= 2\big[\delta(y) - \delta(y - \pi R)\big]. \end{aligned} \tag{B.31}$$

For $y \le -\pi R, \pi R < y$, σ and ϵ are defined by the translational symmetry

$$\sigma(y + 2\pi R) = \sigma(y), \qquad\qquad \epsilon(y + 2\pi R) = \epsilon(y). \tag{B.32}$$

B.2 Background gauge

$$A_M = A^c_M + A'_M. \tag{B.33}$$

The gauge kinetic Lagrangian is

$$\mathcal{L}_A = -\frac{1}{2}\,\mathrm{tr}\left(F_{MN}F^{MN}\right), \tag{B.34}$$

where

$$F_{MN} = F^c_{MN} + D^c_M A'_N - D^c_N A'_M + ig[A'_M, A'_N]. \tag{B.35}$$

The superscript c denotes that the gauge field is replaced by its classical part A^c so that $D^c_M A'_N = \partial_M A'_N + ig[A^c_M, A'_N]$ etc. When $F^c_{MN} = 0$,

$$\begin{aligned}\mathcal{L}_A &= -\frac{1}{2}\,\mathrm{tr}\left(D^c_M A'_N - D^c_N A'_M + ig[A'_M, A'_N]\right)^2, \\ \mathcal{L}_A^{\mathrm{quad}} &= -\frac{1}{2}\,\mathrm{tr}\left(D^c_M A'_N - D^c_N A'_M\right)^2,\end{aligned} \tag{B.36}$$

where of course the square is the general coordinate invariant one. We choose the following gauge fixing function

$$\begin{aligned}f &= e^{2\sigma}\eta^{\mu\nu}D^c_\mu A'_\nu + D^c_y A'_y - t\sigma' A'_y \\ &= e^{2\sigma}\eta^{\mu\nu}D^c_\mu A'_\nu + e^{t\sigma}D^c_y(e^{-t\sigma}A'_y).\end{aligned} \tag{B.37}$$

When $t = 4$, f becomes manifesty general covariant $f|_{t=4} = G^{MN}\boldsymbol{\mathcal{D}}^c_M A'_N$. The Lagrangian,

$$\mathcal{L}_f = -\frac{1}{\xi}\,\mathrm{tr}(ff) = -\frac{1}{2\xi}f^a f^a, \tag{B.38}$$

is manifestly invariant under the five-dimensional background gauge transformation:

$$\begin{aligned}\delta A^c_M &= \partial_M\epsilon - ig[\epsilon, A^c_M] = D^c_M\epsilon, \\ \delta A'_M &= -ig[\epsilon, A'_M].\end{aligned} \tag{B.39}$$

where $f = f^a T^a$ and $T^a = \sigma^a/2$ for $SU(2)$.
The true gauge transformation:

$$\begin{aligned}&\Delta_\epsilon A^c_M = 0, \\ &\Delta_\epsilon A'_M = \mathcal{D}_M\epsilon - ig[\epsilon, A^c_M + A'_M] \qquad = \partial_M\epsilon - ig[\epsilon, A^c_M + A'_M] \\ &\qquad = \boldsymbol{\mathcal{D}}^c_M\epsilon - ig[\epsilon, A'_M] \qquad = D^c_M\epsilon - ig[\epsilon, A'_M].\end{aligned} \tag{B.40}$$

Note, that the ghosts are scalars under diffeomorphisms. Then the ghost Lagrangian is:

$$\begin{aligned}\mathcal{L}_{\rm gh} &= (\overline{\omega}^c + \overline{\omega}')^a (\Delta_{\omega^c+\omega'} f)^a \\ &= 2\,\mathrm{tr}\Big[(\overline{\omega}^c + \overline{\omega}')e^{2\sigma}\eta^{\mu\nu} D^c_\mu \big(D^c_\nu(\omega^c+\omega') - ig[\omega^c+\omega', A'_\nu]\big) \\ &\quad + (\overline{\omega}^c + \overline{\omega}')(D^c_y - t\sigma')\big(D^c_y(\omega^c+\omega') - ig[\omega^c+\omega', A'_y]\big)\Big]. \end{aligned} \tag{B.41}$$

The background gauge transformation acts as follows:

$$\begin{aligned} \delta\omega^c &= -ig[\epsilon, \omega^c], & \delta\omega' &= -ig[\epsilon, \omega'], \\ \delta\overline{\omega}^c &= -ig[\epsilon, \overline{\omega}^c], & \delta\overline{\omega}' &= -ig[\epsilon, \overline{\omega}']. \end{aligned} \tag{B.42}$$

The total Lagrangian,

$$\mathcal{L}_{\rm total} = \mathcal{L}_A + \mathcal{L}_f + \mathcal{L}_{\rm gh}, \tag{B.43}$$

is invariant under the five-dimensional background gauge transformation of Eqs. (B.39) and (B.42).
For the case at hand we need to set $A^c_\mu = \omega^c = \overline{\omega}^c = 0$:

$$\begin{aligned}\sqrt{-G}\mathcal{L}^{\rm quad}_A &= -\,\mathrm{tr}\Big[-(A'\cdot\Box A') - (\partial\cdot A')^2 + e^{-2\sigma}(D^c_y A'\cdot D^c_y A') \\ &\qquad - e^{-2\sigma}A'_y\Box A'_y + 2e^{-2\sigma}A'_y D^c_y(\partial\cdot A')\Big], \\ \sqrt{-G}\mathcal{L}^{\rm quad}_f &= -\frac{1}{\xi}\,\mathrm{tr}\left[(\partial\cdot A')^2 + 2e^{(t-2)\sigma}(\partial\cdot A')D^c_y(e^{-t\sigma}A'_y) + e^{2(t-2)\sigma}\left[D^c_y(e^{-t\sigma}A'_y)\right]^2\right], \\ \sqrt{-G}\mathcal{L}^{\rm quad}_{\rm gh} &= 2\,\mathrm{tr}\left[e^{-2\sigma}\overline{\omega}'\Box\omega' + e^{-4\sigma}\overline{\omega}'(D^c_y - t\sigma')D^c_y\omega'\right] \\ &= 2\,\mathrm{tr}\left[e^{-2\sigma}\overline{\omega}'\Box\omega' + e^{(t-4)\sigma}\overline{\omega}' D^c_y(e^{-t\sigma}D^c_y\omega')\right]. \end{aligned} \tag{B.44}$$

where $(A\cdot B) = \eta^{\mu\nu}(A_\mu B_\nu)$ and $\Box = \eta^{\mu\nu}\partial_\mu\partial_\nu$. In the gauge $\xi = 1$ with $t = 2$,

$$\begin{aligned}\sqrt{-G}\mathcal{L}^{\rm quad}_{A+f} &= -\,\mathrm{tr}\Big[-(A'\cdot\Box A') + e^{-2\sigma}(D^c_y A'\cdot D^c_y A') \\ &\qquad - e^{-2\sigma}A'_y\Box A'_y + \left[D^c_y e^{-2\sigma}A'_y\right]^2 \\ &\qquad + 2D^c_y\left[e^{-2\sigma}A'_y(\partial\cdot A')\right]\Big], \\ \sqrt{-G}\mathcal{L}^{\rm quad}_{\rm gh} &= 2\,\mathrm{tr}\left[e^{-2\sigma}\overline{\omega}'\Box\omega' + e^{-4\sigma}\overline{\omega}'(D^c_y - 2\sigma')D^c_y\omega'\right] \\ &= 2\,\mathrm{tr}\left[e^{-2\sigma}\overline{\omega}'\Box\omega' + e^{-2\sigma}\overline{\omega}' D^c_y(e^{-2\sigma}D^c_y\omega')\right]. \end{aligned} \tag{B.45}$$

Bibliography

[1] W. A. Bardeen, FERMILAB-CONF-95-391-T *Presented at the 1995 Ontake Summer Institute, Ontake Mountain, Japan, Aug 27 - Sep 2, 1995*

[2] See review by H. E. Haber in S. Eidelman *et al.* [Particle Data Group], Phys. Lett. B **592**, 1 (2004) and references therein.

[3] S. Weinberg, Phys. Rev. D **13**, 974 (1976); Phys. Rev. D **19**, 1277 (1979); L. Susskind, Phys. Rev. D **20**, 2619 (1979).

[4] For a review, see C. T. Hill and E. H. Simmons, Phys. Rept. **381**, 235 (2003) [Erratum-ibid. **390**, 553 (2004)] [arXiv:hep-ph/0203079].

[5] D. B. Kaplan and H. Georgi, Phys. Lett. B **136**, 183 (1984) B **136**, 187 (1984);
H. Georgi, D. B. Kaplan and P. Galison, Phys. Lett. B **143**, 152 (1984);
H. Georgi and D. B. Kaplan, Phys. Lett. B **145**, 216 (1984);
M. J. Dugan, H. Georgi and D. B. Kaplan, Nucl. Phys. B **254**, 299 (1985).

[6] C. T. Hill, Phys. Lett. B **266**, 419 (1991); C. T. Hill, Phys. Lett. B **345**, 483 (1995) [arXiv:hep-ph/9411426]; K. D. Lane and E. Eichten, Phys. Lett. B **352**, 382 (1995) [arXiv:hep-ph/9503433].

[7] N. Arkani-Hamed, A. G. Cohen, E. Katz, A. E. Nelson, T. Gregoire and J. G. Wacker, JHEP **0208**, 021 (2002) [arXiv:hep-ph/0206020]; N. Arkani-Hamed, A. G. Cohen, E. Katz and A. E. Nelson, JHEP **0207**, 034 (2002) [arXiv:hep-ph/0206021]. For a review and more references, see M. Schmaltz and D. Tucker-Smith, arXiv:hep-ph/0502182. For string models which lead to the ADD scenario, see D. Cremades, L.E.Ibanez and F.Marchesano, Nucl. Phys. B643 (2002) 93, [hep-th/0205074]; C. Kokorelis, Nucl. Phys. B677 (2004) 115, [hep-th/0207234].

[8] N. Arkani-Hamed, S. Dimopoulos and G. R. Dvali, Phys. Lett. B **429**, 263 (1998) [arXiv:hep-ph/9803315]; I. Antoniadis, N. Arkani-Hamed, S. Dimopoulos and G. R. Dvali, Phys. Lett. B **436**, 257 (1998) [arXiv:hep-ph/9804398].

[9] L. Randall and R. Sundrum, *Phys. Rev. Lett.* **83** (1999) 3370–3373, [arXiv:hep-ph/9905221].

[10] A. J. Buras, P. Gambino, M. Gorbahn, S. Jager and L. Silvestrini, Phys. Lett. B **500** (2001) 161 [arXiv:hep-ph/0007085].

[11] A. J. Buras, Acta Phys. Polon. B **34**, 5615 (2003) [arXiv:hep-ph/0310208].

[12] A. J. Buras, M. Spranger and A. Weiler, Nucl. Phys. B **660**, 225 (2003) [arXiv:hep-ph/0212143].

[13] A. J. Buras, A. Poschenrieder, M. Spranger and A. Weiler, Nucl. Phys. B **678**, 455 (2004) [arXiv:hep-ph/0306158].

[14] S. R. Choudhury, N. Gaur, A. Goyal and N. Mahajan, Phys. Lett. B **601**, 164 (2004) [arXiv:hep-ph/0407050]; A. J. Buras, A. Poschenrieder and S. Uhlig, arXiv:hep-ph/0410309; A. J. Buras, A. Poschenrieder and S. Uhlig, arXiv:hep-ph/0501230.

[15] A. J. Buras and M. K. Harlander, Adv. Ser. Direct. High Energy Phys. **10**, 58 (1992).

[16] M. Bona *et al.* [UTfit Collaboration], Phys. Rev. Lett. **97** (2006) 151803 [arXiv:hep-ph/0605213].

[17] G. D'Ambrosio, G.F. Giudice, G. Isidori and A. Strumia, Nucl. Phys. **B645** (2002) 155.

[18] A. J. Buras, Phys. Lett. B **566** (2003) 115 [arXiv:hep-ph/0303060].

[19] A. Ali, E. Lunghi, C. Greub and G. Hiller, Phys. Rev. D **66** (2002) 034002 [arXiv:hep-ph/0112300].

[20] G. Hiller and F. Krüger, Phys. Rev. D **69**, 074020 (2004) [arXiv:hep-ph/0310219].

[21] P. Gambino, U. Haisch and M. Misiak, Phys. Rev. Lett. **94**, 061803 (2005) [arXiv:hep-ph/0410155].

[22] F. Wilczek, Phys. Rev. Lett. **49** (1982) 1549.

[23] T. Kaluza, Sitzungsber. Preuss. Akad. Wiss. Berlin (Math. Phys.) **1921** (1921) 966; O. Klein, Z. Phys. **37** (1926) 895 [Surveys High Energ. Phys. **5** (1986) 241].

[24] T. Appelquist, H. C. Cheng and B. A. Dobrescu, Phys. Rev. D **64** (2001) 035002 [arXiv:hep-ph/0012100].

[25] T. Appelquist and H. U. Yee, Phys. Rev. D **67**, 055002 (2003) [hep-ph/0211023]; T. Flacke, D. Hooper and J. March-Russell, Phys. Rev. D **73**, 095002 (2006) [Erratum-ibid. D **74**, 019902 (2006)] [hep-ph/0509352]; I. Gogoladze and C. Macesanu, Phys. Rev. D **74**, 093012 (2006) [hep-ph/0605207].

[26] K. Agashe, N. G. Deshpande and G. H. Wu, Phys. Lett. B **511** (2001) 85 [arXiv:hep-ph/0103235].

[27] J. F. Oliver, J. Papavassiliou and A. Santamaria, Phys. Rev. D **67** (2003) 056002 [arXiv:hep-ph/0212391].

[28] G. Servant and T. M. P. Tait, Nucl. Phys. B **650** (2003) 391 [arXiv:hep-ph/0206071].

[29] S. L. Glashow, J. Iliopoulos and L. Maiani, Phys. Rev. D **2** (1970) 1285.

[30] J. Papavassiliou and A. Santamaria, Phys. Rev. D **63** (2001) 016002 [arXiv:hep-ph/0008151]; J. F. Oliver, J. Papavassiliou and A. Santamaria, arXiv:hep-ph/0209021.

[31] T. Inami and C. S. Lim, Prog. Theor. Phys. **65** (1981) 297 [Erratum-ibid. **65** (1981) 1772].

[32] A. J. Buras, W. Slominski and H. Steger, Nucl. Phys. B **238** (1984) 529; Nucl. Phys. B **245** (1984) 369.

[33] G. Buchalla, A. J. Buras and M. K. Harlander, Nucl. Phys. B **349** (1991) 1.

[34] D. Chakraverty, K. Huitu and A. Kundu, Phys. Lett. B **558** (2003) 173 [arXiv:hep-ph/0212047].

[35] E. Barberio *et al.* [Heavy Flavor Averaging Group (HFAG)], arXiv:hep-ex/0603003.

[36] T. Becher and M. Neubert, arXiv:hep-ph/0610067.

[37] M. Misiak *et al.*, arXiv:hep-ph/0609232.

[38] K. Agashe, N. G. Deshpande and G. H. Wu, Phys. Lett. B **514** (2001) 309 [arXiv:hep-ph/0105084].

[39] J. Kaneko *et al.* [Belle Collaboration], Phys. Rev. Lett. **90** (2003) 021801 [arXiv:hep-ex/0208029].

[40] T. Hurth, arXiv:hep-ph/0212304.

[41] G. Burdman, Phys. Rev. D **57** (1998) 4254 [arXiv:hep-ph/9710550].

[42] H. H. Asatrian, H. M. Asatrian, C. Greub and M. Walker, Phys. Lett. B **507** (2001) 162 [arXiv:hep-ph/0103087]; Phys. Rev. D **65** (2002) 074004 [arXiv:hep-ph/0109140]; Phys. Rev. D **66** (2002) 034009 [arXiv:hep-ph/0204341]; H. M. Asatrian, K. Bieri, C. Greub and A. Hovhannisyan, Phys. Rev. D **66** (2002) 094013 [arXiv:hep-ph/0209006].

[43] A. Ghinculov, T. Hurth, G. Isidori and Y. P. Yao, Nucl. Phys. B **648** (2003) 254 [arXiv:hep-ph/0208088]; arXiv:hep-ph/0211197.

[44] A. J. Buras and R. Fleischer, Phys. Rev. D **64** (2001) 115010 [arXiv:hep-ph/0104238]; A. J. Buras and R. Buras, Phys. Lett. B **501** (2001) 223 [arXiv:hep-ph/0008273]; S. Bergmann and G. Perez, JHEP **0008** (2000) 034 [arXiv:hep-ph/0007170]; Phys. Rev. D **64** (2001) 115009 [arXiv:hep-ph/0103299]; S. Laplace, Z. Ligeti, Y. Nir and G. Perez, Phys. Rev. D **65** (2002) 094040 [arXiv:hep-ph/0202010]; A. J. Buras, arXiv:hep-ph/0303060.

[45] A. J. Buras and M. Jamin, arXiv:hep-ph/0306217.

[46] C. Bobeth, M. Bona, A. J. Buras, T. Ewerth, M. Pierini, L. Silvestrini and A. Weiler, Nucl. Phys. B **726** (2005) 252 [arXiv:hep-ph/0505110].

[47] G. Buchalla, A. J. Buras and M. E. Lautenbacher, Rev. Mod. Phys. **68**, 1125 (1996) [arXiv:hep-ph/9512380].

[48] G. Isidori, F. Mescia and C. Smith, [arXiv:hep-ph/0308008].

[49] A. J. Buras, M. Gorbahn, U. Haisch and U. Nierste, Phys. Rev. Lett. **95**, 261805 (2005) [arXiv:hep-ph/0508165]; A. J. Buras, M. Gorbahn, U. Haisch and U. Nierste, JHEP **0611**, 002 (2006) [arXiv:hep-ph/0603079].

[50] G. Buchalla, G. D'Ambrosio and G. Isidori, Nucl. Phys. B **672**, 387 (2003) [arXiv:hep-ph/0308008].

[51] G. Isidori, C. Smith and R. Unterdorfer, Eur. Phys. J. C **36**, 57 (2004) [arXiv:hep-ph/0404127].

[52] A. Ali and C. Greub, Z. Phys. C **49**, 431 (1991); A. Ali and C. Greub, Phys. Lett. B **259**, 182 (1991); A. Ali and C. Greub, Phys. Lett. B **361**, 146 (1995) [arXiv:hep-ph/9506374]; A. J. Buras, A. Czarnecki, M. Misiak and J. Urban, Nucl. Phys. B **631**, 219 (2002) [arXiv:hep-ph/0203135]; K. Adel and Y. P. Yao, Phys. Rev. D **49**, 4945 (1994) [arXiv:hep-ph/9308349]; C. Greub and T. Hurth, Phys. Rev. D **56**, 2934 (1997) [arXiv:hep-ph/9703349]; A. J. Buras, A. Kwiatkowski and N. Pott, Nucl. Phys. B **517**, 353 (1998) [arXiv:hep-ph/9710336]; M. Ciuchini, G. Degrassi,

P. Gambino and G. F. Giudice, Nucl. Phys. B **527**, 21 (1998) [arXiv:hep-ph/9710335]; C. Bobeth, M. Misiak and J. Urban, Nucl. Phys. B **567**, 153 (2000) [arXiv:hep-ph/9904413]; K. G. Chetyrkin, M. Misiak and M. Munz, Nucl. Phys. B **520**, 279 (1998) [arXiv:hep-ph/9711280]; M. Misiak and M. Munz, Phys. Lett. B **344**, 308 (1995) [arXiv:hep-ph/9409454]; N. Pott, Phys. Rev. D **54**, 938 (1996) [arXiv:hep-ph/9512252]; Z. Ligeti, M. E. Luke, A. V. Manohar and M. B. Wise, Phys. Rev. D **60**, 034019 (1999) [arXiv:hep-ph/9903305]; C. Greub, T. Hurth and D. Wyler, Phys. Lett. B **380**, 385 (1996) [arXiv:hep-ph/9602281]; C. Greub, T. Hurth and D. Wyler, Phys. Rev. D **54**, 3350 (1996) [arXiv:hep-ph/9603404]; A. J. Buras, A. Czarnecki, M. Misiak and J. Urban, Nucl. Phys. B **611**, 488 (2001) [arXiv:hep-ph/0105160].

[53] A. Ghinculov, T. Hurth, G. Isidori and Y. P. Yao, Nucl. Phys. B **685**, 351 (2004) [arXiv:hep-ph/0312128]; C. Bobeth, P. Gambino, M. Gorbahn and U. Haisch, JHEP **0404**, 071 (2004) [arXiv:hep-ph/0312090]; C. Bobeth, M. Misiak and J. Urban, Nucl. Phys. B **574**, 291 (2000) [arXiv:hep-ph/9910220]; H. H. Asatryan, H. M. Asatrian, C. Greub and M. Walker, Phys. Rev. D **65**, 074004 (2002) [arXiv:hep-ph/0109140]; H. H. Asatryan, H. M. Asatrian, C. Greub and M. Walker, Phys. Rev. D **66**, 034009 (2002) [arXiv:hep-ph/0204341]; A. Ghinculov, T. Hurth, G. Isidori and Y. P. Yao, Nucl. Phys. B **648**, 254 (2003) [arXiv:hep-ph/0208088]; H. M. Asatrian, K. Bieri, C. Greub and A. Hovhannisyan, Phys. Rev. D **66**, 094013 (2002) [arXiv:hep-ph/0209006]; H. M. Asatrian, H. H. Asatryan, A. Hovhannisyan and V. Poghosyan, Mod. Phys. Lett. A **19**, 603 (2004) [arXiv:hep-ph/0311187]; A. Ghinculov, T. Hurth, G. Isidori and Y. P. Yao, Eur. Phys. J. C **33**, S288 (2004) [arXiv:hep-ph/0310187].

[54] M. Bona *et al.* [UTfit Collaboration], in preparation; Talk given by M. Pierini at the CKM 2005 Workshop, http://ckm2005.ucsd.edu/speakers/WG6/Pierini-WG6-fri2.pdf.

[55] S. Chen *et al.* [CLEO Collaboration], Phys. Rev. Lett. **87**, 251807 (2001) [arXiv:hep-ex/0108032].

[56] P. Koppenburg *et al.* [Belle Collaboration], Phys. Rev. Lett. **93**, 061803 (2004) [arXiv:hep-ex/0403004];

[57] J. Walsh for the Babar Collaboration, talk presented at Moriond QCD, 2005, http://moriond.in2p3.fr/QCD/2005/SundayAfternoon/Walsh.ppt.

[58] M. Neubert, Eur. Phys. J. C **40**, 165 (2005) [arXiv:hep-ph/0408179]; D. Benson, I. I. Bigi and N. Uraltsev, Nucl. Phys. B **710**, 371 (2005) [arXiv:hep-ph/0410080].

[59] V. V. Anisimovsky *et al.* [E949 Collaboration], Phys. Rev. Lett. **93**, 031801 (2004) [arXiv:hep-ex/0403036].

[60] A. Alavi-Harati *et al.* [The E799-II/KTeV Collaboration], Phys. Rev. D **61**, 072006 (2000) [arXiv:hep-ex/9907014].

[61] R. Barate *et al.* [ALEPH Collaboration], Eur. Phys. J. C **19**, 213 (2001) [arXiv:hep-ex/0010022].

[62] M. Herndon[CDF and D0 Collaborations], FERMILAB-CONF-04-391-E SPIRES entry *To appear in the proceedings of 32nd International Conference on High-Energy Physics (ICHEP 04), Beijing, China, 16-22 Aug 2004*

[63] M. Ciuchini *et al.*, JHEP **0107**, 013 (2001) [arXiv:hep-ph/0012308].

[64] A. J. Buras and R. Fleischer, Phys. Rev. D **64** (2001) 115010 [arXiv:hep-ph/0104238].

[65] A. J. Buras, A. Romanino and L. Silvestrini, Nucl. Phys. B **520**, 3 (1998) [arXiv:hep-ph/9712398]; G. Colangelo and G. Isidori, JHEP **9809**, 009 (1998) [arXiv:hep-ph/9808487]; A. J. Buras, G. Colangelo, G. Isidori, A. Romanino and L. Silvestrini, Nucl. Phys. B **566**, 3 (2000) [arXiv:hep-ph/9908371]; G. Buchalla, G. Hiller and G. Isidori, Phys. Rev. D **63**, 014015 (2001) [arXiv:hep-ph/0006136]; D. Atwood and G. Hiller, arXiv:hep-ph/0307251; A. J. Buras, R. Fleischer, S. Recksiegel and F. Schwab, Nucl. Phys. B **697**, 133 (2004) [arXiv:hep-ph/0402112]; A. J. Buras, T. Ewerth, S. Jager and J. Rosiek, Nucl. Phys. B **714**, 103 (2005) [arXiv:hep-ph/0408142].

[66] M. Blanke, A. J. Buras, A. Poschenrieder, S. Recksiegel, C. Tarantino, S. Uhlig and A. Weiler, arXiv:hep-ph/0610298.

[67] G. Burdman, Phys. Rev. D **57**, 4254 (1998) [arXiv:hep-ph/9710550].

[68] A. G. Akeroyd *et al.*[SuperKEKB Physics Working Group], arXiv:hep-ex/0406071; J. L. Hewett *et al.*, arXiv:hep-ph/0503261.

[69] A. L. Kagan and M. Neubert, Phys. Rev. D **58**, 094012 (1998) [arXiv:hep-ph/9803368].

[70] T. Hurth, E. Lunghi and W. Porod, Nucl. Phys. B **704**, 56 (2005) [arXiv:hep-ph/0312260].

[71] K. Bieri, C. Greub and M. Steinhauser, Phys. Rev. D **67** (2003) 114019 [[arXiv:hep-ph/0302051]; M. Misiak and M. Steinhauser, Nucl. Phys. B **683**, 277 (2004) [arXiv:hep-ph/0401041]; M. Gorbahn and U. Haisch, Nucl. Phys. B **713** (2005) 291 [arXiv:hep-ph/0411071]; M. Gorbahn, U. Haisch

and M. Misiak, arXiv:hep-ph/0504194; H. M. Asatrian, C. Greub, A. Hovhannisyan, T. Hurth and V. Poghosyan, arXiv:hep-ph/0505068.

[72] K. S. Babu and C. F. Kolda, Phys. Rev. Lett. **84**, 228 (2000) [arXiv:hep-ph/9909476]; C. S. Huang, W. Liao and Q. S. Yan, Phys. Rev. D **59**, 011701 (1999) [arXiv:hep-ph/9803460]; S. R. Choudhury and N. Gaur, Phys. Lett. B **451**, 86 (1999) [arXiv:hep-ph/9810307]; C. S. Huang, W. Liao, Q. S. Yan and S. H. Zhu, Phys. Rev. D **63**, 114021 (2001) [Erratum-ibid. D **64**, 059902 (2001)] [arXiv:hep-ph/0006250]; C. Bobeth, T. Ewerth, F. Kruger and J. Urban, Phys. Rev. D **64** (2001) 074014 [arXiv:hep-ph/0104284]; A. Dedes, Mod. Phys. Lett. A **18**, 2627 (2003) [arXiv:hep-ph/0309233]; A. J. Buras, P. H. Chankowski, J. Rosiek and L. Slawianowska, Phys. Lett. B **546**, 96 (2002) [arXiv:hep-ph/0207241]; A. J. Buras, P. H. Chankowski, J. Rosiek and L. Slawianowska, Nucl. Phys. B **659**, 3 (2003) [arXiv:hep-ph/0210145]; S. Baek, P. Ko and W. Y. Song, JHEP **0303**, 054 (2003) [arXiv:hep-ph/0208112]; G. L. Kane, C. Kolda and J. E. Lennon, arXiv:hep-ph/0310042; A. Dedes and B. T. Huffman, Phys. Lett. B **600**, 261 (2004) [arXiv:hep-ph/0407285].

[73] A. J. Buras, P. Gambino, M. Gorbahn, S. Jager and L. Silvestrini, Nucl. Phys. B **592**, 55 (2001) [arXiv:hep-ph/0007313].

[74] K. Agashe, N. G. Deshpande and G. H. Wu, Phys. Lett. B **514**, 309 (2001) [arXiv:hep-ph/0105084].

[75] M. Trodden, Rev. Mod. Phys. **71** (1999) 1463 [arXiv:hep-ph/9803479].

[76] V. Cirigliano, B. Grinstein, G. Isidori and M. B. Wise, Nucl. Phys. B **728** (2005) 121 [arXiv:hep-ph/0507001].

[77] G. C. Branco, A. J. Buras, S. Jager, S. Uhlig and A. Weiler, arXiv:hep-ph/0609067.

[78] P. Minkowski, Phys. Lett. B **67** (1977) 421; M. Gell-Mann, P. Ramond and R. Slansky, in *Supergravity*, eds. P. van Nieuwenhuizen et al., (North-Holland, 1979), p. 315; S.L. Glashow, in *Quarks and Leptons*, Cargèse, eds. M. Lévy et al., (Plenum, 1980), p. 707; T. Yanagida, in *Proceedings of the Workshop on the Unified Theory and the Baryon Number in the Universe*, eds. O. Sawada et al., (KEK Report 79-18, Tsukuba, 1979), p. 95; R. N. Mohapatra and G. Senjanovic, Phys. Rev. Lett. **44** (1980) 912.

[79] M. Fukugita and T. Yanagida, Phys. Lett. B **174** (1986) 45.

[80] For a review, see e.g. W. Buchmüller, R. D. Peccei and T. Yanagida, hep-ph/0502169.

[81] B. Pontecorvo, Sov. Phys. JETP **6** (1957) 429 [Zh. Eksp. Teor. Fiz. **33** (1957) 549]; Z. Maki, M. Nakagawa and S. Sakata, Prog. Theor. Phys. **28** (1962) 870.

[82] J. A. Casas and A. Ibarra, Nucl. Phys. B **618** (2001) 171 [arXiv:hep-ph/0103065].

[83] S. T. Petcov, W. Rodejohann, T. Shindou and Y. Takanishi, arXiv:hep-ph/0510404.

[84] G. C. Branco, R. Gonzalez Felipe, F. R. Joaquim and B. M. Nobre, Phys. Lett. B **633** (2006) 336 [arXiv:hep-ph/0507092].

[85] V. Cirigliano, G. Isidori and V. Porretti, arXiv:hep-ph/0607068.

[86] A. Pilaftsis, Phys. Rev. D **56** (1997) 5431.

[87] A. Pilaftsis and T. E. J. Underwood, Nucl. Phys. B **692** (2004) 303 [arXiv:hep-ph/0309342].

[88] G. D'Ambrosio, G. F. Giudice and M. Raidal, Phys. Lett. B **575** (2003) 75 [hep-ph/0308031] ; Y. Grossman, T. Kashti, Y. Nir and E. Roulet, Phys. Rev. Lett. **91** (2003) 251801 [arXiv:hep-ph/0307081].

[89] W. A. Bardeen, A. J. Buras, D. W. Duke and T. Muta, Phys. Rev. D **18** (1978) 3998.

[90] P. H. Chankowski and Z. Pluciennik, Phys. Lett. B **316** (1993) 312 [arXiv:hep-ph/9306333]; K. S. Babu, C. N. Leung and J. T. Pantaleone, Phys. Lett. B **319** (1993) 191 [arXiv:hep-ph/9309223]; S. Antusch, M. Drees, J. Kersten, M. Lindner and M. Ratz, Phys. Lett. B **519** (2001) 238 [arXiv:hep-ph/0108005]; S. Antusch, M. Drees, J. Kersten, M. Lindner and M. Ratz, Phys. Lett. B **525** (2002) 130 [arXiv:hep-ph/0110366]; S. Antusch and M. Ratz, JHEP **0207** (2002) 059 [arXiv:hep-ph/0203027]; P. H. Chankowski and S. Pokorski, Int. J. Mod. Phys. A **17** (2002) 575 [arXiv:hep-ph/0110249]; S. Antusch, J. Kersten, M. Lindner and M. Ratz, Phys. Lett. B **538** (2002) 87 [arXiv:hep-ph/0203233].

[91] F. Borzumati and A. Masiero, Phys. Rev. Lett. **57** (1986) 961; J. Hisano, T. Moroi, K. Tobe, M. Yamaguchi and T. Yanagida, Phys. Lett. B **357** (1995) 579 [arXiv:hep-ph/9501407]; J. Hisano, T. Moroi, K. Tobe and M. Yamaguchi, Phys. Rev. D **53** (1996) 2442 [arXiv:hep-ph/9510309].

[92] S. Antusch, J. Kersten, M. Lindner and M. Ratz, Nucl. Phys. B **674** (2003) 401 [arXiv:hep-ph/0305273].

[93] S. Antusch, J. Kersten, M. Lindner, M. Ratz and M. A. Schmidt, JHEP **0503** (2005) 024 [hep-ph/0501272].

[94] A. Strumia and F. Vissani, Nucl. Phys. B **726**, 294 (2005) [arXiv:hep-ph/0503246].

[95] F. Deppisch, H. Pas, A. Redelbach and R. Ruckl, arXiv:hep-ph/0511062.

[96] S. Kanemura, K. Matsuda, T. Ota, T. Shindou, E. Takasugi and K. Tsumura, Phys. Rev. D **72** (2005) 055012 [Erratum-ibid. D **72** (2005) 059904] [arXiv:hep-ph/0507264].

[97] S. T. Petcov and T. Shindou, arXiv:hep-ph/0605204.

[98] T. Hambye, Talk given at SEESAW25: International Conference on the Seesaw Mechanism and the Neutrino Mass, Paris, France, 10-11 Jun 2004. Published in Paris 2004, Seesaw 25, p. 151-168; hep-ph/0412053.

[99] G. C. Branco, T. Morozumi, B. M. Nobre and M. N. Rebelo, Nucl. Phys. B **617** (2001) 475; G. C. Branco, R. González Felipe, F. R. Joaquim and M. N. Rebelo, Nucl. Phys. B **640** (2002) 202; M. N. Rebelo, Phys. Rev. D **67** (2003) 013008; G. C. Branco, R. González Felipe, F. R. Joaquim, I. Masina, M. N. Rebelo and C. A. Savoy, Phys. Rev. D **67** (2003) 073025.

[100] S. Kaneko and M. Tanimoto, Phys. Lett. B **551** (2003) 127; S. Pascoli, S. T. Petcov and W. Rodejohann, Phys. Rev. D **68** (2003) 093007; E. K. Akhmedov, M. Frigerio and A. Y. Smirnov, JHEP **0309** (2003) 021; L. Velasco-Sevilla, JHEP **0310** (2003) 035; A. Ibarra and G. G. Ross, Phys. Lett. B **591** (2004) 285; P. H. Chankowski, J. R. Ellis, S. Pokorski, M. Raidal and K. Turzynski, Nucl. Phys. B **690** (2004) 279; M. Bando, S. Kaneko, M. Obara and M. Tanimoto, hep-ph/0405071; R. N. Mohapatra and S. Nasri, Phys. Rev. D **71** (2005) 033001; Z. Z. Xing and S. Zhou, Phys. Lett. B **606** (2005) 145; N. Sahu and S. Uma Sankar, hep-ph/0501069. G. C. Branco, M. N. Rebelo and J. I. Silva-Marcos, Phys. Lett. B **633** (2006) 345 [arXiv:hep-ph/0510412].

[101] R. González Felipe and F. R. Joaquim, JHEP **0109** (2001) 015.

[102] K. Hamaguchi, H. Murayama and T. Yanagida, Phys. Rev. D **65** (2002) 043512; T. Hambye, Nucl. Phys. B **633** (2002) 171; S. Davidson and A. Ibarra, Phys. Lett. B **535** (2002) 25; W. Buchmüller, P. Di Bari and M. Plümacher, Nucl. Phys. B **643** (2002) 367; W. Buchmüller, P. Di Bari and M. Plümacher, Nucl. Phys. B **665** (2003) 445; T. Hambye, Y. Lin, A. Notari, M. Papucci and A. Strumia, Nucl. Phys. B **695** (2004) 169.

[103] G. F. Giudice, A. Notari, M. Raidal, A. Riotto and A. Strumia, Nucl. Phys. B **685** (2004) 89.

[104] M.Y. Khlopov and A.D. Linde, Phys. Lett. **B138** (1984) 265; J. Ellis, J.E. Kim and D.V. Nanopoulos, Phys. Lett. **B145** (1984) 181; M. Kawasaki and T. Moroi, Prog. Theor. Phys. **93** (1995) 879.

[105] R. González Felipe, F. R. Joaquim and B. M. Nobre, Phys. Rev. D **70** (2004) 085009; F. R. Joaquim, Nucl. Phys. Proc. Suppl. **145** (2005) 276.

[106] K. Turzynski, Phys. Lett. B **589** (2004) 135.

[107] D. N. Spergel *et al.* [WMAP Collaboration], Astrophys. J. Suppl. **148** (2003) 175; M. Tegmark *et al.* [SDSS Collaboration], Phys. Rev. D **69** (2004) 103501 [arXiv:astro-ph/0310723].

[108] A. Pilaftsis and T. E. J. Underwood, Phys. Rev. D **72** (2005) 113001 arXiv:hep-ph/0506107; T. E. J. Underwood, arXiv:hep-ph/0605232.

[109] R. Barbieri, P. Creminelli, A. Strumia and N. Tetradis, Nucl. Phys. B **575**, 61 (2000) [arXiv:hep-ph/9911315].

[110] A. Abada, S. Davidson, F. X. Josse-Michaux, M. Losada and A. Riotto, arXiv:hep-ph/0601083; A. Abada, S. Davidson, A. Ibarra, F. X. Josse-Michaux, M. Losada and A. Riotto, arXiv:hep-ph/0605281.

[111] E. Nardi, Y. Nir, E. Roulet and J. Racker, JHEP **0601**, 164 (2006) [arXiv:hep-ph/0601084].

[112] S. Blanchet and P. Di Bari, arXiv:hep-ph/0607330.

[113] S. Blanchet and P. Di Bari, arXiv:hep-ph/0603107.

[114] L. Covi, E. Roulet and F. Vissani, Phys. Lett. B **384**, 169 (1996) [arXiv:hep-ph/9605319].

[115] P. Di Bari, arXiv:hep-ph/0406115.

[116] G. F. Giudice and R. Rattazzi, Nucl. Phys. B **757** (2006) 19 [arXiv:hep-ph/0606105].

[117] N. S. Manton, Nucl. Phys. B **158** (1979) 141; D. B. Fairlie, Phys. Lett. B **82** (1979) 97; J. Phys. G **5** (1979) L55; P. Forgacs, N. S. Manton, Commun. Math. Phys. **72** (1980) 15; S. Randjbar-Daemi, A. Salam, J. Strathdee, Nucl. Phys. B **214** (1983) 491; N. V. Krasnikov, Phys. Lett. B **273** (1991) 246; H. Hatanaka, T. Inami, C. Lim, Mod. Phys. Lett. A **13** (1998) 2601; G. R. Dvali, S. Randjbar-Daemi and R. Tabbash, Phys. Rev. D **65** (2002) 064021.

[118] C. A. Scrucca, M. Serone and L. Silvestrini, Nucl. Phys. B **669**, 128 (2003) [arXiv:hep-ph/0304220].

[119] Y. Hosotani, *Phys. Lett.* **B126** (1983) 309;
Y. Hosotani, *Phys. Lett.* **B129** (1983) 193;
Y. Hosotani, *Ann. Phys.* **190** (1989) 233.

[120] K. Agashe, R. Contino and A. Pomarol, Nucl. Phys. B **719** (2005) 165.

[121] K. y. Oda and A. Weiler, Phys. Lett. B **606** (2005) 408 [arXiv:hep-ph/0410061].

[122] M. Kubo, C. S. Lim, and H. Yamashita, *Mod. Phys. Lett.* **A17** (2002) 2249–2264, `hep-ph/0111327`;
N. Haba, M. Harada, Y. Hosotani, and Y. Kawamura, *Nucl. Phys.* **B657** (2003) 169–213, `hep-ph/0212035`;
N. Haba and T. Yamashita, *JHEP* **02** (2004) 059,`hep-ph/0401185`;
Y. Hosotani, S. Noda, and K. Takenaga, *Phys. Rev.* **D69** (2004) 125014, `hep-ph/0403106`.

[123] N. Haba, Y. Hosotani, and Y. Kawamura, *Prog. Theor. Phys.* **111** (2004) 265–289, `hep-ph/0309088`.

[124] L. J. Hall, H. Murayama, and Y. Nomura, *Nucl. Phys.* **B645** (2002) 85–104, `hep-th/0107245`.

[125] A. Delgado, A. Pomarol and M. Quiros, JHEP **0001** (2000) 030 [arXiv:hep-ph/9911252].

[126] H. Verlinde, *Nucl. Phys.* **B580** (2000) 264–274, `hep-th/9906182`;
S. B. Giddings, S. Kachru, and J. Polchinski, *Phys. Rev.* **D66** (2002) 106006,`hep-th/0105097`.

[127] C. Csaki, arXiv:hep-ph/0404096.

[128] R. Contino, Y. Nomura, and A. Pomarol, *Nucl. Phys.* **B671** (2003) 148–174, `hep-ph/0306259`.

[129] K. Oda and A. Weiler, in preparation.

[130] W. D. Goldberger and M. B. Wise, *Phys. Rev. Lett.* **83** (1999) 4922–4925, `hep-ph/9907447`.

[131] T. Gherghetta and A. Pomarol, *Nucl. Phys.* **B586** (2000) 141–162, `hep-ph/0003129`.

[132] J. Garriga, O. Pujolas, and T. Tanaka, *Nucl. Phys.* **B605** (2001) 192–214, `hep-th/0004109`.

[133] D. J. Toms, *Phys. Lett.* **B484** (2000) 149–153, hep-th/0005189.

[134] W. D. Goldberger and I. Z. Rothstein, *Phys. Lett.* **B491** (2000) 339–344, hep-th/0007065.

Acknowledgement

First, I would like to thank my advisor, Andrzej Buras, for providing such a stimulating and enthusing environment where both new ideas and proven 'gut feeling' are equally present. I have learned a lot from him, both directly through his mastery of the field of weak decays but also on how to generally approach physics problems. He has supported me in an exceptional way and provided funds in that I could travel extensively to summer schools, conferences and work-shops. During my time in Munich I have also benefitted from discussions with Luca Silvestrini, who visited our group for six months. He was always accessible and quick to understand the core of a problem. The open and exciting discussions with him and the pizza dinners afterwards are gratefully acknowledged. I also would like to thank Kin-ya Oda with whom I had to walk through a long desert led astray by mirages many times before we could find the trick which made it all possible.
Sebastian Jäger I'd like to thank for many insightful discussions on life, physics and the curbing of one's enthusiasm. Next, I would like to thank my coworkers from whom I have benefited through discussions during the course of our common projects: Monika Blanke, Christoph Bobeth, Gustavo Branco, Thorsten Ewerth, Uli Haisch, Anton Poschenrieder, Stefan Recksiegel, Felix Schwab, Michael Spranger, Cecilia Tarantino, and Selma Uhlig. I want to thank Stefan additionally for his quick and always knowledgeable help with the computer system. Finally, I also would like to thank everybody in the group for the pleasant and friendly atmosphere.
I also thank my family for their unconditional support and their never ending questions and interest even when faced with mostly obscure and detached physics problems. I am very grateful for their encouragement and their understanding during sometimes difficult periods.
Vasso, $\alpha\gamma\alpha\pi\eta\ \mu o\upsilon$, I want to thank for showing me beauty and for coming with and for bearing with me.